ÉCOLE DE TECHNOLOGIE SUPÉRIEURE
UNIVERSITÉ DU QUÉBEC

THÈSE PAR ARTICLES PRÉSENTÉE À
L'ÉCOLE DE TECHNOLOGIE SUPÉRIEURE

COMME EXIGENCE PARTIELLE
À L'OBTENTION DU
DOCTORAT EN GÉNIE
Ph.D.

PAR
Martin GAGNON

CONTRIBUTION À L'ÉVALUATION DE LA FIABILITÉ EN FATIGUE DES TURBINES HYDROÉLECTRIQUES

MONTRÉAL, LE 3 JUILLET 2013

PRÉSENTATION DU JURY

CETTE THÈSE A ÉTÉ ÉVALUÉE

PAR UN JURY COMPOSÉ DE:

M. Souheil-Antoine Tahan, directeur de thèse
Département de génie mécanique

M. Philippe Bocher, codirecteur
Département de génie mécanique

M. Robert Sabourin, président du jury
Département de génie de la production automatisée

M. Nicolas Saintier, examinateur externe
École nationale supérieure d'arts et métiers (ENSAM) - Centre Bordeaux-Talence

M. Denis Thibault, examinateur invité
Institut de recherche d'Hydro-Québec (IREQ)

M. André Coutu, examinateur invité
Andritz Hydro Ltée

IL A FAIT L'OBJET D'UNE SOUTENANCE DEVANT JURY ET PUBLIC

LE "19 JUIN 2013"

À L'ÉCOLE DE TECHNOLOGIE SUPÉRIEURE

REMERCIEMENTS

J'aimerais remercier tous les gens que j'ai convaincus de participer aux différentes activités reliées aux travaux de cette thèse. Mentionnons particulièrement les groupes suivants: Andritz Hydro Ltée, l'Institut de recherche d'Hydro-Québec (IREQ) et l'École de technologie supérieure (ÉTS). Ces groupes, par leur support, ont rendu possible le parachèvement de cette thèse. De plus, j'aimerais souligner l'apport financier du CRSNG et du FQRNT qui m'a permis de concentrer la majorité de mon temps à mes activités de recherche.

CONTRIBUTION À L'ÉVALUATION DE LA FIABILITÉ EN FATIGUE DES TURBINES HYDROÉLECTRIQUES

Martin GAGNON

RÉSUMÉ

Cette recherche a pour objectifs le développement, la validation et l'application d'outils pour estimer la fiabilité en fatigue des aubes de turbines hydroélectriques. Au cours des dernières années, la déréglementation des marchés et la position croissante qui est donnée aux modes de production intermittents, telle que la production d'électricité à partir de l'énergie éolienne, ont forcé les producteurs d'hydroélectricité à modifier leur façon d'opérer leurs équipements de production électrique. Une des conséquences est l'augmentation des fluctuations sur le chargement des équipements qui ,en contrepartie, augmente leurs risques de défaillance. Ces changements rendent difficile la planification de la maintenance pour garantir des niveaux de disponibilité adéquats. Donc, pour les manufacturiers de ces équipements et pour les producteurs d'électricité, avoir la possibilité d'évaluer l'influence de tels changements devient essentiel.

Les résultats de cette thèse sont présentés sous la forme de trois chapitres. Ceux-ci couvrent successivement les aspects suivants : la caractérisation du chargement, la construction d'un modèle d'endommagement et le calcul de la fiabilité des aubes de turbines hydroélectriques. Une introduction ainsi qu'une revue de la littérature sont présentés avant les chapitres qui forment le corps de la thèse pour mettre en perspective les travaux effectués. Dans le Chapitre 1, la modélisation du chargement des aubes de turbines hydroélectriques est abordée avec l'application de modèles de simulation stochastique à la simulation de la réponse transitoire des aubes de turbines hydroélectriques lors du démarrage de celles-ci. Nos résultats révèlent que ces méthodes sont utiles lorsque les données observées sont limitées. Le démarrage des turbines hydroélectriques se révèle un cas intéressant, car cet évènement ne se reproduit jamais de manière identique. Ensuite, dans le Chapitre 2, nous proposons un modèle de fiabilité en fatigue spécifiquement adapté aux aubes de turbines hydroélectriques. Dans ce chapitre, un état limite qui permet d'estimer la fiabilité des aubes de turbines hydroélectriques est défini. Cet état limite permet de déterminer à partir de quel moment une fissure devient critique et par le fait même peut être détectée pour éventuellement être réparée. Finalement, au Chapitre 3, l'effet et la portée des hypothèses émises lors de l'établissement du profil de chargement dans le calcul de la fiabilité d'une turbine hydroélectrique sont discutés. Une étude de cas effectuée sur une turbine provenant d'une centrale hydroélectrique qui appartient à Hydro-Québec est utilisée pour illustrer l'influence de ces hypothèses émises sur le chargement. Plusieurs profils de chargement simplifiés sont proposés avec des caractéristiques définies à partir des données observées *in situ*.

La conclusion de cette thèse montre les avancées scientifiques qu'ont générés nos travaux sur la fiabilité en fatigue des turbines hydroélectrique. De plus, nous portons un intérêt particulier aux perspectives de recherche soulevées par les travaux présentés dans cette thèse et aussi aux travaux que nous avons initiés parallèlement à ceux-ci.

Mot-clés : Turbine hydroélectrique, Fiabilité, Propagation de fissure, Modèle stochastique, Chargement en fatigue

CONTRIBUTION À L'ÉVALUATION DE LA FIABILITÉ EN FATIGUE DES TURBINES HYDROÉLECTRIQUES

Martin GAGNON

ABSTRACT

The goal of this thesis is to develop, validate, and apply reliability assessment methodologies to estimate the probability of fatigue cracking in hydroelectric runner blades. In the recent years, the growing influence of intermittent energy source, such as wind turbines, on hydroelectric facility operation force hydroelectricity producer to change their operation scenarios in order to account for this new variability. This new variability tends to augment the risk of failure which renders difficult maintenance planning and the achievement of the desired level of reliability. Hence, both the manufacturer and the operator of hydroelectric turbines need tools to evaluate the influence of these changes on the reliability of their structure.

The results presented in this thesis cover the following aspects: Loading characterization, damage modeling, and reliability assessment. After a rapid introduction, a literature review gives an overview of research made in each field. Next, in the first chapter, the loading of runner blades is studied. Loading generated by transient events such as turbine startups are modeled using stochastic models. Our results show that such models are particularly useful in case where limited data is available to estimate the variability of such events. In Chapter 2, we propose a limit state for the HCF onset on turbine runner blades. This limit state combined with probabilistic method render possible fatigue reliability and likelihood of crack detection estimate. Subsequently in Chapter 3, our reliability model is applied using the data gathered from one of Hydro-Québec's power plant. Our objective was to evaluate the influence of loading assumptions. As a result, loading spectra are proposed with different level of simplification in order to determine the minimal number of parameters necessary to adequately estimate the reliability.

Finally, in the conclusion, we discuss the contributions to the reliability assessment of hydroelectric turbine runner blades of the work presented in this thesis. Furthermore, at the same time, we highlight new and emerging research opportunities uncovered during our research activities.

Keywords: Hydroelectric runner, Reliability, Crack growth, Stochastic model, fatigue loading

TABLE DES MATIÈRES

LISTE DES TABLEAUX

Page

LISTE DES FIGURES

LISTE DES ABRÉVIATIONS, SIGLES ET ACRONYMES

ASTM	American Society for Testing and Materials
EEMD	Ensemble Empirical Mode Decomposition
EMD	Empirical Mode Decomposition
ÉTS	École de technologie supérieure
ϵN	Deformation vs Number of cycles
FORM	First Order Reliability Method
HCF	High Cycle Fatigue
HL	Hasofer-Lind
IEA	International Energy Agency
IEEE	Institute of Electrical and Electronics Engineers
IMF	Intrinsic Mode Function
IREQ	Institut de recherche d'Hydro-Québec
LCF	Low Cycle Fatigue
LEFM	Linear Elastic Fracture Mechanics
MC	Monte Carlo
MPP	Most Probable Point
NSERC	National Sciences and Engineering Research Council of Canadian
SORM	First Order Reliability Method
SN	Stress vs Number of cycles
SNL	Spin no-load

SWD	Stationary Wavelet Decomposition

LISTE DES SYMBOLES ET UNITÉS DE MESURE

a	Dimension de la fissure [mm]
a_0	Transition entre la limite d'endurance $\Delta\sigma_0$ et le seuil ΔK_{th} [mm]
$A(t)$	Amplitude instantanée
$A_j(t)$	Amplitude instantanée pour le niveau de décomposition j
$A_N(t)$	Approximation du niveau N
β_{HL}	Indice de fiabilité de Hasofer-Lind
C	Constante qui permet de modéliser la vitesse de propagation de fissure
$C_j(t)$	IMF du niveau de décomposition j
da/dN	Propagation de fissure par cycle de contrainte [$mm/cycle$]
$D_j(t)$	Détail du niveau j
ΔK	Variation du facteur d'intensité de contrainte [$N/mm^{3/2}$]
ΔK_{th}	Seuil de propagation de fissure [$N/mm^{3/2}$]
ΔK_{onset}	Seuil de propagation pour le chargement HCF [$N/mm^{3/2}$]
$\Delta\sigma$	Variation de contrainte [$N/mm^2(MPa)$]
$\Delta\sigma_{HCF}$	Étendue des cycles de contraintes HCF [$N/mm^2(MPa)$]
$\Delta\sigma_{Shutdown}$	Étendue du cycle de contraintes lors de l'arrêt [$N/mm^2(MPa)$]
$\Delta\sigma_{SNL}$	Étendue des cycles de contraintes à la condition d'opération SNL [$N/mm^2(MPa)$]
$\Delta\sigma_{Startup}$	Étendue du cycle de contraintes au démarrage [$N/mm^2(MPa)$]
$\Delta\sigma_{th}$	Seuil de propagation de fissure [$N/mm^2(MPa)$]
$\Delta\sigma_0$	Limite d'endurance [$N/mm^2(MPa)$]

E	Énergie d'une fonction quelconque dépendant du temps
$f(t)$	Fonction quelconque dépendant du temps
$f(x)$	Fonction quelconque
$F(x)$	Fonction cumulée de $f(x)$ tel que $F(x) = \int_{-\infty}^{x} f(x)\, dx$
$H(t)$	Transformée de Hilbert
K	Facteur d'intensité de contrainte [$N/mm^{3/2}$]
m	Constante qui permet de modéliser la vitesse de propagation de fissure
$N_{Startup}$	Nombre de démarrages
N_{SNL}	Nombre de passages par la condition d'opération SNL
$\omega(t)$	Fréquence instantanée [radian/s]
$\omega_j(t)$	Fréquence instantanée du niveau de décomposition j [radian/s]
p	Distance par rapport à la surface [mm]
P	Valeur principale de Cauchy
P_f	Probabilité de dépasser la limite ou seuil
ϕ	Phase [radian]
ϕ_j	Phase du niveau de décomposition j [radian]
$r_N(t)$	Résidu
$\theta(t)$	Phase instantanée [radian]
W	Largeur de la section [mm]
$X(t)$	Série temporelle
$X_a(t)$	Série temporelle analytique

$\hat{X}(t)$	Série temporelle estimée
$Y(a)$	Facteur de correction pour une géométrie donnée

INTRODUCTION

Problématique

L'hydroélectricité représente 16.3% de la production mondiale d'électricité (approximativement 3500 TWh en 2010) comparativement à 67.2% pour les énergies fossiles et 12.8% pour le nucléaire (IEA, 2012). La moitié de cette production d'hydroélectricité provient, par ordre d'importance: de la Chine (694 TWh), du Brésil (403 TWh), du Canada (376 TWh) et des États-Unis (328 TWh). Notons qu'en Amérique du Nord, uniquement 39% de la ressource est développée et que cela représente un potentiel de développement de 1659 TWh ou 388 GW (IEA, 2012). Au Québec, Hydro-Québec a produit à elle seule en 2011 un total de 189 TWh d'électricité. La production d'Hydro-Québec est à 98% d'origine hydraulique et provient d'un parc de production comprenant 60 centrales hydroélectriques avec une puissance installée de 37 GW (Hydro-Québec, 2011). Dans ce contexte, la maintenance et la pérennité des équipements de production hydroélectrique représentent des enjeux majeurs, non seulement localement, pour Hydro-Québec, mais aussi mondialement.

On observe que la déréglementation des marchés et la position croissante qui est donnée aux modes de production intermittents d'électricité, telle que la production d'électricité à partir de l'énergie éolienne, forcent les producteurs à modifier leur façon d'opérer les équipements de production hydroélectrique. On observe dans plusieurs centrales hydroélectriques que des groupes turbine-alternateurs doivent maintenant régulièrement opérer à la limite de leur capacité, et même en dehors des spécifications d'origine. La conséquence de ces changements est une augmentation des risques de défaillance, rendant difficile la planification de la maintenance nécessaire pour garantir les niveaux de disponibilité souhaitée. Il est donc essentiel dans ce contexte, autant pour les manufacturiers de ces équipements que pour les producteurs d'hydroélectricité, de développer des approches qui permettent d'évaluer l'impact de ces nouveaux scénarios d'utilisation.

Un des facteurs qui limitent la vie des turbines hydroélectriques est la dégradation en fatigue du matériau. Pour ce type de structure, ce facteur est associé à la dégradation de la fiabilité.

La fatigue du matériau se caractérise par l'apparition de fissures dans les aubes de la roue de turbine. Le chargement subit par la structure fait évoluer dans le temps la dimension des défauts contenus dans le matériau en fonction de son comportement dynamique. Généralement, des modèles déterministes sont utilisés pour calculer la durée de vie en fatigue. Par contre, l'absence de la notion d'incertitude dans ces modèles rend l'évaluation des risques difficile et surtout approximative. Pour contourner le problème, les valeurs utilisées sont souvent pondérées pour obtenir une marge de sécurité adéquate. Cependant, il est difficile de définir ce qu'est "une marge de sécurité adéquate" sans avoir recours aux probabilités. Il en résulte que, lorsque des modèles déterministes sont utilisés, un composant peut être retiré bien avant la fin de sa vie utile ou subir une défaillance prématurée sans que le risque puisse être quantifié.

Les enjeux économiques et les contraintes environnementales jouent un rôle de plus en plus dominant dans le contexte actuel, et il est difficile aujourd'hui de justifier le remplacement d'un équipement toujours fonctionnel ou le risque de pertes de production générées par de la maintenance non planifiée. Dans cette situation, les approches probabilistes sont mieux adaptées à la prise de décision, car elles permettent de quantifier le risque. Cela est d'autant plus important lorsque l'on doit opérer des équipements de façon économique et sécuritaire en dehors des spécifications d'origine ou de la durée de vie calculée initialement. Les modèles probabilistes répondent à ce genre de problématique, car ils permettent d'évaluer au besoin la probabilité d'une défaillance à un moment donné ou l'incertitude sur le moment de cette défaillance. De plus, par l'analyse de la propagation de l'incertitude à l'intérieur du modèle mathématique utilisé, il est possible de porter un jugement sur la qualité de l'information disponible et la validité de celui-ci.

Objectifs de la thèse

Cette recherche a pour objectifs le développement, la validation et l'application d'outils d'analyse et d'estimation de la fiabilité en fatigue des aubes de turbines hydroélectriques. Face à la dérèglementation des marchés de l'électricité, les équipements de production tel que les turbine hydroélectrique doivent maintenant être opéré selon des scénario souvent différents de

ceux traditionnellement utilisé lors de leurs conception. Ceci soulève deux questions fondamentales:

- Quelle est maintenant la limite à ne pas dépasser?
- Où sommes-nous situés par rapport à la limite?

Nous définissons la fiabilité comme étant "*The ability of a system or component to perform its required functions under stated conditions for a specified period of time*" (IEEE, 1990). C'est-à-dire, la capacité d'un dispositif à accomplir une fonction ou une tâche dans des conditions de fonctionnement données et pour une durée spécifiée. Appliquée aux aubes des roues de turbines hydroélectriques, la **fiabilité en fatigue** devient la probabilité de ne pas avoir une fissure de taille importante causée par la fatigue du matériau qui doit être réparée, dans un intervalle de temps spécifié en fonction de conditions d'opération données.

Le calcul de la durée de vie en fatigue, tel que présenté schématiquement à la Figure 0.1, est centré autour d'un modèle d'endommagement qui fait évoluer dans le temps les propriétés en fatigue de la structure. Le modèle d'endommagement permet d'estimer la durée de vie résiduelle en combinant deux principales sources d'information : l'information relative au comportement dynamique de la structure (qui correspond aux déformations subies par celle-ci sous la forme d'un chargement), et l'information reliée à l'état du matériau à un moment donné dans le temps. De plus, une rétroaction sur les données fournies au modèle peut être ajoutée en utilisant des sources d'information obtenues *a posteriori*. Dans notre cas, ces informations sont typiquement sous la forme de réparations, d'inspections ou de mesures effectuées *a posteriori* qui peuvent avoir une influence sur les paramètres du modèle. Donc, pour exploiter le modèle dans une optique probabiliste, l'incertitude associée à chacun des paramètres doit être estimée et ensuite propagée à travers celui-ci afin d'obtenir la probabilité d'atteindre un objectif de durée de vie spécifiée.

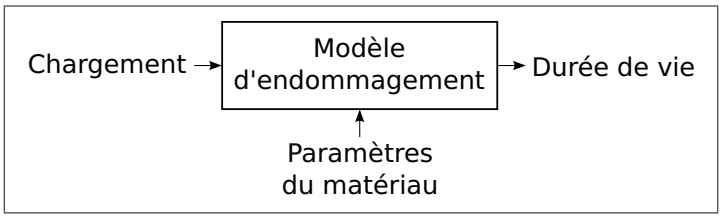

Figure 0.1 Schéma simplifié du calcul de la durée de vie

On distingue deux philosophies de calcul pour estimer la durée de vie en fatigue: le calcul du temps d'initiation d'une fissure et le calcul de la propagation d'une fissure. Les deux approches sont complémentaires. Toutefois, dans notre cas, une approche basée uniquement sur la propagation des fissures et la mécanique de la rupture semble plus adéquate. Pour une aube d'une turbine hydroélectrique, les régions à risque de fissuration sont typiquement localisées près des joints soudés à la jonction avec la couronne ou la ceinture. Or, dans ces régions, la période d'initiation de fissure peut être considérée comme négligeable puisque le procédé de soudage génère une grande quantité de défauts au moment de la fabrication (Chryssanthopoulos et Righiniotis, 2006). Ce type d'approche est nommée tolérance au dommage ("*Damage Tolerance*") et permet le calcul de la propagation des défauts présents initialement dans la structure contrairement à leur "apparition" pour les méthodes basées sur l'initiation de fissure ("*Safe Life*"). Avec ce type d'approche, la structure peut être maintenue en service jusqu'au moment où les défauts (ou fissures) auront atteint une dimension critique à partir de laquelle la structure devra être réparée ou remplacée. Cependant, la notion de dimension critique dans ces modèles pose un problème dans le cas des aubes de turbines hydroélectriques, car les méthodes d'inspection utilisées ne sont pas en mesure de détecter fidèlement un défaut avant que celui-ci devienne de dimension assez grande pour être critique. La conséquence est que tout défaut, lorsque détecté, doit être considéré comme critique et être réparé. Il en résulte qu'une des difficultés principales devient la caractérisation d'un "état limite" adéquat pour permettre un calcul de la fiabilité en fatigue des aubes de turbines hydroélectriques.

Signalons une certaine séquence dans les étapes et une hiérarchie dans les données qui permettent le calcul de la fiabilité en fatigue. Une représentation des étapes du calcul de la fiabilité en fatigue et de la structure de la thèse est présentée à la Figure 0.2. On observe dans cette figure

que le chargement est un paramètre essentiel et que celui-ci est régi par le profil d'opération de la structure. Ce même chargement sert ensuite à établir un profil d'endommagement à partir duquel un calcul probabiliste est effectué pour estimer la fiabilité. De plus, si une validation des résultats est effectuée, à l'aide, par exemple, d'une inspection, une mise à jour des paramètres du modèle d'endommagement peut être envisagée pour améliorer la précision des estimations.

Dans cette thèse, chacun des chapitres correspond à un article publié ou soumis à un journal avec comité de lecture. L'ensemble des chapitres de cette thèse couvre les étapes présentées à la Figure 0.2 à l'exception de la validation et la mise à jour des résultats. Toutefois, ces deux étapes seront considérées dans la revue de littérature et la conclusion de cette thèse puisqu'elles jouent un rôle important dans l'amélioration de la précision des prédictions effectuées.

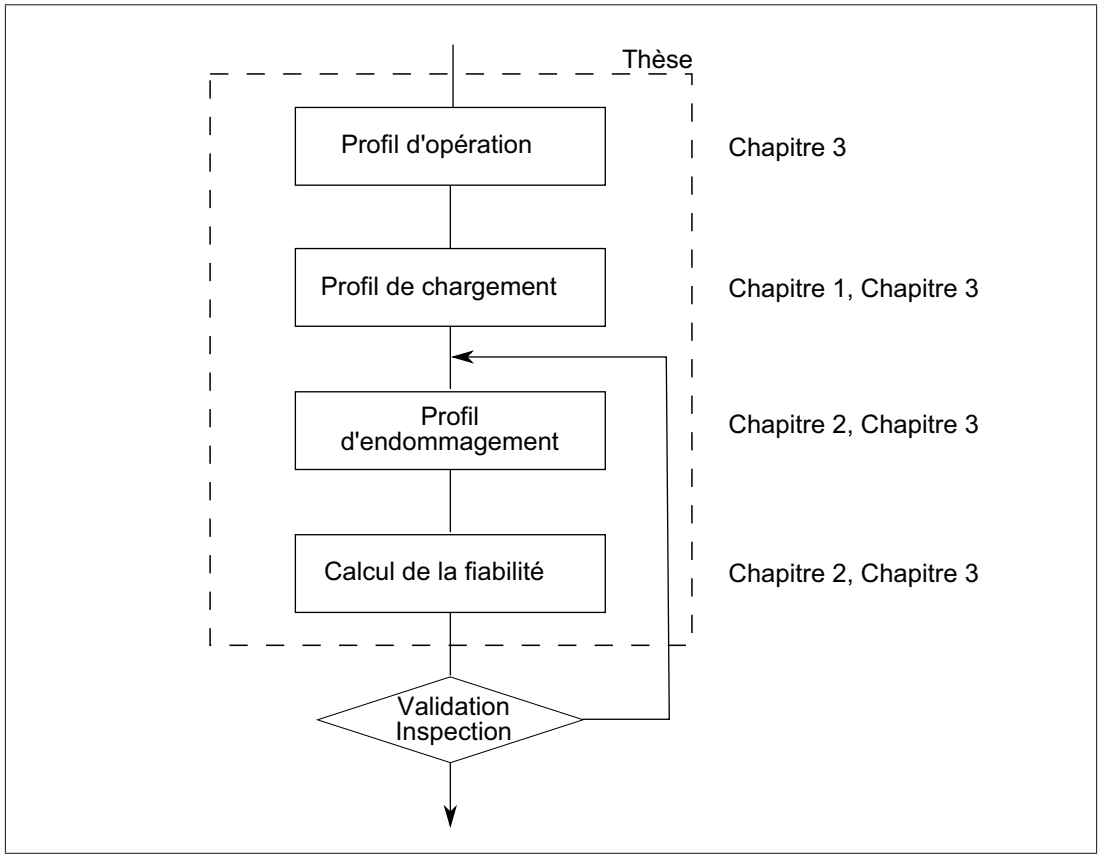

Figure 0.2 Étapes du calcul de la fiabilité en fatigue et structure de la thèse

Structure de la thèse

Le contenu de cette thèse, tel que présenté à la Figure 0.2, est constitué de trois chapitres qui couvrent la caractérisation du chargement, la construction d'un modèle d'endommagement et le calcul de la fiabilité des aubes de turbines hydroélectriques. Plus précisément, nous cherchons à répondre aux trois questions suivantes:

- Chapitre 1: Peut-on estimer l'incertitude sur le chargement d'un évènement transitoire?
- Chapitre 2: Comment définir l'état limite pour la fatigue d'une aube de turbine?
- Chapitre 3: Nos hypothèses sur le chargement ont-elles une influence sur la fiabilité?

Premièrement, suite à l'introduction, une revue de la littérature est présentée afin de mettre en perspective l'état de l'art et les travaux effectués. Ensuite, dans le Chapitre 1, la modélisation du chargement des aubes de turbines est abordée avec l'application de modèles de simulation stochastique initialement développés pour la simulation des évènements transitoires générés par des phénomènes naturels tels que le vent et les tremblements de terre. Dans notre cas, ces méthodes sont appliquées à la simulation de la réponse transitoire des aubes de turbines hydroélectriques lors du démarrage de celles-ci. Nos résultats révèlent que ces méthodes sont très utiles lorsque peu de données observées sont disponibles pour des évènements transitoires qui ne se reproduisent jamais de manière identique. Dans le Chapitre 2, un modèle de fiabilité en fatigue spécifiquement adapté aux aubes de turbines hydroélectriques est proposé. L'état limite qui permet le calcul de la fiabilité des aubes de turbines hydroélectriques y est défini. Cet état limite permet de déterminer à partir de quel moment une fissure devient critique et peut être détectée pour éventuellement être réparée. Puis, au Chapitre 3, l'effet et la portée des hypothèses émises lors de la définition d'un profil de chargement sont discutés. Une étude de cas basée sur une turbine provenant du parc de centrales hydroélectriques d'Hydro-Québec est utilisée pour illustrer l'influence des hypothèses utilisées au niveau du chargement sur la fiabilité estimée. Dans ce chapitre, plusieurs profils de chargement simplifiés sont proposés avec des caractéristiques définies à partir des déformations observées *in situ*. L'objectif est d'identifier un nombre minimal de paramètres essentiels et de quantifier leurs effets. Finalement, dans la conclusion,

nous synthétisons l'apport de chacun des articles de cette thèse à l'amélioration des méthodes d'estimation de la fiabilité en fatigue des turbines hydroélectriques et nous présentons les perspectives de recherche dictées par nos travaux.

REVUE DE LITTÉRATURE

Introduction

Au cours de la dernière décennie, on remarque un regain d'intérêt pour l'aspect probabiliste en fatigue des matériaux et des structures. Parmi les problématiques abordées, on observe une croissance dans les domaines suivants: l'utilisation de données incomplètes, l'effet des activités de maintenance, les impacts des conditions d'opération envisagées et la précision des résultats obtenus (Heng *et al.*, 2009). L'estimation de l'espérance de vie en fatigue peut se calculer selon deux principales philosophies: une approche est basée sur l'espérance de vie en fonction de l'initiation de fissures et une autre approche est basée sur la propagation de celles-ci avec la mécanique de la rupture (Castillo *et al.*, 2008). Les concepts reliés à ces deux types d'approche sont présentés à la Figure 0.3. Les méthodologies basées sur le premier type d'approche s'intéressent au calcul du nombre d'évènements nécessaires pour qu'un défaut d'une taille donnée apparaisse. D'un autre côté, les méthodologies basées sur le deuxième type d'approche sont basées sur la mécanique de la rupture et s'intéressent à la progression de ces défauts sous forme de fissure. Cependant, même si certains chercheurs traitent les deux approches simultanément (Castillo *et al.*, 2008; Jha *et al.*, 2008), on remarque que, généralement, l'initiation et la progression des défauts sont traitées séparément et de manière séquentielle.

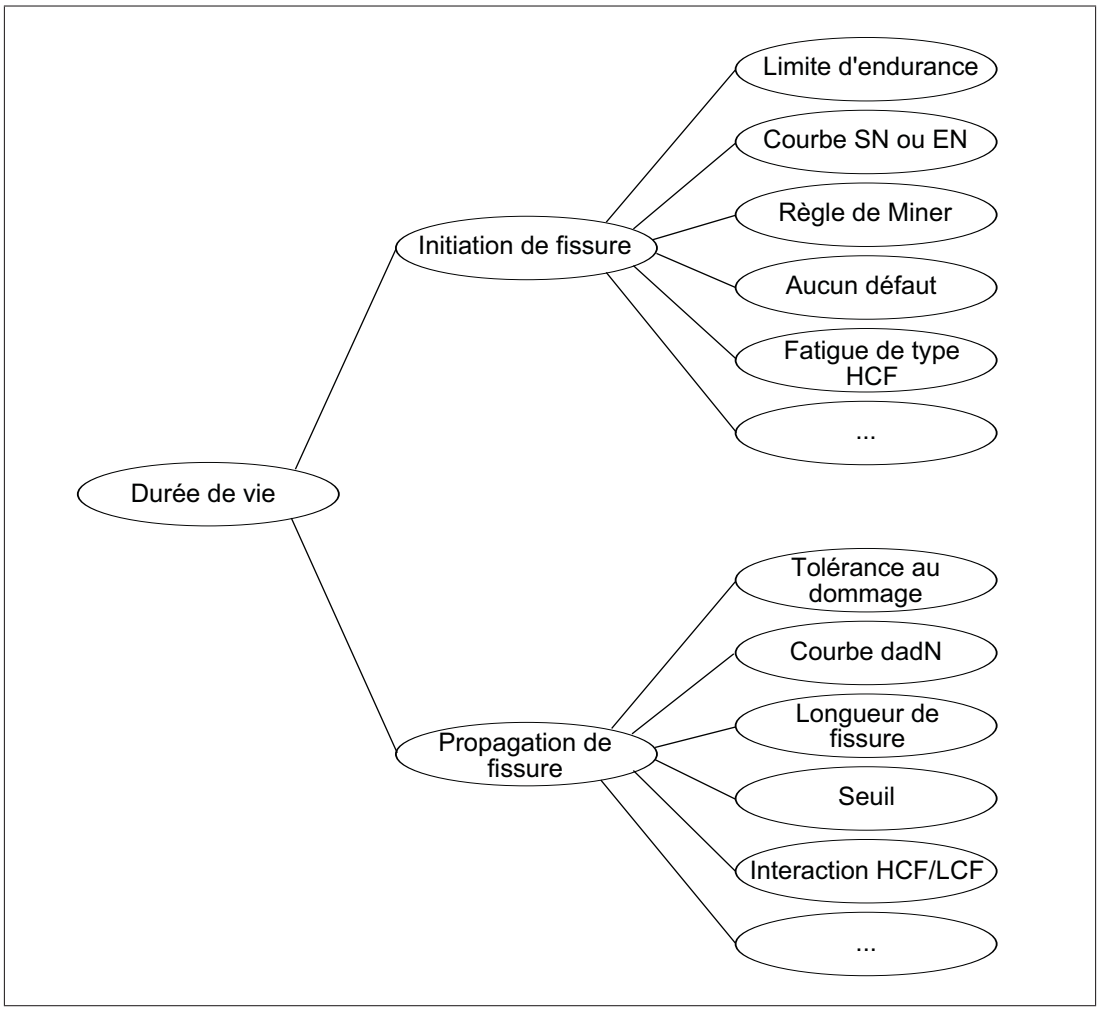

Figure 0.3 Concepts de durée de vie en fatigue

Malgré tout, l'intérêt envers les problématiques reliées à la variabilité des résultats en fatigue n'est pas récent. Les bases du calcul de la fiabilité et du risque en fatigue ont été développées vers la fin des années 60 et au début des années 70. À cette époque, le manque de données et les capacités nécessaires pour effectuer les calculs numériques ont nui à l'essor des approches probabilistes en fatigue d'où la prédominance, même aujourd'hui, des approches déterministes (Tong, 2001). On retrouve peu de travaux récents dans la littérature sur la problématique de la fiabilité en fatigue des roues de turbines hydroélectriques, et ce, même si la fissuration est un problème actuel et de plus en plus récurrent dû au vieillissement des installations. Yuan-fang *et al.* (2012), dans leur ouvrage sur l'analyse de l'opération des turbines hydroélectriques, identifient la fissuration comme étant une des principales sources d'endommagement et de

dégradation des groupes turbine-alternateur suite à l'analyse de l'historique de dix centrales hydroélectriques mises en services au cours de la dernière décennie en Chine. Malgré le faible nombre de publications, on remarque chez des producteurs d'électricité, tels Hydro-Québec ainsi que chez plusieurs manufacturiers de turbines hydroélectriques, un intérêt grandissant pour les problématiques liées à la fissuration et à la durée de vie en fatigue des équipements (Sabourin *et al.*, 2010; Lanteigne *et al.*, 2008, 2007; Coutu *et al.*, 2007; Doerfler *et al.*, 2013). Par contre, ces publications ne couvrent pas l'ensemble des problématiques reliées à la prédiction de la fiabilité et des risques de fissuration dans ce type de structure, mais seulement certains aspects.

Dans ce chapitre, la littérature sur les méthodes de calcul de la fiabilité en fatigue sera passée en revue. Nous nous concentrerons sur les méthodes de type "tolérance au dommage" issues de la mécanique de la rupture. Nous jugeons que ces méthodes sont mieux adaptées à la problématique des aubes de turbines hydroélectriques. Trois thèmes seront abordés: l'opération et le chargement, la tolérance au dommage puis la fiabilité. Ces thèmes correspondent aux aspects abordés dans les chapitres subséquents et permettront de mettre en perspective les travaux de recherche effectués dans le cadre de cette thèse.

Opération et chargement

Le profil d'opération et le chargement peuvent être établis de plusieurs façons. Ceux-ci peuvent être définis par l'utilisation de données observées, par simulation à l'aide de modèles ou encore par une combinaison des deux approches. Lors du calcul de la fiabilité, les données d'opération et le chargement anticipé ont une influence significative sur les valeurs obtenues. En observant la séquence utilisée pour le calcul de la fiabilité à la Figure 0.2, on constate qu'une variation ou une incertitude sur les données d'opération se répercutera sur chaque étape du calcul de fiabilité. À ce titre, on distingue dans la littérature scientifique un effort important déployé par l'industrie aéronautique pour limiter cet impact. Une grande partie des efforts sont concentrés sur le développement de spectres standardisés pour le chargement (Heuler et Klatschke, 2005; Divenah et Beaufils, 2004; Potter et Watanabe, 1989; Bryan et Potter, 1980). Les spectres standardisés de chargement sont particulièrement utiles lors de la conception et pour la caracté-

risation des propriétés en fatigue, car ils permettent de prendre en considération un chargement réaliste, mais standard pour faciliter les comparaisons entre différents matériaux. Cependant, dans bien des cas, ils ne peuvent pas se substituer au chargement réel de la structure. Ceci est particulièrement vrai lors de la prédiction de la durée de vie anticipée. Notons, tel que répertorié par Heuler et Klatschke (2005), qu'au cours des 30 dernières années, des chargements standardisés ont été établis dans une large variété d'industries. En plus du secteur aéronautique, on observe des chargements standardisés dans l'industrie automobile, des éoliennes et des plateformes pétrolières. Cependant, dans l'industrie hydroélectrique, l'étude formelle des cycles d'opération réelle des centrales hydroélectriques s'avère un phénomène relativement récent dans la littérature (Yuanfang *et al.*, 2012). Par contre, une littérature importante traite des phénomènes hydrauliques et vibratoires complexes générés par l'opération de celles-ci (Doerfler *et al.*, 2013; Naudascher et Rockwell, 1994).

En vue d'obtenir le chargement réel, il est possible de mesurer le chargement directement après la mise en service d'un équipement ou d'une structure. Cela éliminerait la problématique reliée à l'estimation de celui-ci. Par contre, le processus n'est pas si simple à réaliser. Pour utiliser les données ainsi obtenues, les signaux doivent être décomposés en cycles de chargement simples pour être exploités dans l'évaluation de la durée de vie en fatigue (ASTM Standard E1049, 2011). La méthode la plus couramment utilisée pour effectuer cette décomposition pour un signal complexe est l'algorithme du "Rainflow" (Anthes, 1997; Rychlik, 1996, 1993, 1987). Par la suite, l'historique de chargement est généralement simplifié pour éliminer les cycles de chargement causant peu ou pas de dommage. Donc, en plus d'extraire les cycles de chargement mesurés, il est nécessaire de les classer selon le dommage induit. Par exemple, tel qu'effectué par Xiong et Shenoi (2008), on peut caractériser et discriminer les cycles de chargement en les classant selon qu'ils soient principaux, secondaires ou porteurs.

Malgré qu'il soit possible de mesurer et caractériser le chargement sur un intervalle de temps donné, en général celui-ci ne se reproduit jamais de façon identique. En fait, pour des chargements observés dans les mêmes conditions sur des périodes similaire mais à des moments différents, on constate une variabilité qui peut souvent être significative. Si la période d'obser-

vation est relativement courte, cette variabilité devient difficile à quantifier. Donc, même si le chargement réel est disponible, il est nécessaire de le modéliser sous la forme d'un processus aléatoire en vue d'estimer le chargement sur une période plus longue. Pour ce faire, les paramètres du processus aléatoire sont alors estimés à partir des données observées sur un intervalle de temps disponible pour ensuite être utilisés dans la simulation du chargement sur l'intervalle désiré. À ce titre, deux principales familles de méthodes se distinguent pour l'extrapolation de signaux: les méthodes qui effectuent l'extrapolation dans le domaine temporel et celles qui effectuent celle-ci dans le domaine du "Rainflow" ou de Markov. Les résultats obtenus avec les deux familles de méthodes ont été comparés pour des cas particuliers par Carboni *et al.* (2008) et par Cerrini *et al.* (2006). Notons que la différence principale entre le domaine de Markov et celui du "Rainflow" est la possibilité de distinguer les transitions vers un maximum des transitions vers un minimum, et ce, pour chacun des cycles de chargement. Cependant, peu importe que l'on passe dans le domaine de Markov ou du "Rainflow", une partie de l'information contenue dans le signal temporel original est perdue et uniquement des blocs de chargement équivalent peuvent être générés par la suite dans le domaine temporel à partir des informations détenues.

Les méthodes d'extrapolation utilisées dans le domaine temporel consistent à répéter autant de fois que nécessaire un bloc de chargement tout en permettant aux amplitudes de "varier" par rapport à des valeurs de référence. Ces variations peuvent être modélisées statistiquement en fonction de la théorie des valeurs extrêmes (Johannesson, 2006), à l'aide de réseaux neuronaux (Klemenc et Fajdiga, 2002) ou à l'aide de modèles de simulation stochastiques (Kareem, 2008; Gurley *et al.*, 1997). Ce type d'extrapolation permet d'éviter les difficultés reliées à la perte d'information telle que la séquence des cycles de chargement rencontrée avec les méthodes opérant dans le domaine du "Rainflow" ou de Markov.

D'un autre côté, dans le domaine du "Rainflow" ou de Markov, même si la séquence exacte de chargement n'est pas explicitement conservée, il est toutefois possible de la simuler (Rychlik, 1996) et de retourner dans le domaine temporel. Les méthodes d'extrapolation de ce type consistent à convertir l'histogramme obtenu à partir des données observées en une densité de

probabilité à partir de laquelle de nouveaux histogrammes sont générés à volonté (Klemenc et Fajdiga, 2008; Socie, 2001; Klemenc et Fajdiga, 2004; Nagode *et al.*, 2001; Klemenc et Fajdiga, 2000; Nagode et Fajdiga, 1999; Johannesson, 1999). Notons que la modélisation adéquate des zones de l'histogramme qui comportent peu de points constitue une des difficultés principales de cette approche (Socie et Pompetzki, 2004).

D'autres méthodes, telles que les réseaux neuronaux, ont démontré, en plus de l'extrapolation, la possibilité de générer des chargements pour des conditions d'opération non observées à partir des données provenant de conditions d'opération observées (Klemenc et Fajdiga, 2006, 2005). On note aussi certains phénomènes qui peuvent être modélisés comme un renouvellement de processus intermittents (Sykora, 2006). Plus spécifiquement, dans le cas de l'opération des centrales hydrauliques, Szczota *et al.* (2011) ont démontré que la séquence d'opération peut être extrapolée en utilisant des modèles semi-Markoviens et que ceux-ci offrent une meilleure flexibilité que les modèles Markoviens traditionnels.

Fatigue et mécanique de la rupture

Le calcul de l'endommagement en fatigue par des approches basées sur la mécanique de la rupture utilise la vitesse avec laquelle les défauts déjà présents dans la structure se propagent pour en estimer la durée de vie. Avec ces méthodes, il est essentiel de considérer l'hypothèse fondamentale de la présence d'un défaut initial, mesurable ou non, dans la structure. Ce type d'approches constitue la base du concept de tolérance au dommage. L'endommagement est alors défini en fonction de la taille des défauts qui sont généralement considérés comme des fissures. Puis, à l'aide de la courbe de propagation qui représente la vitesse de propagation des fissures en fonction du facteur d'intensité de contrainte telle que présentée à la Figure 0.4, il est possible d'estimer la progression de celles-ci. Sur ce diagramme, le paramètre da/dN correspond à la vitesse de propagation d'une fissure longue, a est la longueur de la fissure, N est le nombre de cycles et ΔK est la variation du facteur d'intensité de contrainte qui est fonction de la dimension du défaut combiné au chargement. On distingue trois régions principales sur ce diagramme. La première région est caractérisée par un seuil ΔK_{th} défini comme la variation minimale d'intensité de contrainte pour faire progresser la fissure. Ensuite, on observe une

région où la vitesse augmente linéairement (région de Paris). Finalement, il y a une région où la vitesse augmente exponentiellement et qui correspond à la rupture (Schijve, 2003; Hu *et al.*, 2006).

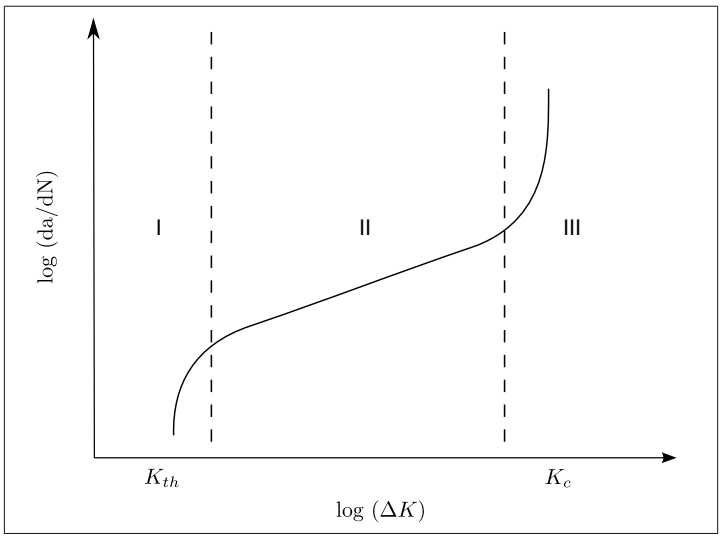

Figure 0.4 Diagramme de propagation de fissure

Cependant, la vitesse de propagation da/dN est estimée empiriquement à partir de valeurs mesurées qui comportent une certaine dispersion. Donc, en plus de la valeur estimée, l'incertitude autour de celle-ci nécessite d'être quantifiée lorsque des modèles probabilistes sont utilisés. Une vaste gamme de modèles probabilistes sont disponibles pour la modélisation de la propagation de fissures. Par contre, on recommande souvent d'utiliser initialement des modèles simples pour ensuite, au besoin, utiliser des modèles plus complexes si les données le prescrivent (Wu et Ni, 2007, 2004, 2003). Classiquement, le diagramme de propagation tel que présenté à la Figure 0.4 est construit avec des données obtenues pour des ΔK constants, contrairement au chargement réel qui comporte souvent des cycles d'amplitude variables. Il s'en suit que des interactions entre les cycles d'amplitudes différentes peuvent survenir et nécessiter d'être modélisées (Skorupa, 1998). Par exemple, les cycles de grandes amplitudes et les cycles de faibles amplitudes peuvent dans certains cas ne pas partager le même seuil d'intensité minimale de contrainte ΔK_{th} (Nicholas, 2006; Byrne *et al.*, 2003). Ceci peut générer

un biais significatif entre la propagation estimée et la propagation observée, si ces interactions ne sont pas correctement prises en compte.

Fiabilité

Tel que mentionné précédemment, la notion de fiabilité correspond à la probabilité qu'un dispositif accomplisse une fonction dans des conditions données pendant une durée spécifiée (IEEE, 1990). Lorsque l'on parle de fiabilité en fatigue, celle-ci est reliée à la probabilité qu'une fissure de longueur donnée ne soit pas présente après un certain nombre d'évènements. Tel que présenté à la Figure 0.5, cette probabilité peut être calculée soit en termes de longueur de fissure à un instant donné ou soit en termes de nombre de cycles de contrainte (ou blocs de chargement) pour atteindre une longueur de fissure donnée. Le type de représentation utilisée à la Figure 0.5 est appelé modèle de dégradation, comparativement au modèle de survie, traditionnellement utilisé en fiabilité. On note que dans la littérature scientifique l'intérêt pour l'effet de la fatigue des matériaux sur la fiabilité, la maintenance et la disponibilité n'est pas récent. Par exemple, on constate que dans les années 80, on s'intéressait aux mêmes problématiques qu'aujourd'hui (Bloom et Ekvall, 1983). Ces problématiques sont: l'utilisation des données mesurées *in situ*, la dispersion des résultats expérimentaux de propagation de fissure, l'incertitude des modèles, les techniques de détection des fissures et l'influence des données d'inspection sur les paramètres du modèle.

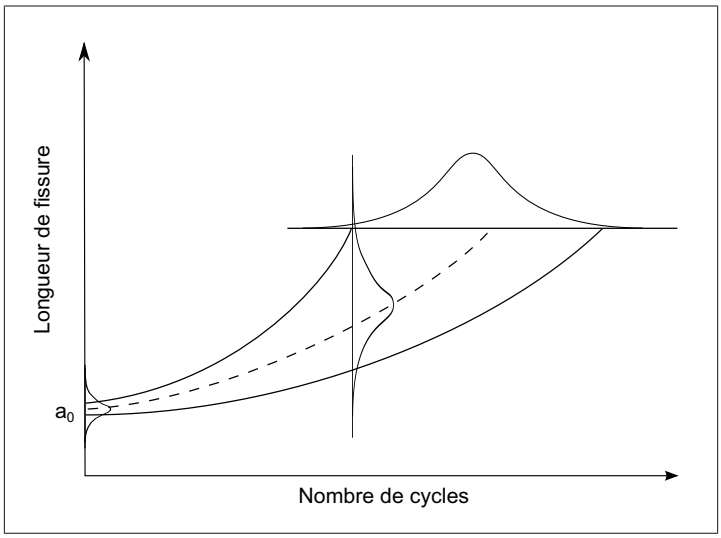

Figure 0.5 Approche probabiliste en propagation de fissure

L'industrie aéronautique, particulièrement dans le domaine militaire, est au premier plan des développements scientifiques dans le domaine de la fiabilité en fatigue (Kappas, 2002). On retrouve également plusieurs travaux pour les structures en mer (Chryssanthopoulos et Righiniotis, 2006), dans l'industrie automobile (Genet, 2006), au niveau des éoliennes (Lange, 1996) et même au niveau des composantes de vélos (Tovo, 2001; Ellens *et al.*, 1997). Une des principales difficultés du calcul de la fiabilité est le choix des modèles et méthodologies de calcul utilisées (Cross *et al.*, 2006). Cela comprend aussi des difficultés reliées aux implications des hypothèses utilisées pour quantifier l'incertitude des paramètres ainsi que la fiabilité elle-même. Par exemple, le fait d'ignorer de possibles corrélations entre les paramètres peut engendrer des erreurs majeures (Annis, 2004). Malgré les similitudes entre les méthodologies utilisées, il n'y a présentement aucune méthodologie unique et universelle répertoriée dans la littérature puisque chaque domaine d'application possède ses propres particularités. Par exemple, le fait d'utiliser des approximations de premier ordre ou de second ordre (FORM/-SORM) simplifie le calcul, mais restreint la possibilité d'utiliser certains modèles numériques avec une précision adéquate. D'un autre côté, l'utilisation de simulations de type Monte-Carlo offre une plus grande flexibilité mais comporte le risque de nécessiter un nombre d'itérations souvent prohibitif pour obtenir des résultats satisfaisants dans les zones de faibles probabilités.

De plus, il ne faut pas négliger l'impact que peut avoir la mise à jour de l'information détenue *a priori* par des données obtenues *a posteriori* sur la précision des valeurs estimées. Les méthodes traditionnelles de calcul de fiabilité utilisent l'information disponible à un moment donné sans mettre à jour les informations détenues lors des calculs effectués précédemment (Ayala-Uraga et Moan, 2007; Chryssanthopoulos et Righiniotis, 2006). Dans la majorité des cas, l'incertitude associée aux paramètres initiaux est très grande, car l'information disponible initialement est limitée. Ce manque d'information rend les valeurs estimées très incertaines. Une solution consiste à utiliser les observations effectuées *a posteriori* pour mettre à jour les valeurs estimées *a priori* (Wang *et al.*, 2009). On qualifie ce type d'approche de bayésienne. Les approches bayésiennes permettent d'utiliser les informations au fur et à mesure de leur disponibilité pour consolider les hypothèses de départ ou pour valider le modèle. Dans le cas des aubes de turbines hydroélectriques, les inspections périodiques sont notre principale source d'information *a posteriori*. Celles-ci servent à définir les paramètres reliés aux défauts présents dans la structure. Potentiellement, les inspections peuvent permettre d'estimer la distribution des défauts tant au niveau de leur localisation que de leur dimension. Signalons que l'incertitude sur la dimension des défauts présents dans un matériau représente à elle seule un domaine de recherche important (Altamura et Beretta, 2012; Liu et Mahadevan, 2009; Liao, 2009; Sharpe *et al.*, 2004). Ce paramètre a une influence directe sur les conditions initiales des approches de type tolérance au dommage. En d'autres termes, l'utilisation d'approches bayésiennes peut, en plus de la calibration des conditions initiales, permettre la validation des modèles à chaque instant où une nouvelle information devient disponible sur la structure étudiée (Sankararaman *et al.*, 2011).

Conclusion

La revue de la littérature a permis de couvrir divers aspects de la fiabilité dans une optique de tolérance au dommage. Nous avons présenté une perspective générale de la littérature sur la fiabilité en fatigue en couvrant les principaux domaines d'application de celle-ci. Les aspects plus spécifiques reliés à l'application de ces méthodes aux turbines hydroélectriques seront couverts à l'intérieur des chapitres subséquents. Le large éventail de littérature disponible sur

la fiabilité en fatigue permet de constater que la problématique n'est pas exclusive aux turbines hydroélectriques et qu'elle est commune à plusieurs domaines d'application. La fiabilité en fatigue est un champ de recherche qui montre une intense activité dans plusieurs domaines d'application.

CHAPITRE 1

ON THE STOCHASTIC SIMULATION OF HYDROELECTRIC TURBINE BLADES TRANSIENT RESPONSE

Martin Gagnon[1], Antoine Tahan[1], Philippe Bocher[1], Denis Thibault[2]

[1] École de technologie supérieure (ÉTS), Montréal, Québec, H3C 1K3, Canada

[2] Institut de recherche d'Hydro-Québec (IREQ), Varennes, Québec, J3X 1S1, Canada

Article published in "Mechanical Systems and Signal Processing", Volume 32, October 2012, Pages 178–187, Uncertainties in Structural Dynamics

1.1 Abstract

This paper describes a methodology for the extrapolation of a single measured non-stationary time series to an expected long-term service history. Within the context of limited data availability, stochastic simulation is used to generate an ensemble of surrogate realizations from which expected long-term service histories can be derived. Two non-stationary stochastic simulation algorithms are implemented. Both simulation algorithms are compared using the transient response measured on hydroelectric turbine blades during startup. In both algorithms, an independent random phase shift is introduced in the analytic signal given by the Hilbert transform of each time series subcomponent. The subcomponents are obtained either by Empirical Mode Decomposition (EMD) or by Stationary Wavelet Decomposition (SWD). The simulated realizations will invariably include some inherent variations arising from the process itself, combined with epistemic uncertainty due to the assumptions made during modeling. To ensure the quality of the simulated realizations, the following quantitative criteria are used to compare the simulated ensemble to the reference data: cumulative energy, extreme value distribution and rainflow amplitude spectra.

1.2 Introduction

Reliable prediction of structural component fatigue life depends mostly on the proper assessment of damaging events severity and variability during the expected service life. The cost of *in situ* measurement and the limited time period over which some structures can be monitored often render the extrapolation of the available data difficult. The extrapolation methods generally used for fatigue analysis involve statistical modeling of the rainflow amplitude histogram, in which rainflow amplitude histograms are randomly generated using kernel smoothing to convert a reference rainflow histogram to a probability distribution (Dressler *et al.*, 1996; Socie, 2001; Socie et Pompetzki, 2004). Other known methods involve the use of extreme value theory (Johannesson et Thomas, 2001; Johannesson, 2006) or neural network (Klemenc et Fajdiga, 2006, 2005, 2002). The main drawback of these approaches is the need for a large number of measured realizations in order to construct the underlying statistical model.

In structures such as hydroelectric Francis turbine runners, sometimes only a single recorded occurrence of a given transient event is available. Due to time limitations, key events such as runner startup, load rejection or shutdown are often measured only once. Knowing that some of these events account for most of the damage sustained by the structure during its expected life (Gagnon *et al.*, 2010a,b), proper simulation tools are needed in order to build realistic long-term service histories. In this paper, we propose the use of non-stationary stochastic modeling for the simulation of the strain response of Francis turbine runner blades during startup. Two methodologies are investigated: the first, developed by Wang (Wang, 2007), is characterized by the use of Stationary Wavelet Decomposition (SWD), and the second, developed by Wen and Gu (Wen et Gu, 2004, 2005), is characterized by the use of Empirical Mode Decomposition (EMD). In both of these methodologies, the signal is generated using a random phase shift between the analytical signal representation for each subcomponent of the signal. These two methods were initially developed for earthquake and wind loading simulations. We intend to investigate their applicability to rotating machinery such as hydroelectric turbines. The simulated realizations will be evaluated using signal energy, extreme value distribution and rainflow amplitude histogram as quantitative criteria. Both the extreme value distribution

and the rainflow amplitude histogram have been chosen for their relevance in fatigue analysis ; signal energy was chosen as a global indicator of simulation quality.

This paper is organized as follows: first, simulation methodologies and theoretical background are described. Then, measured transient response data are presented, followed by an overview of the quantitative criteria. Finally the results and their implications are discussed. The paper concludes by discussing the applicability of the proposed stochastic model for simulating of transient responses observed in rotating machinery.

1.3 Simulation Methods

Although simulation methods based on stationary processes are widely used and well developed (Grigoriu, 1995), difficulties arise when one needs to construct a stochastic simulation model for the transient events often encountered in physical processes. Many non-stationary simulation methods have been developed based on modulated processes, which were first introduced by Priestly (Priestley, 1965) using the concept of evolutionary power spectra. These methods requires strong assumptions on the parametric form of the modulating function, ergodicity or the piecewise stationarity of the process in order to estimate model parameters. Among the simulation methods cited by Kareem (Kareem, 2008) in his review of the numerical simulation of wind, the method proposed by Wang (Wang, 2007) possesses characteristics which may alleviate some of the difficulties posed by model parameters estimation. In the method developed by Wang (Wang, 2007), the parameters estimation process is simplified by using the Hilbert transform, which requires fewer assumptions. The method combines SWD and the Hilbert transform to simulate earthquakes and down burst wind records from a single observed realization. The approach is similar to the method developed by Wen and Gu (Wen et Gu, 2005, 2004), which uses EMD instead of SWD for earthquake simulation. Both methods have been shown to provide good results using earthquake ground motion records. Because the methodology does not rely on physical models, it has the potential for application to any non-stationary process. This characteristic is essential for the simulation of transient events for which physical models are unavailable, or where parameters are difficult to obtain given the limited number of realizations available.

In both methods, the stochastic process is modeled as follows:

$$\hat{X}(t) = Re\left[\sum_{j=1}^{N} A_j(t)\, e^{i\left(\phi_j + \int w_j(t)\, dt\right)}\right] + r_N(t) \tag{1.1}$$

in which A_j is the instantaneous amplitude for a given level j ; ϕ_j is the phase shift for level j ; $w_j(t)$ is the instantaneous frequencies and $r_N(t)$ is the residue. The model is the sum of a set of subcomponents and a residue. To obtain the random process $\hat{X}(t)$, an independent random phase shift between 0 and 2π is introduced in each subcomponent analytical signal.

The subcomponents can be obtained by using either SWD or EMD, depending on the algorithm chosen. The SWD acts as a dyadic filter bank which decomposes the signal into the following:

$$X(t) = \sum_{j=1}^{N} D_j(t) \; + A_N(t) \tag{1.2}$$

with $D_j(t)$ as the detail function at level j and $A_N(t)$ the approximation at level N which is the resulting trend of $X(t)$. Complete mathematical details and the procedure required for obtaining the detail function $D_j(t)$ and approximation $A_N(t)$ of Eq. (1.2) are available in (Percival et Walden, 2000).

The EMD algorithm, on the other hand, is an iterative process in which decomposition levels are adapted to match a given set of conditions. In EMD, each decomposition level must satisfy two conditions:

a. The number of extrema and the number of zero crossings must either equal or differ by one over the whole signal.

b. The mean value of the envelope defined by the local maxima and the envelope defined by the local minima should be zero at any point in the signal.

A signal that satisfies both conditions is called an Intrinsic Mode Function (IMF). An IMF is expected to be monocomponent, with both locally zero mean and symmetric envelope. The

iterative nature of the EMD algorithm means that the IMFs will be adapted to the nature of the signal, going from fine to coarse scale, and that the solution might not be unique. The solution for a given set of stopping and convergence criteria is represented as follows:

$$X(t) = \sum_{j=1}^{N} C_j(t) + r_N(t) \tag{1.3}$$

in which $C_j(t)$ is the IMF at level j and $r_N(t)$ is the residue of the decomposition. Complete mathematical details and procedures are available in (Huang *et al.*, 1998).

In Eqs. (1.2) and (1.3), we observe that similar representations are obtained. Furthermore, in some specific cases, identical results might be obtained regardless of the decomposition method used. As an example, it was demonstrated that both the SWD and EMD act as dyadic filter banks for white noise and Gaussian fractional processes (Flandrin *et al.*, 2004; Wu et Huang, 2004). More complex implementations are often needed, however, in order to obtain similar decomposition characteristics. Wu and Wang (Wu et Huang, 2009) developed the Ensemble Empirical Mode Decomposition (EEMD) to ensure that the EMD acts in a dyadic manner and to avoid possible mode mixing. Likewise, Olhede and Walden (Olhede et Walden, 2004, 2005) have shown that by using more complex wavelet decomposition algorithms, adaptiveness similar to that of EMD can be obtained.

Next, each subcomponent must be transformed into an analytic signal. The analytic signal is obtained using the Hilbert transform, defined as:

$$H(t) = \frac{1}{\pi} P \int_{-\infty}^{\infty} \frac{X(\tau)}{t - \tau}\, d\tau \tag{1.4}$$

where P is the Cauchy principle and $X(t)$ the untransformed signal. Note that the Hilbert transform represents the convolution of $X(t)$ with $1/\pi t$ resulting in a phase shift of $\pi/2$. $X(t)$ and $H(t)$ form complex conjugate pair which results in an analytic signal $X_a(t)$ expressed as follows:

$$X_a(t) = X(t) + iH(t) = A(t)\, e^{i\theta(t)} \tag{1.5}$$

in which the instantaneous amplitude $A(t)$ and the instantaneous phase $\theta(t)$ are obtained with:

$$A(t) = \sqrt{X(t)^2 + H(t)^2} \tag{1.6}$$

$$\theta(t) = \arctan \frac{H(t)}{X(t)} \tag{1.7}$$

The instantaneous phase $\theta(t)$ can be expressed as

$$\theta(t) = \phi + \int \omega(t)\, dt \tag{1.8}$$

$$\omega(t) = \frac{d\,\theta(t)}{dt} \tag{1.9}$$

in which ϕ is the initial phase and $\omega(t)$ is the instantaneous frequency.

One important characteristic of the Hilbert transform is the set of conditions imposed on the signal for proper separation of envelope $A(t)$ from its carrier $e^{i\theta(t)}$, as expressed in the following:

$$H\left\{A(t)\, cos\, \theta(t)\right\} = A(t)\, H\left\{cos\, \theta(t)\right\} \tag{1.10}$$

The conditions are summarized by the Bedrosian (Bedrosian, 1963) and Nuttall (Nuttall, 1966) theorems. Bedrosian (Bedrosian, 1963) established that in order for Eq. (1.10) to be true, the Fourier spectra of envelope $A(t)$ and carrier $cos\, \theta(t)$ should be non-overlapping. In addition to the Bedrosian (Bedrosian, 1963) theorem, Nuttall (Nuttall, 1966) established the necessary condition under which the Hilbert transform represents the quadrature signal which sets uncertainty on its instantaneous frequencies. We would like to note that Huang and Wu (Huang *et al.*, 2009) have developed methods for circumventing some of the difficulties posed by both theorems. However, the Hilbert transform was chosen in this study for its simplicity. As a result, some numerical artefacts are expected, since none of the conditions imposed by the cited theorems are enforced by either of the decomposition methods used.

1.4 Transient Response Data

In situ measurements made by Hydro-Québec in summer 2002 at the Beauharnois hydroelectric power plant were used to obtain measured strain response during runner startup. The Beauharnois facility is a low head run-of-the-river power plant located in Quebec, Canada. During the *in situ* measurements, one of the plant's Francis turbine runners was instrumented with strain gauges at critical locations on two blades. Only the location where maximum dynamic amplitudes were expected was used in this study. The strain gauges were located in a cutout near the runner's crown, as shown in Figure 1.1.

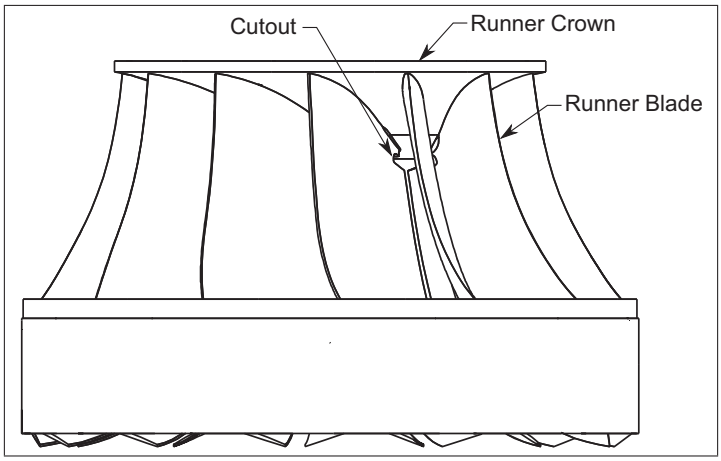

Figure 1.1 Francis runner diagram showing the measurement locations used

The data obtained from two similar startups were selected for this study. The two startups shared nearly identical wicket gate opening rates and plant operating parameters, which leads to the assumption that both startups could arise from the same stochastic process. However, neither of the blade measurements are expected to arise of the same stochastic process due to variations in blade geometries, gauge position, calibration and measurement error. These assumptions were not enforced in simulation algorithm. Results were obtained independently for each dataset. We expected the simulation results to corroborate our preliminary assumptions. The measured strains for both startups and both blades are shown in Figure 1.2.

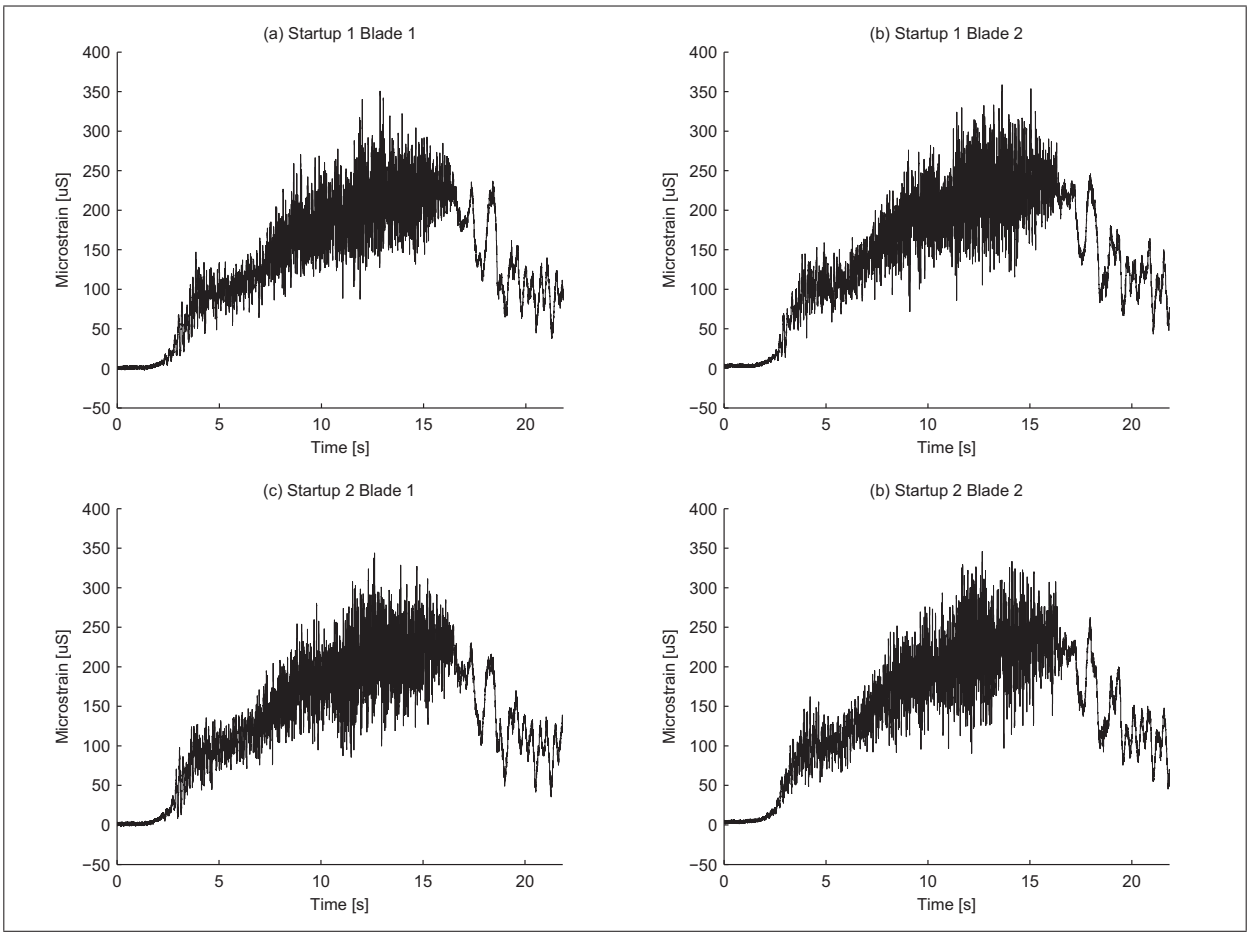

Figure 1.2 Measured strain history datasets

The time series for each dataset appear to be similar. They are characterized by one large overall strain cycle, followed by a few intermediate-amplitude strain cycles and many low-amplitude cycles. This becomes more obvious after the time series is rainflow counted, as shown in Figure 1.3. In Figure 1.3, we observe one large amplitude deformation cycle that is well separated from the others. This deformation cycle was generated by the maximum value of the time series and would cause most of the fatigue damage.

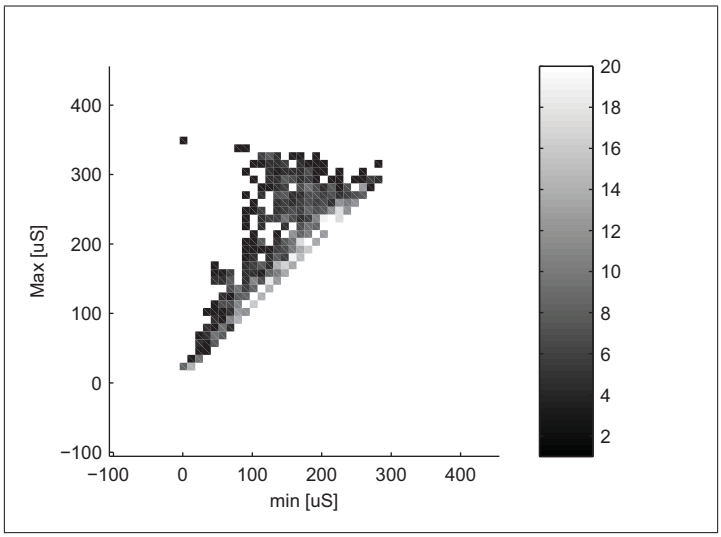

Figure 1.3 Rainflow results for dataset Startup 1 Blade 1

1.5 Comparison Criteria

We limited our study to three simulation quality indicators. The first comparison criterion is a quality indicator related to signal amplitude. This criterion is defined for continuous signal as:

$$E = \int_{\infty}^{\infty} |f(t)|^2 dt \tag{1.11}$$

in which E is the time series total energy and $f(t)$ is the time series. The distribution of total energy for an ensemble of simulated time series should include the energy level of the original time series. A significant discrepancy would mean that part of the time series amplitudes as been either over- or under-evaluated.

The second criterion is also related to the signal amplitude, but limited to extreme values. Given that the time series maximum value generates most of the fatigue damage, the extremes of the ensemble of simulated results are compared to the maximum value of the original time series. As with total energy, the original time series maximum value should be highly probable, and the ensemble distribution should also include values from every measured time series that is expected to arise from the stochastic process.

Lastly, the ensemble of simulated amplitude spectra was compared to the original amplitude spectra. We expect the ensemble of simulated spectra to include the spectrum from the original dataset without excessive discrepancy. The amplitude spectra for our four measured datasets are shown in Figure 1.4.

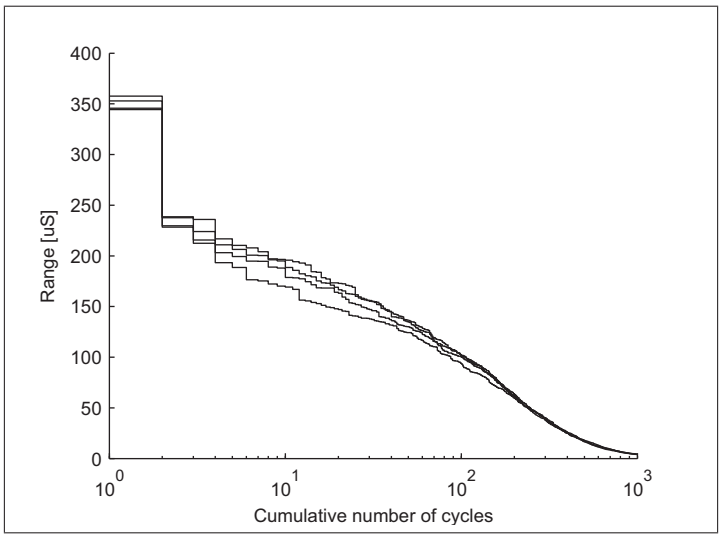

Figure 1.4 Measured amplitude spectra for the four datasets

1.6 Simulation Results

The SWD-based simulation method was the first to be implemented. An example of simulated signal using ten decomposition levels for blade one of the first startup is shown in Figure 1.5. Here we observe good overall shape agreement, but a side-by-side comparison reveals a slightly lower vibration amplitude over the entire length of the time series.

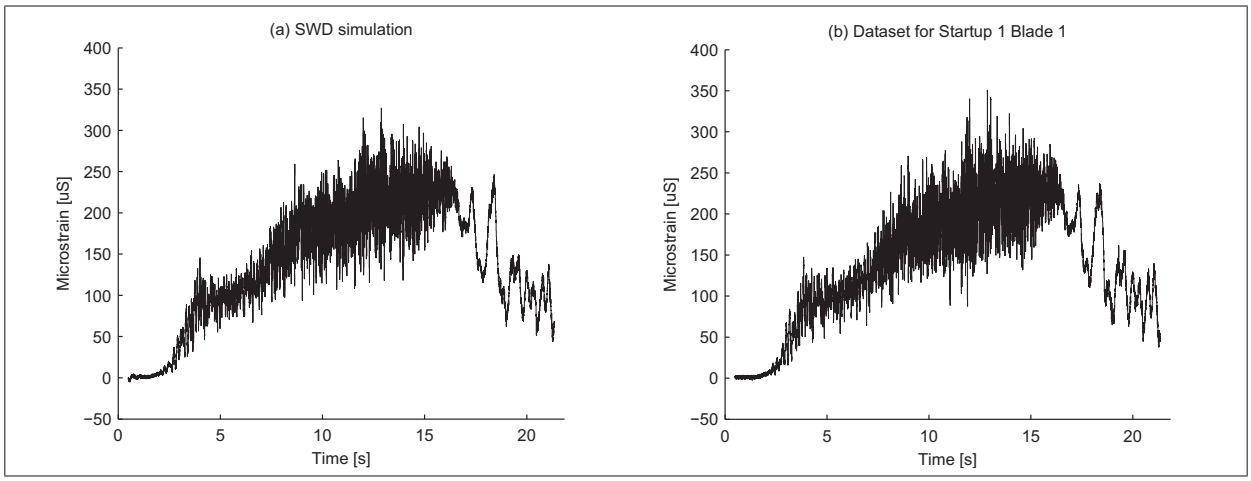

Figure 1.5 Simulated realization using the SWD method for dataset Startup 1 Blade 1

A comparison of the first two criteria is shown in Figure 1.6, using two hundred simulated realizations. In this figure, the dashed line represents the expected value from the original dataset. We observe that all the simulated realizations using the SWD method have signal energy that are below the dataset used to build the model. Furthermore, the extreme value distribution barely includes the value of the original data.

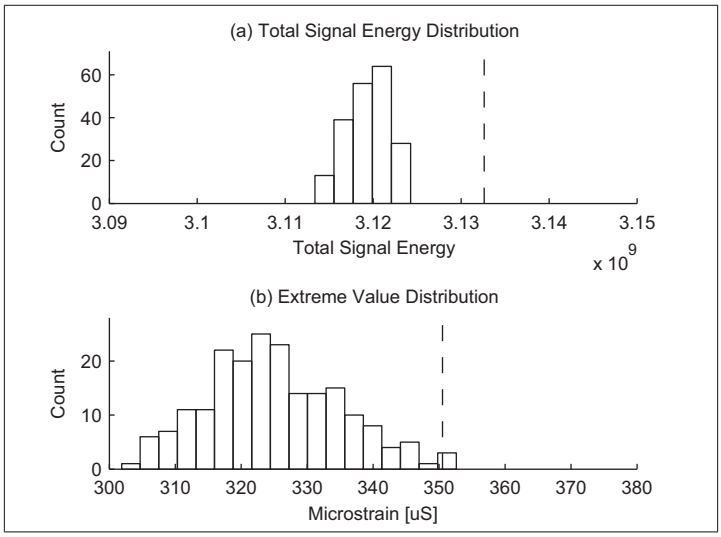

Figure 1.6 Energy and extreme value distribution obtained using the SWD method for dataset Startup 1 Blade 1

A comparison of the simulated amplitude spectra with the original dataset is shown in Figure 1.7. The lower signal energy observed in Figure 1.6 is corroborated by the lower amplitudes observed across the whole spectrum. Notice that for clarity, only five simulations have been shown.

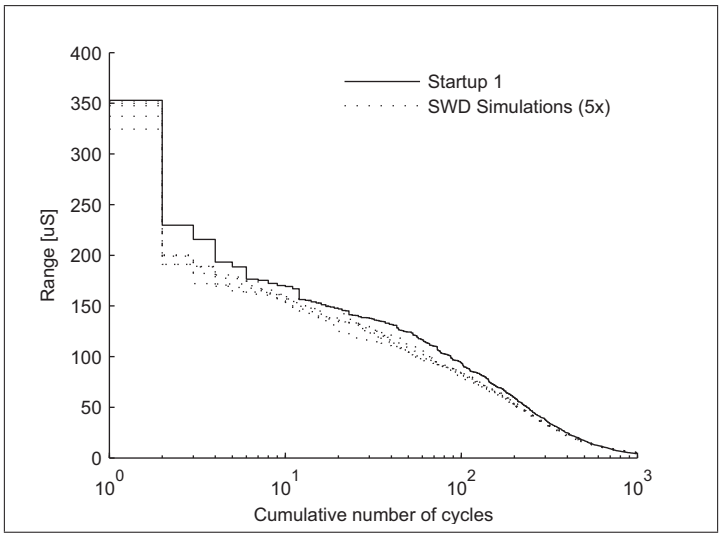

Figure 1.7 Simulated spectra obtained with the SWD method for dataset Startup 1 Blade 1

Next, the EMD-based simulation method was applied to the same dataset. Figure 1.8 shows the results from one simulation using ten decomposition levels, as was done with the SWD simulation method. We observe that both the shape and amplitude of the simulated signal are similar to those of the original dataset.

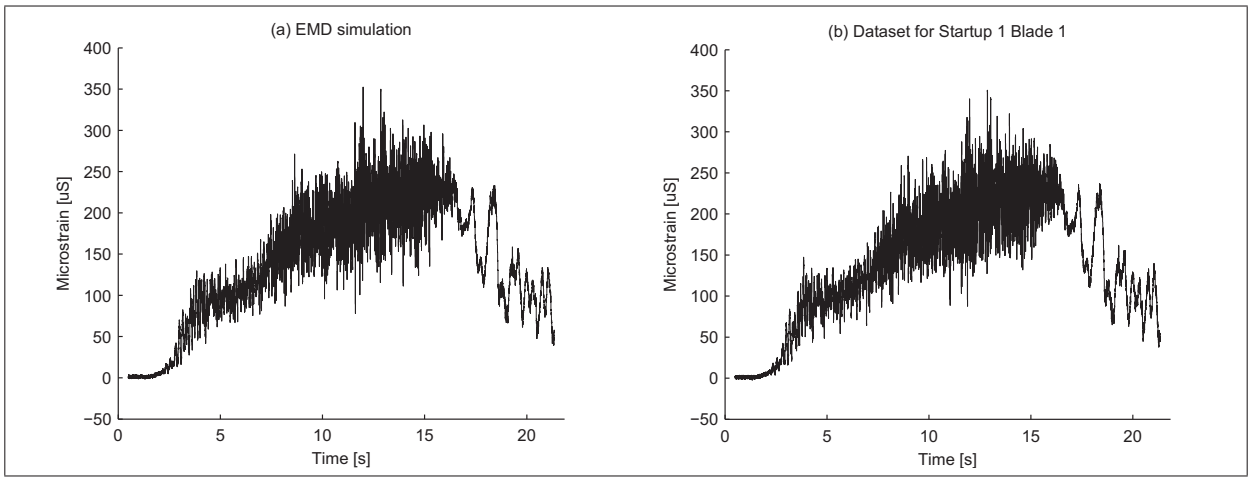

Figure 1.8 Simulated realization using the EMD method for dataset Startup 1 Blade 1

The results of two hundred simulation realizations using the EMD method are shown in Figure 1.9. Better agreement is observed between the simulated realizations and the original dataset, when compared with the SWD realizations in Figure 1.5. While the distribution of simulated signal energy and extreme values includes the value from the original data, we observe that the median is relatively far from the expected value for this dataset.

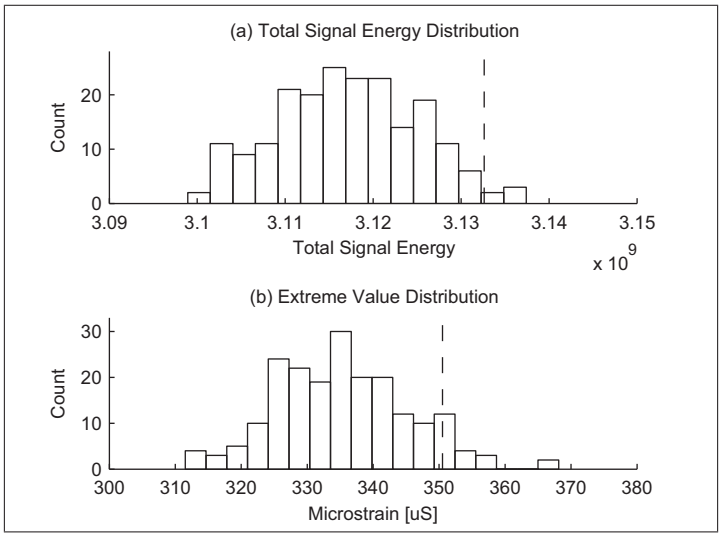

Figure 1.9 Energy and extreme value distribution obtained using the EMD method for dataset Startup 1 Blade 1

The amplitude spectra from five simulation realizations are compared to the original dataset in Figure 1.10. Good agreement with the original signal is observed, even though in some areas of the spectrum, amplitudes tend to be slightly lower than the original data. The lower simulated amplitude areas corroborates the discrepancy observed in Figure 1.9.

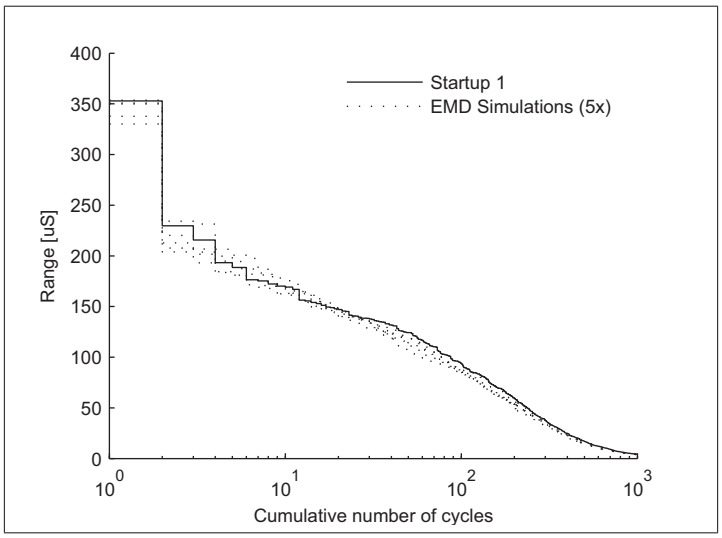

Figure 1.10 Simulated spectra obtained with the EMD method for dataset Startup 1 Blade 1

The simulated extreme value results obtained from each dataset are compared in Figure 1.11. Overall, the EMD method performed significantly better than anticipated, based on the results from the first dataset presented in Figure 1.9. These results support the preliminary assumption that the startups might be similar enough to be considered as arising from the same stochastic process. We observed that for both startups, distribution modes are similar for measurements on the same blade. On the other hand, both blades exhibit dissimilar distribution modes and shapes. These discrepancies might be explained by differences in calibration, positioning and blade geometry, as predicted in our preliminary assumptions.

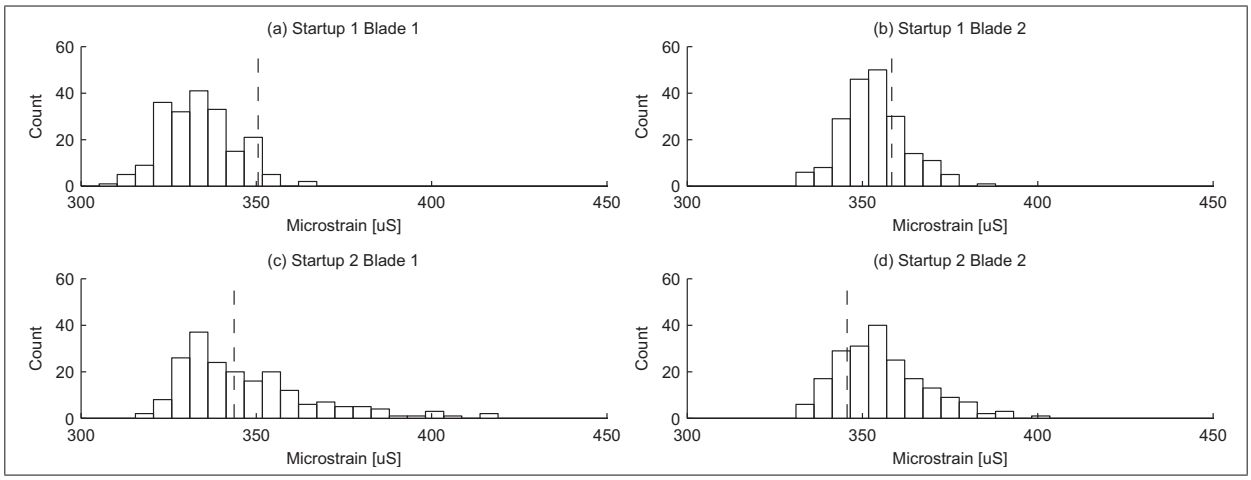

Figure 1.11 Comparison of the EMD extreme value distribution for the four datasets

1.7 Discussion

We observe that the SWD method tends to underestimate the amplitude spectra for our datasets. The results are characterized by lower simulated signal energy and extreme value amplitude, which can be explained by the Bedrosian theorem. Using the SWD method, the signal is split in an arbitrary dyadic fashion without constraint enforcing the monocomponent assumption or the condition dictated by the Bedrosian theorem. The proper separation of the carrier from its envelope cannot be assumed. With our datasets, the envelope obtained using the SWD method contains sharp changes which were in the same frequency range as the carrier. These sharp changes tend to occur around the local extremes in the detail functions. The extreme values associated with these sharp envelope changes then become rare events with the introduction of the random phase shift. These sharp envelope changes are spread nearly evenly over the signal length. Since the amplitude is underestimated evenly over the entire spectrum, we could adjust the amplitude from the simulated ensemble *a posteriori* in order to conform to our comparison criteria. However, this *a posteriori* correction would not remove either the signal distortion or artefacts introduced in the simulated time series.

The results obtained using EMD method show a better replication of the reference time series characteristic. The improvement comes mainly from the constraints used in the decomposition algorithm. Since, as for the SWD method, no constraints are imposed to conform to the

Bedrosian theorem, the results obtained with the datasets used in this study cannot be generalized for an arbitrary reference signal. A detailed analysis of the IMFs obtained using the EMD method shows that sharp envelope changes are still present, though less frequent than with the SWD method. The amplitude spectrum was not significantly affected by these distortions, which means that the method could in fact be used to derive long-term service histories without inducing significant bias in fatigue assessment. A side-by-side comparison of the realization obtained with SWD and EMD method is shown in Figure 1.12.

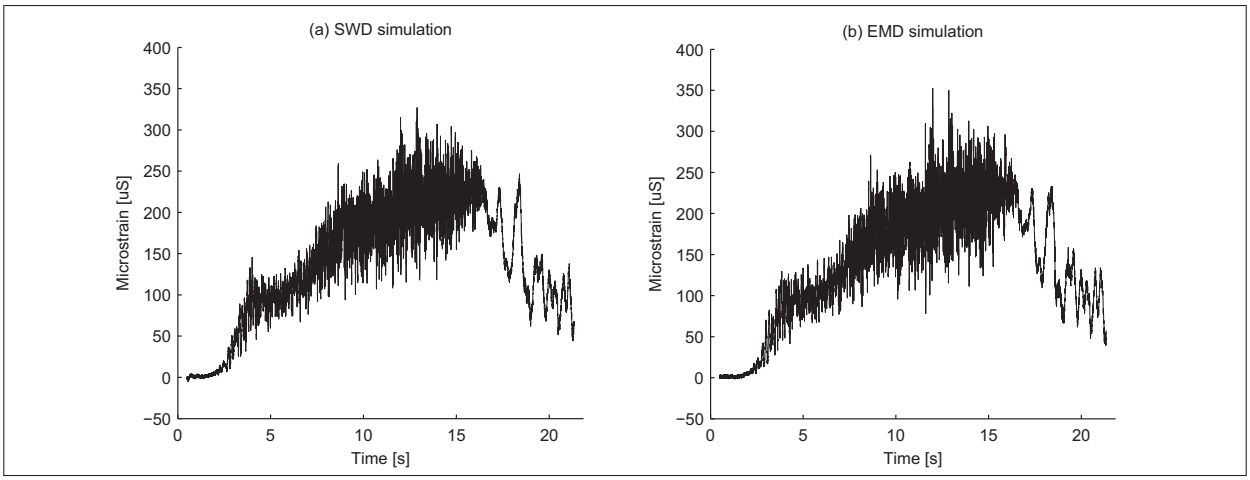

Figure 1.12 Side-by-side comparison of simulated realizations for dataset Startup 1 Blade 1

We note that neither decomposition method can ensure that the Bedrosian theorem will be respected. The quality of the stochastic process modeled using Eq. (1.1) by imposing a random phase shift is directly related to the ability of the Hilbert transform to separate the envelope from its carrier. Our results show superiority for the EMD method, but this is specific to the datasets used in this study. Hence, the choice of quality criteria is critical, as each application has different requirements. For fatigue analysis, any artefact or distortion that has no effect on the amplitude spectrum can be ignored, which might not be the case if the results are used as input for another type of model. Wavelet decomposition in general provides more rigorous mathematical development and physical uniqueness (Huang et Wu, 2008). These qualities might warrant the use of a wavelet-based decomposition method rather than the EMD, when applicable.

1.8 Conclusions

Our study has demonstrated that the extreme value characteristics and amplitude spectra generated using only one realization of a Francis turbine runner startup may be used to obtain long-term service histories. The stochastic simulation methods used in this study were initially developed for earthquake simulation (Wang, 2007; Wen et Gu, 2004, 2005). In these methods, the Hilbert transform is used to bypass the need for many of the assumptions and approximations needed to construct a model of the physical process. Given the complex nature of the dynamic behaviour of the runner during startup, and the small number of realizations available, the methods proved to be well adapted for our needs. Our results show that even when the physics of the problem are completely ignored, the necessary features for fatigue analysis and life assessment can be retained. Our study also highlights the need for careful results assessment when selecting the decomposition algorithm. Signal decomposition in subcomponents that are compatible with the Bedrosian theorem – which is an implicit assumption of the Hilbert transform – is not trivial. Our results show that with proper signal decomposition, the stochastic simulation model used in this study holds great potential for simulating transient events in large rotating machinery.

Acknowledgments

The authors would like to thank *Institut de recherche d'Hydro-Québec* (IREQ), the National Sciences and Engineering Research Council of Canadian (NSERC) and *École de technologie supérieure* (ÉTS) for their support and financial contribution.

CHAPITRE 2

A PROBABILISTIC MODEL FOR THE ONSET OF HIGH CYCLE FATIGUE (HCF) CRACK PROPAGATION: APPLICATION TO HYDROELECTRIC TURBINE RUNNER

Martin Gagnon[1], Antoine Tahan[1], Philippe Bocher[1], Denis Thibault[2]

[1] École de technologie supérieure (ÉTS), Montréal, Québec, H3C 1K3, Canada

[2] Institut de recherche d'Hydro-Québec (IREQ), Varennes, Québec, J3X 1S1, Canada

Article published in "International Journal of Fatigue", Volume 47, February 2013, Pages 300–307

2.1 Abstract

A fatigue reliability model for hydroelectric turbine runners is presented in this paper. In the proposed model, reliability is defined as the probability of not exceeding a threshold above which HCF contribute to crack propagation. In the context of combined LCF-HCF loading, the Kitagawa diagram is used as the limit state threshold. Two types of crack geometries are investigated: circular surface flaw and embedded flaw in a semi-infinite medium. The accuracy of FORM/SORM approximations was considered acceptable for engineering purpose in our application given the minimal numerical burden posed by such a method compared to Monte Carlo simulations. Our results show that the probability of an embedded flaw close to the surface has a major influence on reliability. Furthermore, we observe that the assumption that crack geometrical characteristics are independent leads to non-conservative results.

2.2 Introduction

The reliability assessment of structural components is often limited by our capacity to select relevant models and proper limit states. In structures, such as large Francis hydroelectric turbine runners, where the cost of downtime is high and *in situ* inspection methods are limited, cracks

often reach a detectable size only after the onset of High Cycle Fatigue (HCF). Furthermore, because large Francis runners can sustain significant amount of damage without incurring safety issues, the main concerns are repair cost and downtime. Hence, a crack must be repaired as soon as possible in order to minimize the cost of repair and concurrently the time between inspections must be maximized to reduce downtime. This leads to the following dilemma: if the HCF onset has occurred, longer time between inspection leads to longer cracks to repair ; yet, if the component is inspected before the HCF onset, we incur downtime and maintenance costs with limited information on the state of the structure because the detectable flaw size is not reached. Therefore, we propose to move away from the typical fatigue limit, as commonly seen in SN curve and critical crack length, which do not adequately reflect this reality, in favour of a limit state directly related to the HCF onset.

In this paper, the HCF is defined as the contribution to crack propagation by small amplitude stress cycles, leading to the rapid growth. In this case, the Low Cycle Fatigue (LCF) part of the loading is composed of the large amplitude stress cycles which contribute initially to the crack growth. These large amplitude cycles are less frequent than the small amplitude cycles of the HCF part of the loading. A schematic representation of an LCF+HCF combination is presented in Figure 2.1 (Byrne *et al.*, 2003). We observe, in Figure 2.2, that this representation is similar to the strain measured during a typical loading sequence if the startup phase of the sequence is neglected. The overall amplitude of the transient observed during the startup phase is directly related to the control scheme used (Gagnon *et al.*, 2010a, 2012a) and its impact on the runner reliability will not be investigated in this paper. For a typical hydroelectric turbine runner, we assume that the HCF will induce a rapid crack growth to a size above detection limits, which will then becomes proportional to HCF loading rather than to a limited number of transients LCF events. Notice that this definition is compatible with the one used in the review work done by Nicholas (Nicholas, 2006).

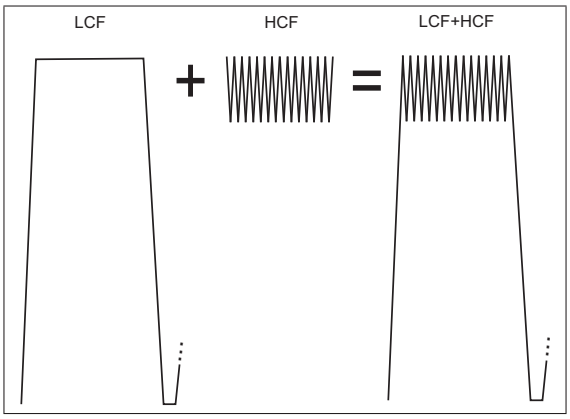

Figure 2.1 Schematic example of combined LCF+HCF loading

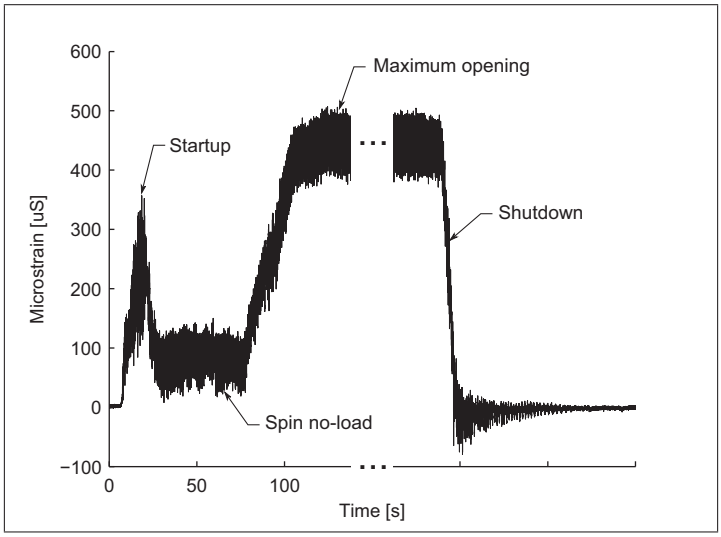

Figure 2.2 Example of loading measured on a large Francis runner

Reliability, for its part, is generally defined as: “The ability of a system or component to perform its required functions under stated conditions for a specified period of time" (IEEE, 1990). For a large Francis turbine runner, because cracks need to be repaired as soon as detected to minimize cost, the limit state for reliability becomes the onset of HCF crack propagation after which a flaw will rapidly become a detectable crack. The problem is illustrated in Figure 2.3 using British Standard BS7910:2005 (British Standards Institute, 2005) deterministic crack growth procedure and the loading presented in Figure 2.2 Gagnon *et al.* (2010a). The LCF

only curve represents the results for the loading with minimal time at the maximum opening condition and the HCF+LCF curve, on the other hand, includes 24hrs of operation time at this condition for each loading block. In this case, we observe that using any critical crack size above the HCF onset point could be almost equally acceptable but would hide the real limit state and would cloud our understanding of the reliability problem. Obviously, we have not accounted for stress gradient and other factors which would affect crack growth but this simple example illustrates the difficulty of assigning a arbitrary critical crack length when, in facts, the moment of interest is the HCF onset.

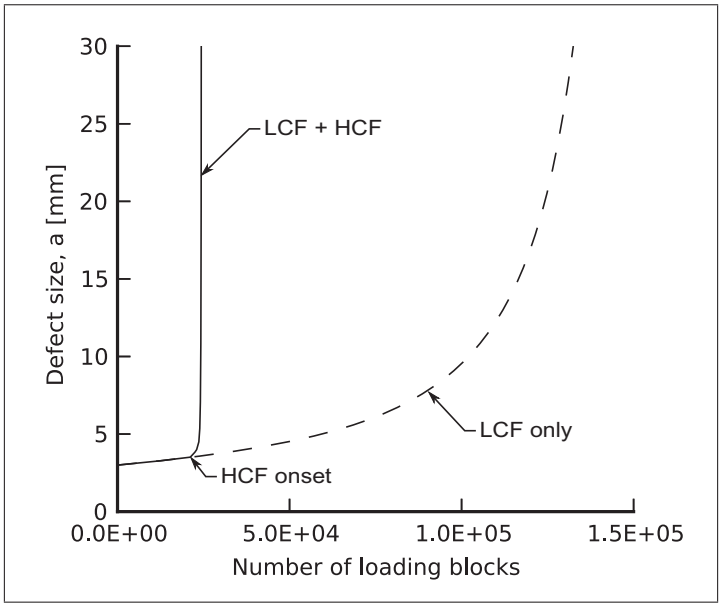

Figure 2.3 Deterministic crack growth exemple using Figure 2.2 loading

Kitagawa and Takahashi (Kitagawa et Takahashi, 1976) established that the threshold which differentiates a propagating from a non-propagating crack is characterized by at least two thresholds ; the first threshold is the stress intensity range for crack growth ΔK_{th} as defined by Linear Elastic Fracture Mechanics (LEFM), and the second threshold is the fatigue limit, which usually corresponds to 10^7 stress cycles for materials exhibiting an endurance limit. The limit state defined by Kitagawa and Takahashi (Kitagawa et Takahashi, 1976) can also be extended to include other parameters like notch effect (Atzori et Lazzarin, 2002) and multi-axial crite-

ria (Thieulot-Laure *et al.*, 2007). We refer the reader to the work of Atzori and Lazarin (Atzori *et al.*, 2003) for an overview of the experimental data available in the literature that support such limit. In the present study, the limit state for HCF is derived only from the thresholds established by Kitagawa and Takahashi (Kitagawa et Takahashi, 1976), combined with the correction factor developed by El Haddad et al. (El Haddad *et al.*, 1979), which accounts for short crack propagation. This limit state can be visualized on a two-dimensional diagram with defect size and stress range for axes, as shown in Figure 2.4.

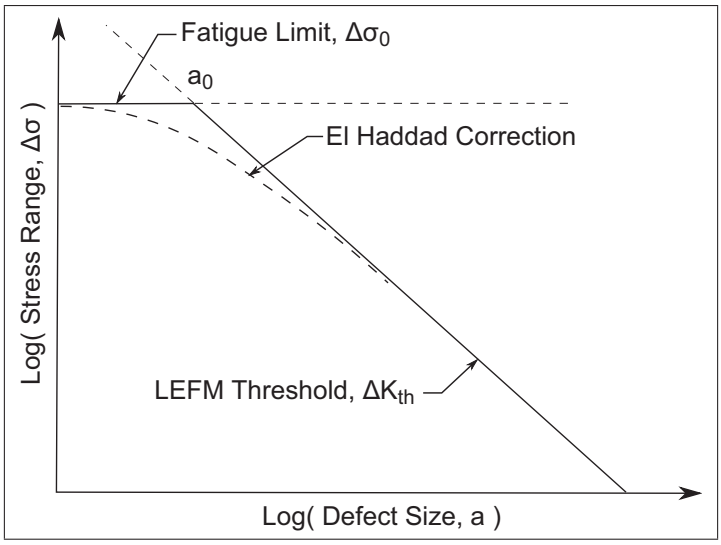

Figure 2.4 Schematic Kitagawa diagram

In order to use this model in a probabilistic approach, we propose the use of an isoprobabilist transformation combined with the Hasofer-Lind index to obtain the probability of exceeding a specified threshold using First- or Second-Order Reliability Methods (FORM/SORM). The premise in this study is that defect geometry and size uncertainty have already been defined either from inspections data or probabilistic crack growth simulations. The study of both inspection data and crack growth models are beyond the scope of this paper. From that premise, the reliability assessment is reduced to the probability of exceeding a threshold which follow this general procedure:

a. Definition of the variables of interest, limit state and input variables

b. Quantification of the uncertainty sources

c. Isoprobabilist transform

d. Most Probable Point (MPP) search

e. Reliability approximation

f. Sensitivity analysis and ranking of uncertainty sources

Then, two application examples are investigated to assess the speed and accuracy of the FORM/-SORM approximations versus the conventional Monte Carlo simulations. Finally, we conclude with a limited sensitivity analysis on some parameters considered important for our application and the applicability of the developed probabilistic criteria for the reliability assessment of large rotating machinery such as large Francis runner.

2.3 High Cycle Fatigue (HCF) reliability

To assess the fatigue reliability of a structure, the following elements are needed: a properly defined limit state model, a reliability criterion and characterized uncertainty sources. In this study, the limit state is defined as the thresholds proposed by Kitagawa and Takahashi (Kitagawa et Takahashi, 1976) combined with the correction factor developed by El Haddad et al. (El Haddad *et al.*, 1979). This correction factor accounts for short crack growth by asymptotically matching the LEFM threshold and the fatigue limit. This limit state, commonly called the Kitagawa diagram, is shown in Figure 2.4, and in it, the limit formed by the LEFM threshold is obtained from the stress intensity factor solution defined as follows:

$$\Delta K = \Delta\sigma\sqrt{\pi a}\, Y(a) \tag{2.1}$$

where ΔK is the stress intensity factor variation, $\Delta\sigma$ is the stress cycle range, a is the crack length and $Y(a)$ is the stress intensity correction factor for a given geometry. The limit state equation is obtained by replacing ΔK by the LEFM threshold ΔK_{th} in Eq. (2.1) which is

rewritten as follows:

$$\Delta\sigma_{th} = \frac{\Delta K_{th}}{\sqrt{\pi a}\, Y(a)} \tag{2.2}$$

We note that the values ΔK_{th} is known to be influenced by the stress ratio R (Doker, 1997). If needed, ΔK_{th} could be modeled as a function of R to account for change in the steady state conditions. However, the study of such variation is beyond the scope of this paper since an hydroelectric turbine runner generally operates under rather constant and high R ratio most the time leading to concern only for the worst steady state condition in the time interval of interest. In order to capture short crack growth, El Haddad et al. (El Haddad *et al.*, 1979) proposed to asymptotically match the limits defined by LEFM and the fatigue limit $\Delta\sigma_0$ using the reference crack length a_0 as a correction factor. The correction factor a_0 is added to the crack length a in Eq. (2.2) to obtain:

$$\Delta\sigma_{th} = \frac{\Delta K_{th}}{\sqrt{\pi\,(a + a_0)}\, Y(a + a_0)} \tag{2.3}$$

where the constant a_0 represents the transition crack size between both limits, and is obtained by solving the following equation:

$$a_0 = \frac{1}{\pi}\left(\frac{\Delta K_{th}}{\Delta\sigma_0\, Y(a_0)}\right)^2 \tag{2.4}$$

For infinite life, $\Delta\sigma_0$ is the endurance limit. However, in some cases, the limit state for a finite number of cycles N might also be of interest either because the number of cycles for infinite life might not have been reached in a given time interval or because the material has no endurance limit. In those instances, a finite number of stress cycles N can be accounted for using the fatigue limit at N cycles rather than the endurance limit. This approach is similar to the model developed by Ciavarella and Monno (Ciavarella et Monno, 2006). In the current approach, to account for a limited number of cycles N, Eq. (2.3) and Eq. (2.4) can be rewritten as follows:

$$\Delta\sigma_{th} = \frac{\Delta K_{th}}{\sqrt{\pi\,(a + a_0(N))}\, Y(a + a_0(N))} \tag{2.5}$$

$$a_0(N) = \frac{1}{\pi}\left(\frac{\Delta K_{th}}{\Delta\sigma_0(N)\, Y(a_0(N))}\right)^2 \tag{2.6}$$

It is relevant to note that any of the parameters in Eq. (2.5) and Eq. (2.6) can be used as an independent random variable. Now that the limit state has been defined, the criteria for failure must be defined and is expressed as follows:

$$g(x) \leq 0 \tag{2.7}$$

with a probability of failure:

$$P_f = \int_{g(x)\leq 0} f_X(x)\, dx \tag{2.8}$$

in which, x is an n-dimensional vector of random variables with a joint density function $f_X(x)$. By defining the failure as the HCF onset, $g(x)$ becomes:

$$g(a, \Delta\sigma) = \Delta\sigma - \frac{\Delta K_{onset}}{\sqrt{\pi\ (a + a_0(N))}\, Y(a + a_0(N))} \tag{2.9}$$

Where ΔK_{th} has been replaced by ΔK_{onset} for generality to differentiate the onset from LEFM threshold ΔK_{th} because in some case the onset could be different due to interaction between HCF and LCF cycles (Byrne *et al.*, 2003). Furthermore, we observe that two time-dependant parameters are found in Eq. (2.9). The first one is $a_0(N)$ which increases with time because $\Delta\sigma_0$ decreases with the number of stress cycles N until it reaches the endurance limit. The second parameter is the defect size a which concurrently increases with time due to the LCF part of the loading spectrum. To illustrate Eq. (2.9), the limit state with the associated parameters uncertainties are shown in Figure 2.5.

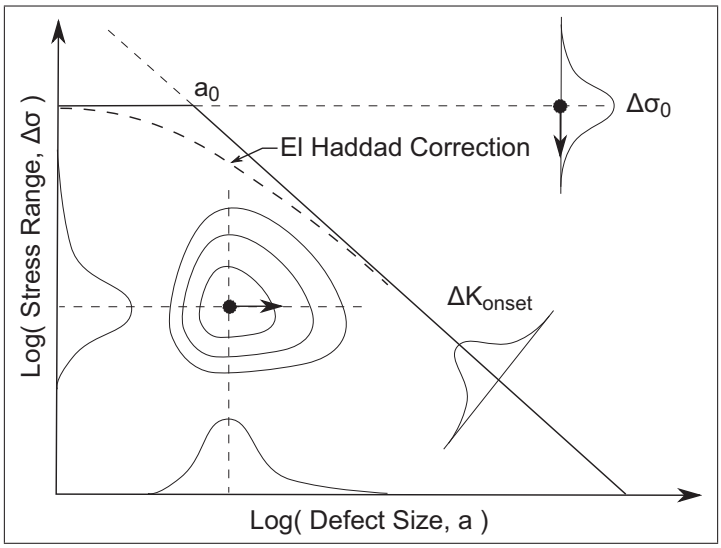

Figure 2.5 Schematic probabilistic Kitagawa diagram

Then, to properly define the model, uncertainty sources must be characterized. For the purpose of this study $\Delta\sigma_0$ and ΔK_{onset} are considered deterministic which reduces the model in the simplest case to two random parameters: defect size and stress range. Our assumption is that for a given element of volume subjected to a uniform stress level, the HCF onset will occur at the largest flaw due to the largest stress cycle in the HCF loading. For both random variables, the largest value uncertainty can be characterized using the Extreme Value Theory (EVT). Within EVT, two models can be used: the General Extreme Value (GEV) distribution and the General Pareto Distribution (GPD). The GEV cumulative distribution is expressed as follows:

$$F(x) = exp\left(-\left(1+\frac{\xi(x-\mu)}{\sigma}\right)^{-1/\xi}\right) \tag{2.10}$$

where $\xi \in \mathbb{R}$ is the shape factor, $\mu \in \mathbb{R}$ is the location parameter and $\sigma > 0$ the scale parameter. The case where $\xi > 0$ and $\xi < 0$ correspond respectively to the Fréchet and Weibull distribution. Note that $\xi = 0$ is a special case which leads to the Gumbel distribution for which the cumulative is reduced to:

$$F(x) = exp\left(-e^{\frac{-(x-\mu)}{\sigma}}\right) \tag{2.11}$$

Because GEV distribution characterizes the uncertainty around a sample largest event(i.e. block maxima), only a small part of the available data can be used for parameter estimation. This

limitation can be alleviated by the use of GPD model which characterizes the observations exceeding a given threshold (i.e. peak-over-threshold). Using a GDP model, a larger part of the available data can be used for parameter estimation. The GPD cumulative probability distribution is expressed as follows:

$$F(x) = 1 - \left(1 + \frac{\xi(x-\mu)}{\sigma}\right)^{-1/\xi} \tag{2.12}$$

where $\xi \in \mathbb{R}$ is the shape factor, $\mu \in \mathbb{R}$ is the location parameter and $\sigma > 0$ the scale parameter. The special case $\xi = 0$ corresponds to the exponential distribution which reduce Eq. (2.12) to the following:

$$F(x) = 1 - e^{\frac{-(x-\mu)}{\sigma}} \tag{2.13}$$

We would like to note that the GEV distribution can be obtained from the GPD or vice versa, using the assumption that the peaks over a high enough threshold follow a Poisson process (Coles, 2001). The exponential and Gumbel distribution are simplified versions of their generalized counterpart. As such, the Gumbel distribution was chosen to model both random variables. Note that this distribution has already been used in the literature to model both the extremes of load spectra (Johannesson, 2006) and the defect size (Murakami, 2002; Beretta *et al.*, 2006). This assumption should be reasonable for a wide range of applications because many distributions, like the normal, log-normal and Weibull distribution, are approximatly exponentially distributed above a high enough threshold (Pickands III, 1975; Davison et Smith, 1990). However, there is no restriction on the distribution to be used.

2.4 Isoprobabilist transformation and Hasofer-Lind reliability index

Two numerical approaches can be used to solve the probability of HCF onset defined by Eq. (2.8) in the previous section. The approaches can either be simulation-based, like the Monte Carlo (MC) simulation and its variants, or analytical, using approximations like the First-Order Reliability Method (FORM) and the Second-Order Reliability Method (SORM). An advantage with the simulation-based method, like the Crude MC, is that it asymptotically converges to the exact values for a number of simulations $N \to \infty$ but nevertheless has a drawback, common

to all simulation-based methods, of possibly requiring a prohibitive number of simulations in order to obtain reliable results, for a low-probability estimate. On the other hand, analytical methods are based on the approximation of the probability of failure leading to a minimal numerical burden in exchange for accuracy.

FORM/SORM approximations rely on the assumption that a transformation in the form $\underline{U} = T(\underline{X})$ exists, mapping the physical space to a standard space. The transformation is expressed as follows:

$$P_f = \int_{g(\underline{X})\leq 0} f(\underline{x})\ d\underline{x} = \int_{g(T(\underline{X}))\leq 0} \varphi(\underline{u})\ d\underline{u} \tag{2.14}$$

where $\varphi(u)$ is an n-dimensional standard normal density with independent components. Several such transformation methods are available. The Rosenblatt transform (Lebrun et Dutfoy, 2009b) was chosen in this study because of its flexibility to impose a dependency structures between the random variables modeled using the copula theory. The Rosenblatt transform is defined as follow:

$$\underline{U} = T(\underline{X}) = T_2(\underline{X}) \circ T_1(\underline{X}) \tag{2.15}$$

$$\begin{aligned} T_1 :\quad & \mathbb{R}^n \to \mathbb{R}^n \\ & \underline{X} \mapsto \underline{Y} = \begin{pmatrix} F_1(X_1) \\ F_2(X_2|X_1) \\ F_3(X_3|X_1, X_2) \\ \vdots \\ F_n(X_n|X_1, X_2, \ldots, X_{n-1}) \end{pmatrix} \end{aligned} \tag{2.16}$$

$$\begin{aligned} T_2 :\quad & \mathbb{R}^n \to \mathbb{R}^n \\ & \underline{Y} \mapsto \underline{U} = \begin{pmatrix} \Phi^{-1}(Y_1) \\ \Phi^{-1}(Y_2) \\ \vdots \\ \Phi^{-1}(Y_n) \end{pmatrix} \end{aligned} \tag{2.17}$$

where $\underline{X}$ in $\mathbb{R}^n$ is a continuous random vector defined by its marginal cumulative distributions F_i and copula. It should be noted that the conditioning order in Eq. (2.16) will influence

the shape limit state in the standard space $\underline{U}$ and impact the results of the FORM/SORM approximation. Because the stress ranges are considered independent of the defect size, the assumption can be made that the random vector $\underline{X}$ has an independent copula. The independent copula assumption simplifies the Rosenblatt transform and Eq. (2.15) becomes:

$$\underline{U} = \begin{pmatrix} \Phi^{-1}(F_1(X_1)) \\ \Phi^{-1}(F_2(X_2)) \\ \vdots \\ \Phi^{-1}(F_n(X_n)) \end{pmatrix} \tag{2.18}$$

In the standard space $\underline{U}$, the probability of failure can be obtained either with a linear approximation (FORM) or a quadratic approximation (SORM) as shown in Figure 2.6. In this space, the Most Probable Point (MPP) of failure, also named the design point u^*, is located at the shortest distance between the origin and the limit state $g(\underline{U}) = 0$. The distance to the MPP is called the Hasofer-Lind reliability index β_{HL}.

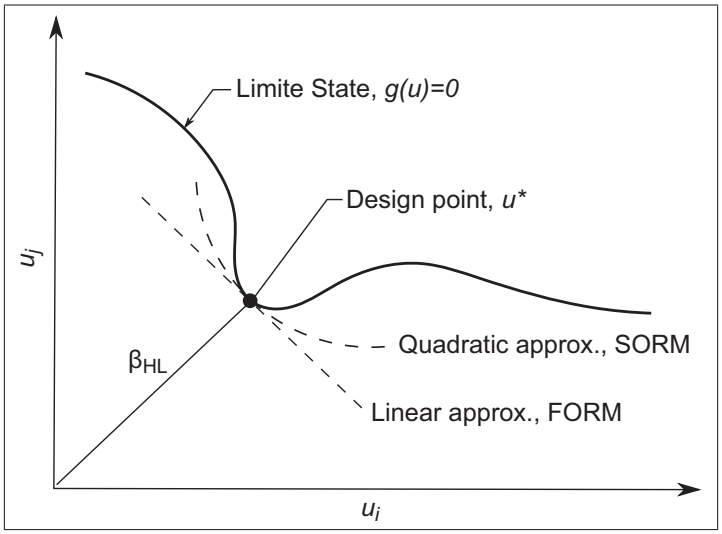

Figure 2.6 Schematic isoprobabilist space

The FORM approximation of the probability of failure P_f is calculated directly from the Hasofer-Lind index β_{HL} and is given by:

$$P_f = 1 - \Phi(\beta_{HL}) = \Phi(-\beta_{HL}) \tag{2.19}$$

where $\beta_{HL} = \|\underline{u}^*\|$, Φ is the standard normal cumulative function and $\underline{u}^* = min\|\underline{u}\|$ for $g(\underline{U}) \leq 0$. The main numerical burden of this approximation resides in finding the location of the design point $\underline{u}^*$. Note that the results obtained with the FORM approximation are only accurate when the limit state is linear in the standard space $\underline{U}$. Likewise, results from the SORM approximations are only accurate when the limit state at the design point is close to quadratic in the standard space $\underline{U}$. Many formulation are available for SORM approximations, three of which will be used in this paper: the Tveld formulation (Tvedt, 1988), the Breitung formulation (Breitung, 1989), and the Hohenbichler formulation (Hohenbichler et Rackwitz, 1988). The SORM solution requires $n(n+1)/2$ additional function calls over the FORM approximation to compute the main curvatures around the design point in the standard space (Rackwitz, 2001). We refer the reader to the work of Rackwitz (Rackwitz, 2001) and to the work of Ditlevsen and Madsen (Ditlevsen et Madsen, 2007) for a complete overview of the theory and the methods used in structural reliability analysis.

2.5 Application examples

For a structure like a hydroelectric Francis runner, two types of material flaws are usually considered critical: surface flaws and near-surface embedded flaws. Figure 2.7 shows the flaw geometries used in our application examples. In both cases, simple, circular, two-dimensional flaws in a semi-infinite medium are used to limit the number of parameters. The surface flaw has only one parameter, the size a, which enables the visualization of the reliability problem on a two-dimensional diagram similar to Figure 2.5. On the other hand, a near-surface embedded flaw geometry is characterized by at least two parameters: the position p and size a. For both flaw type the only the direction where the maximum stress intensity factor ΔK is expected will be considered. For surface flaw the maximum stress intensity factor ΔK is expected parallel to

the surface and for embedded flaw the maximum stress intensity factor ΔK is expected at the closest point to the surface.

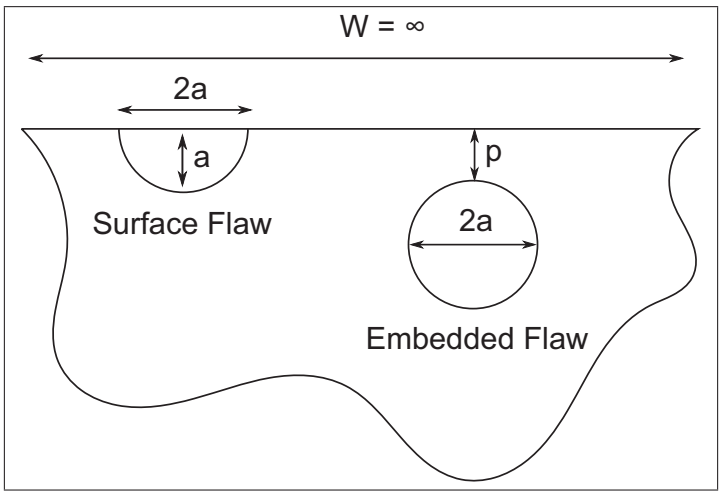

Figure 2.7 Surface flaw and embedded flaw

The correlation between parameters is not a concern for surface flaws, however, for an embedded flaw, the stress intensity correction factor Y in Eq. (2.1) is a function of both the position p and size a which we cannot assume independent. In this case, a correlation could have been induced either because of the manufacturing process or the crack propagation process itself. As an example, defects closer to the surface will propagate faster because of the higher stress intensity leading, with time, to larger flaws closer to the surface. For such cases, as an example, a dependency between random variables could be introduced in the form of a Gumbel copula which would characterizes the correlation between the extreme values of each parameter.

In our application examples, only the uncertainties on the HCF stress range and defect geometry are studied to enable easier visualization of results and all the other parameters are treated as deterministic. Furthermore, if not specified otherwise, all random parameters are considered independent. The parameter values used are presented in Table 2.1.Typical design requirements are used for the endurance limit $\Delta\sigma_0\,(N = 10^7)$. Both the LEFM threshold and stress intensity factor solution ΔK are taken from the British Standard BS7910:2005 (British Standards Institute, 2005). Notice that we assume $\Delta K_{onset} = \Delta K_{th}$ in this study meaning that the LCF

influence on the material HCF fatigue strength is neglected (Nicholas, 2006). However, we recommend the use of actual experimental data combined with their associated uncertainties if available. Furthermore, we would like to highlight that the parameter values used for stress and defect size have been chosen for illustrative purposes and do not reflect the state of an actual structure.

Tableau 2.1 Limit state parameters

	Location	**Scale**	**Distribution**	**Units**
$\Delta K_{onset} = \Delta K_{th}$	2.0	-	-	MPa $m^{1/2}$
$\Delta\sigma_0\,(N = 10^7)$	85.6	-	-	MPa
p	-	-	Uniform [0,10]	mm
a	1.5	0.5	Gumbel	mm
σ	20.0	1.0	Gumbel	MPa

2.6 Results and discussion

The results displayed in Figure 2.7 show, for the surface flaw example, the influence of the reduction of $\Delta\sigma_0$ until the number of HCF cycles reaches the endurance limit ($N = 1.0E{+}07$). For a hydroelectric turbine runner with a rotating speed of 75RPM, $N = 1.0E + 07$ represents 0.25 years of operation for a stress fluctuations at the rotating speed frequency. The design point shown in Figure 2.7 is obtained for a number of HCF cycles above the endurance limit. Detailed results are presented in Table 2.2.

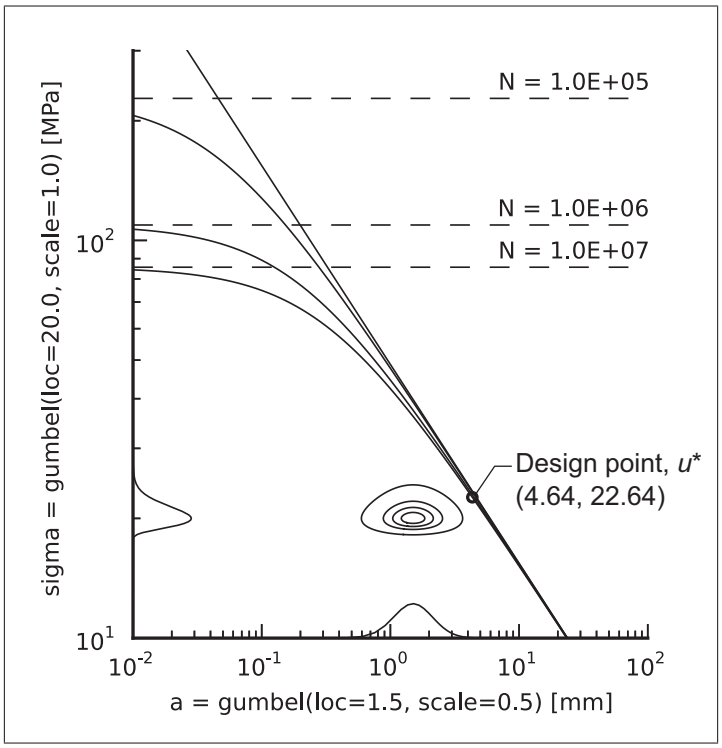

Figure 2.8 Surface flaw example

Tableau 2.2 Detailed results for the surface flaw example

Description	**Value**
Physical space design point	$(4.64, 22.64)$
Standard space design point	$(2.90, 1.49)$
Hasofer-Lind reliability index β	3.26
FORM probability	$5.64E-04$
Tveld SORM probability	$6.79E-04$
Breitung SORM probability	$6.71E-04$
Honenbicher SORM probability	$6.83E-04$
Monte Carlo (10^6 simulations)	$6.30E-04$

We observe in Table 2.2 that the results from SORM approximations are closer to the MC results than to the FORM approximation. However, for such low probability values, the ob-

served discrepancy might not be considered significant in some engineering applications. A comparison of event probability as a function of defect size distribution location for each flaw type is shown in Figure 2.9. In this figure, we observe larger discrepancies between MC and FORM/SORM results for the embedded flaw compared to the surface flaw. Nonetheless, these discrepancies might still be considered negligible if we consider that the FORM results in Table 2.2 are obtained using only 45 function calls, as compared to the 10^6 function calls needed to obtain a convergent MC estimate.

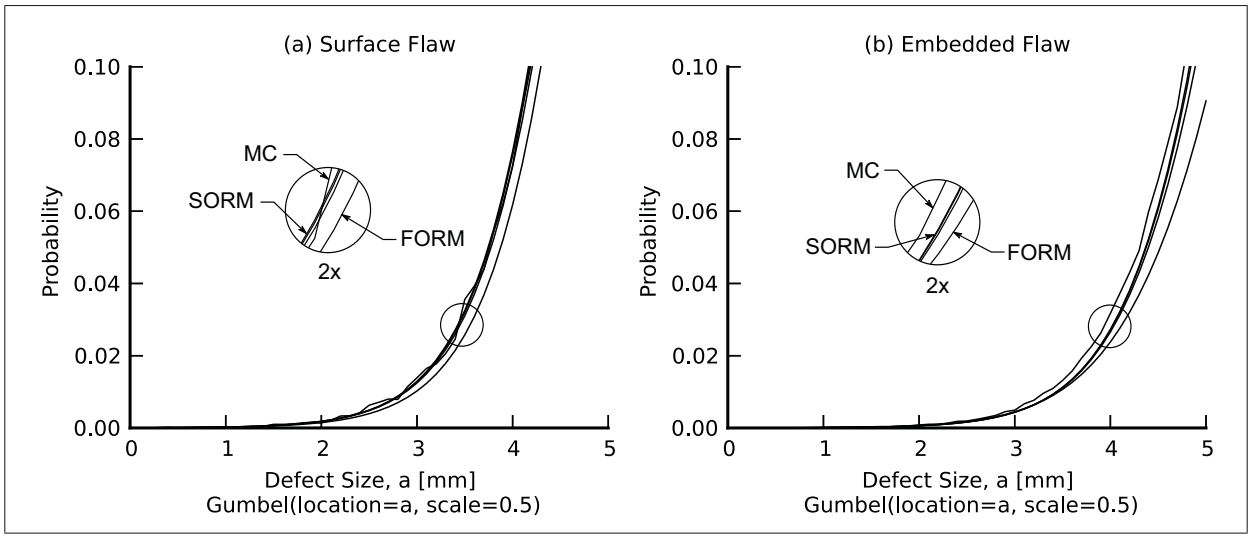

Figure 2.9 Event probability vs. defect size for surface flaw and embedded flaw examples

Also, in Figure 2.9, we might believe their is a lack of sensitivity in the low probability region for both examples. However, the is only due to the non-linearity of the results which renders comparison and visualisation difficult across different level of probability. These difficulties can be alleviated by the use of the reliability index β as a comparison basis instead of the event probability. The reliability index can be visualized as a measure of the shortest distance to the limit state in the standard space and is directly related to the probability of failure P_f. However, the Hasofer-Lind index β_{HL}, as defined previously, is only calculated during FORM/SORM approximations. For an arbitrary probabilistic result, the index β can be generalized using the

following:

$$\beta = \Phi^{-1}(1 - P_f) = -\Phi^{-1}(P_f) \tag{2.20}$$

where P_f is the probability of an event obtained from an arbitrary method. The generalized reliability index offers a general criterion for reliability comparison. We would like to refer the reader to the work of Ditlevsen and Madsen (Ditlevsen et Madsen, 2007) for more information on reliability index. The reliability index β as a function of defect size distribution location a for both flaw types using the values in Table 2.1 and considering all random parameters independent is shown in Figure 2.10.

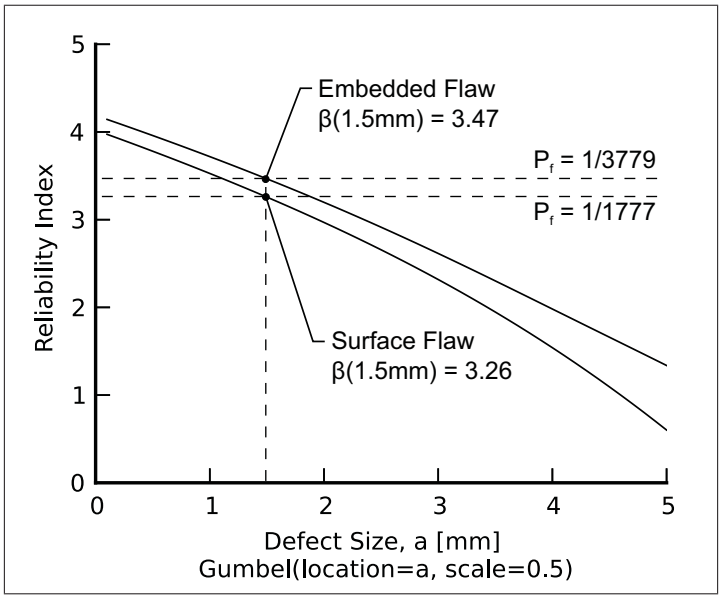

Figure 2.10 Reliability index vs defect size for surface flaw and embedded flaw examples

We observe lower reliability indexes for the surface flaw results compared to the embedded flaw results. These lower β values might be misleading since a close to surface embedded flaw can be more critical than a surface flaw. This is due to the random nature of the position parameter p. The effect of both the defect size a and distance from the surface p can be observed in Figure 2.11. Note that the reliability index increases with the distance from the surface and decreases with the defect size. Compared to a surface flaw, an embedded flaw has a higher reliability index far from the surface and a lower one close to the surface. As a consequence,

when the distance from the surface p is treated as a random variable, the probability of a flaw occurring close to the surface can significantly reduces the overall reliability index.

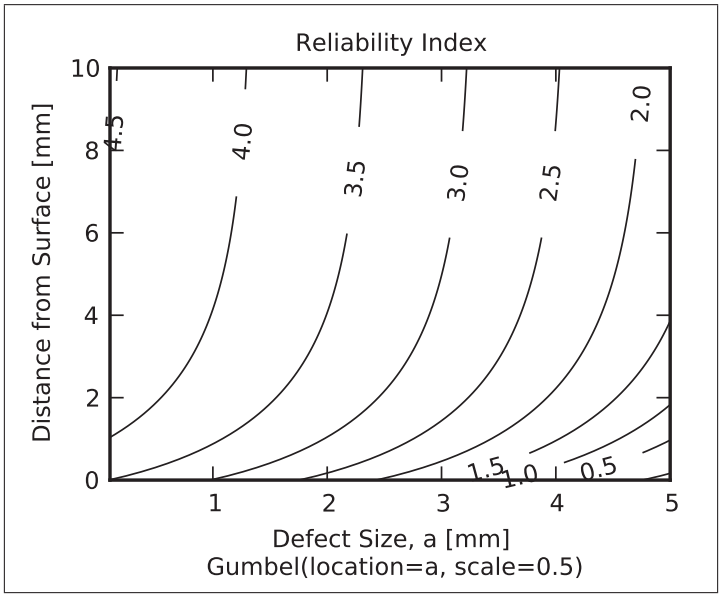

Figure 2.11 Embedded flaw reliability index for deterministic distance from the surface

In such instances, the quantification of marginal distributions might be as important as the correlation structure between the defect size a and distance from the surface p. In our embedded flaw example, the defect size a and the distance from the surface p cannot be assumed independent without proper experimental validation. Ignoring the relationship between random variables can produce significant results bias. For example, the results from a Gumbel copula with a Kendall $\tau = 0.60$ is shown in Figure 2.12. The figure represent one thousand random samples obtained from two uniform distributions. We observe that extreme values from both distribution tend to appear together with a level of dependence measured by the Kendall τ coefficient. Similarly, in Figure 2.13, a Gumbel copula with a Kendall $\tau = 0.60$ is used to model the correlation between the flaw size and position such that large flaws will tend to appear close to the surface, resulting in a significantly lower reliability index compared to the results obtained for the embedded flaw with an independent copula or the surface flaw. These results highlight

the sensitivity of reliability results to such assumption, and even more so if the assumption cannot be validated with observed data.

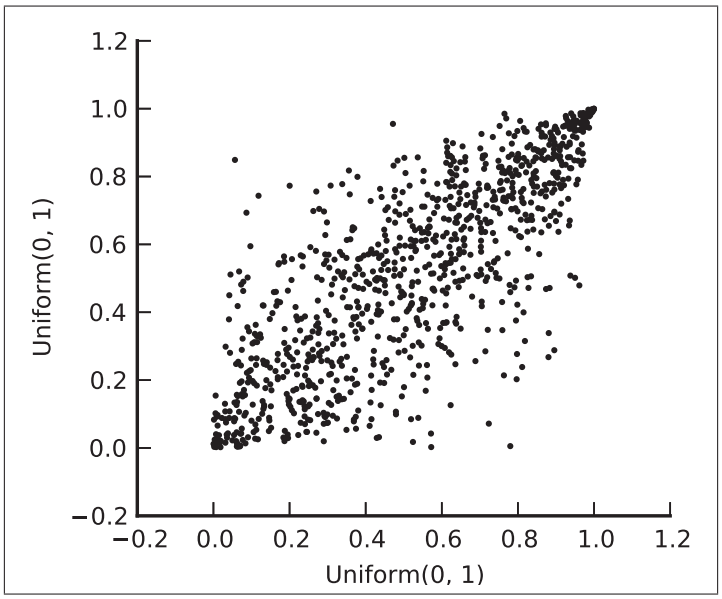

Figure 2.12 Gumbel copula with a Kendall $\tau = 0.60$ (number of samples = 1000)

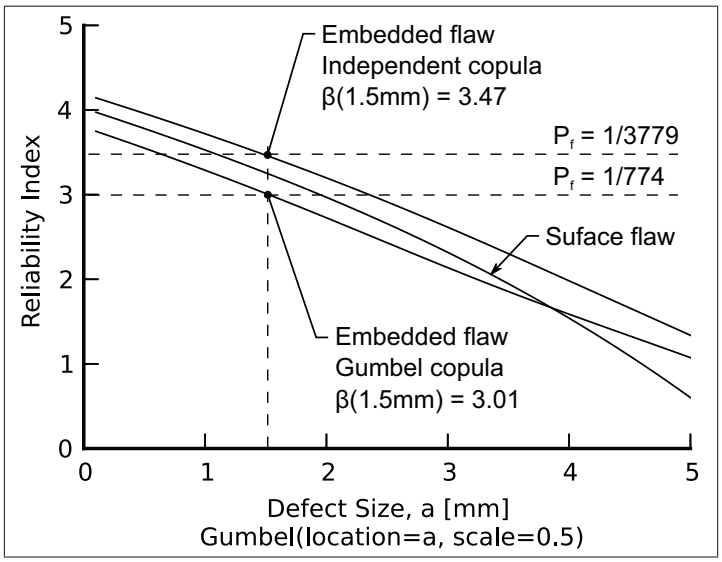

Figure 2.13 Independent copula vs Gumbel copula for the embedded flaw example

2.7 Conclusions

A fatigue reliability model for HCF crack propagation in hydroelectric turbine runner was proposed in this paper. We established that the HCF onset is the proper limit state for a hydroelectric turbine runner since the HCF onset marks the point in time after which a flaw becomes a detectable crack. In the proposed model, the limit state is formed by the Kitagawa and Takahashi (Kitagawa et Takahashi, 1976) diagram combined with the El Haddad et al. (El Haddad *et al.*, 1979) correction factor which defines the region where, for a given set of parameters, a crack will not propagate. Applied in the context of a combined LCF-HCF loading, the proposed model allows the evaluation of the fatigue reliability at any point in time, from the available information about material properties, defect size and HCF loading. The accuracy obtained using FORM/SORM approximations was compared to the results from crude MC simulations using two typical flaw geometries. A lower accuracy was observed for the embedded flaw geometry compared to the surface flaw geometry using FORM/SORM approximations. However, in both cases, the results follow the same overall trend as the crude MC simulations which might warrant their use over more numerically intensive simulation methods, given the minimal numerical burden inherent to such approximations.

The embedded flaw results have highlighted some of the difficulties associated with flaw geometries characterized by more than one random parameter. First, we observed that even if a higher reliability is expected for a flaw far from the surface, the prospect of a flaw close to the surface can lower significantly reliability associated with embedded flaws making them more critical than surface flaws. The results were first obtained by considering the random variables independent which with further investigation proved to be a non-conservative assumption. In the study, a correlation between flaw size and position was induced using a Gumbel copula, such that large flaws tend to appear close to the surface, and a significant reduction in the reliability results was observed making the embedded flaw example more critical than the surface flaw example. As in many structures, like hydroelectric turbine runners, the copula assumption often cannot be validated with observed data which lead to the need for extending sensitivity

assessments to variables such as the copula type and correlation coefficient for proper model assessment.

Our study has shown that HCF reliability can be approximated with minimal numerical burden using a multi-parameter limit state function that combines information from material properties, defect size and HCF loading. The authors believe that such a model has the potential for application to many structures subjected to combined HCF-LCF loading and promote the use of multi-parameter limit states in probabilistic fatigue assessment.

Acknowledgments

The authors would like to thank the *Institut de recherche d'Hydro-Québec* (IREQ), Andritz Hydro Ltd, the National Sciences and Engineering Research Council of Canada (NSERC) and the *École de technologie supérieure* (ÉTS) for their support and financial contribution.

CHAPITRE 3

INFLUENCE OF LOAD SPECTRUM ASSUMPTIONS ON THE EXPECTED RELIABILITY OF HYDROELECTRIC TURBINES: A CASE STUDY

Martin Gagnon[1,2], Antoine Tahan[1], Philippe Bocher[1], Denis Thibault[2]

[1] École de technologie supérieure (ÉTS), Montréal, Québec, H3C 1K3, Canada

[2] Institut de recherche d'Hydro-Québec (IREQ), Varennes, Québec, J3X 1S1, Canada

Submitted to "Structural Safety", February 2013

3.1 Abstract

A lack of observed data can lead to significant discrepancy between estimated and actual fatigue reliability. In this study, the load spectrum derived from the strain measurements and operation history of a hydroelectric turbine are used to identify the information necessary to avoid major bias in the estimated fatigue reliability of such structure. Our results demonstrate that a limited number of parameters need to be considered. Any further simplifications may lead to major reliability estimate discrepancies. Furthermore, we observe that the parameters which influence initial reliability hide the influence of other parameters on the reliability failure rate associated with the structure's life expectancy. We conclude that a typical sensitivity analysis made on parameter values needs to be complemented with a sensitivity study on the chosen assumptions in order to properly evaluate the risks associated with the operation of hydroelectric turbines.

3.2 Introduction

Using oversimplified loading spectra can generate significant bias in fatigue analysis because of neglected features when compared to the actual load sustained by the structure. However, observed data are often lacking during the design of a structure or before measured values

are available. In such cases, both the designer and the analyst have to rely on simplified loading assumptions. The lack in the literature of either standardized load spectra or observed data from existing hydroelectric turbine runners make it difficult for the construction of such *a priori* assumptions. For large Francis hydroelectric turbine runners, every runner is considered a prototype. Generally speaking, the loading patterns used during the design phase simply cannot be based only on previously observed data from similar designs. This often leads to a difference between estimated reliability and actual reliability. Such errors, if unacknowledged, might influence design choices leading to a risk of higher maintenance costs or warranty issues. The nature, consequences and probability of these errors are often not considered in reliability assessments. We believe that the possibility of such errors generates uncertainties which should be acknowledged in a attempt to minimize the risks associated with the operation of these large rotating structures. This is in line with the risk description proposed by Aven (Aven, 2012) in which the probability and the consequences of an event are not sufficient to describe risk. Uncertainties which include assumption credibility also need to be addressed. In many cases, the acknowledgement of such uncertainties may justify the loading spectrum experimental validation in cases where life expectancy is considered an important risk factor. Such observations would be an important step toward the safe operation and standardization of load spectra (Heuler et Klatschke, 2005). In this study, our objective is to define the main damaging features observed on an existing hydroelectric turbine runner and to quantify their effect on the reliability assessment of such structures.

Structures like large hydroelectric turbine runners often have limited inspection possibilities combined with high downtime costs. For these structures, we consider that cracks only need to be repaired after the onset of High Cycle Fatigue (HCF). This statement relies on two basic assumptions:

a. Significant crack growth will be induced after HCF onset and crack growth will then be proportional to operation time rather than the number of low cycle fatigue (LCF) events.

b. A crack needs to be repaired as soon as possible in order to minimize costs only if significant growth is expected.

A typical design assumption is that the stress experienced by the runner blades goes from zero to a given operating condition stress level to zero during a typical load cycle (Lanteigne *et al.*, 2008). This simple loading pattern, shown in Figure 3.1, is similar to the representation of combined HCF/LCF loading commonly used in the literature (Byrne *et al.*, 2003).

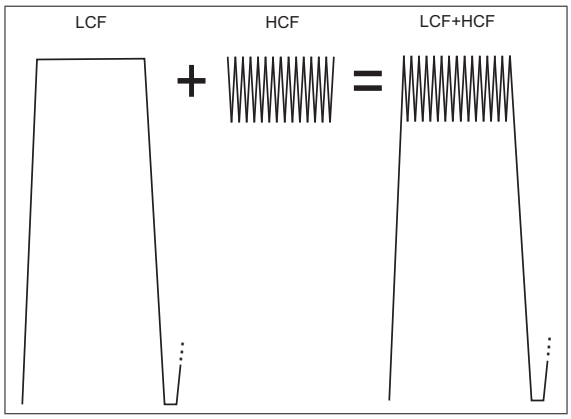

Figure 3.1 Schematic example of combined LCF+HCF loading

This loading pattern loosely matches the strains observed during a typical loading cycle on hydroelectric turbine runner blades. However, when compared with the measured loading shown in Figure 3.2, this load pattern lacks transient events like turbine's startups and shutdowns. Given their amplitudes, these transients have a non-negligible influence which might generate significant bias on life expectancy (Gagnon *et al.*, 2010a). In the industry, the study of such phenomena is recent and is not mentioned in the hydroelectric turbine runner life expectancy literature review compiled by Sabourin *et al.* (Sabourin *et al.*, 2010).

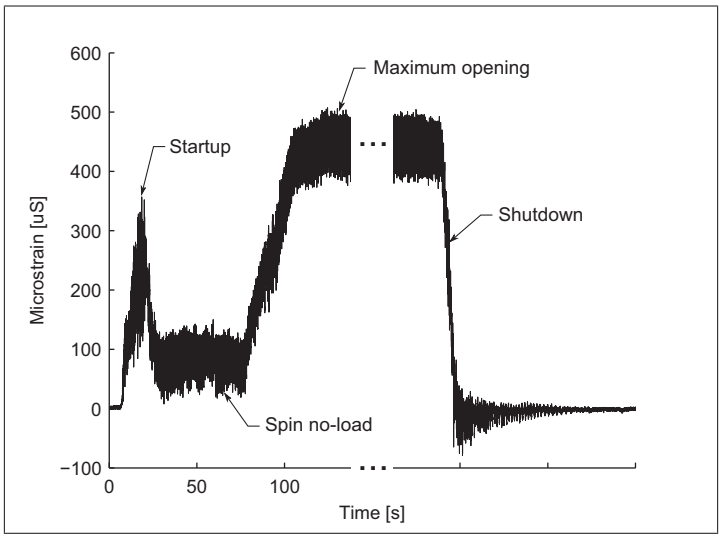

Figure 3.2 Measured loading sequence

The influence of the LCF and HCF part of Figure 3.2 loading sequence can be observed on crack growth simulation from (Gagnon *et al.*, 2010a) shown in Figure 3.3. In this figure, the crack propagation results obtained using the measured strains from Figure 3.2 are presented. We observed a slow crack propagation if a minimal time is spent at maximum opening (LCF only). However, during normal operation, we could expect almost 24 hours of operation at maximum opening for each loading block (LCF+HCF). In this case, the crack reaches a point, identified as the HCF onset, after which crack growth speed increases rapidly due to the loading HCF component contribution.

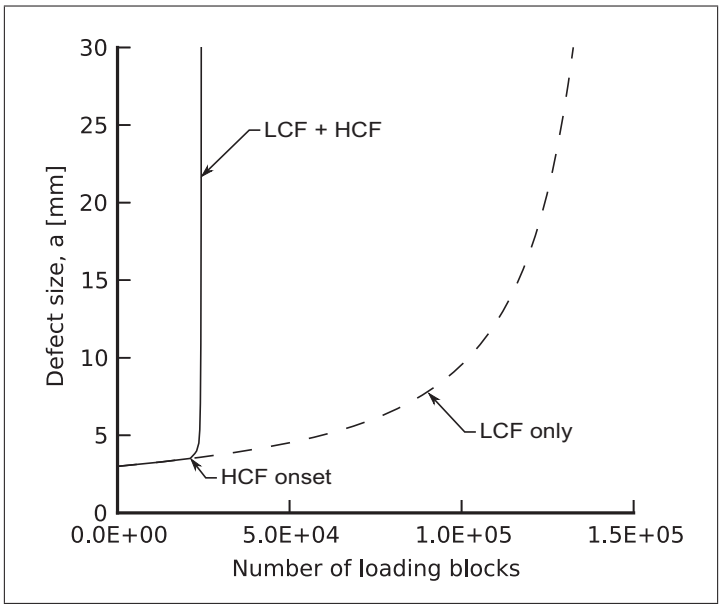

Figure 3.3 LCF vs. LCF+HCF crack propagation results

Life expectancy cannot be defined by the loading pattern alone. It must be combined with other information to generate a representative loading spectrum suitable for life assessment. The information needed to derive a loading spectrum for a hydroelectric turbine runner is typically:

a. The list of all the allowed steady-state conditions.

b. The list and expected number of transient events (startups, shutdowns ...).

c. The location of every critical area on the runner blades.

d. The stresses (static and dynamic contents) for each allowed steady-state and transient operating conditions at each critical area.

e. The residual stress levels at each critical area.

Using these, the loading spectrum is generated and combined with both material fatigue properties and expected defect size to obtain a reliability estimate. Our objective in this study is to highlight the results discrepancy between the *a priori*loading assumptions and observed data. For this purpose the data from an existing structure for which we have both measured strains

at a critical location and an operation history are used to derive simplified load spectra. The reliability results obtained with these spectra are then used to establish guidelines regarding the essential features needed in the loading spectrum to minimize bias due to simplifications while keeping the number of parameters to a minimum. Such guidelines should help limit the number of assumptions needed and facilitate the analysis when observed data are unavailable.

The paper is structured as follows: first, the turbine runner reliability model and the methodology are defined. Next, a case study is proposed based on observed data. Finally, reliability results are presented followed by a discussion on the importance of each parameter in the design, maintenance and operation of large hydroelectric Francis turbine runners.

3.3 Reliability model

To assess the reliability of a structure, we must first define a proper limit state for our application. In this study, Linear Elastic Fracture Mechanics (LEFM) theory will be applied since it is commonly used for the crack propagation of hydroelectric turbine runner blades (Sabourin *et al.*, 2010). According to LEFM, crack growth can be modeled as follows:

$$\frac{da}{dN} = C\,\Delta K^m,\ \Delta K > \Delta K_{th} \tag{3.1}$$

in which a is the crack length, N the number of stress cycles, C a material constant, ΔK the stress intensity variation, and the exponent m also a material constant. In LEFM, no propagation occurs below a defined stress intensity variation level ΔK_{th}. The stress intensity factor variation ΔK is defined using the following:

$$\Delta K = \Delta\sigma\sqrt{\pi a}\,Y(a) \tag{3.2}$$

where $\Delta\sigma$ is the stress cycle range and $Y(a)$ a factor associated to given crack geometry. A limit state equation for crack growth can be obtained simply by replacing ΔK by ΔK_{th} and rewriting eq. 3.2 to obtain:

$$\Delta\sigma_{th} = \frac{\Delta K_{th}}{\sqrt{\pi a}\,Y(a)} \tag{3.3}$$

A representation of the limit described by eq. 3.3 is presented in Figure 3.4. In this figure, *sigma* is the HCF stress range and a the defect size at a given time. Notice that the arrow represents the crack propagation generated by the LCF loading which has stress ranges greater than the defined threshold.

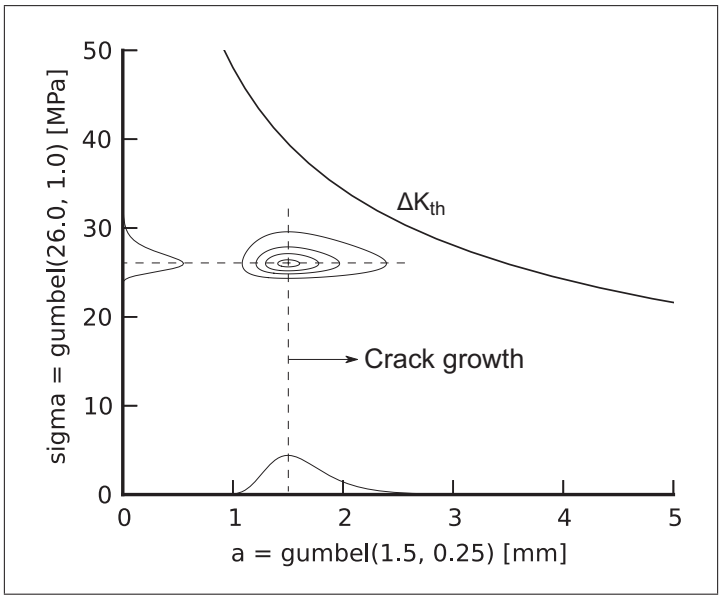

Figure 3.4 Probabilistic representation of the limit state

LEFM is only one part of the limit state for the reliability assessment of hydroelectric turbine runner blades as proposed by Gagnon *et al.* (Gagnon *et al.*, 2013a). Such limit state was initially proposed by Kitagawa and Takahashi (Kitagawa et Takahashi, 1976) and corrected by El Haddad *et al.* (El Haddad *et al.*, 1979) to accounts for short crack growth. This limit state is illustrated in Figure 3.5. Notice that in Figure 3.5, compared to Figure 3.4, both axes are in logarithmic scale.

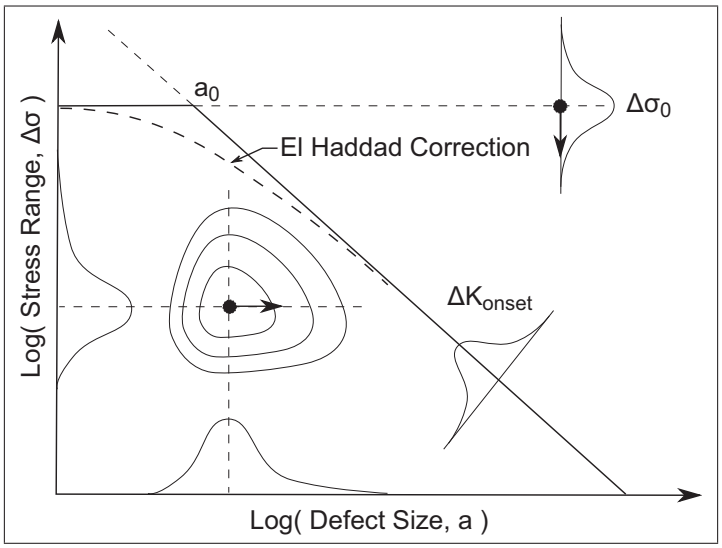

Figure 3.5 Kitagawa representation of the probabilistic HCF threshold

The main difference between the limit state in Figure 3.4 and the one in Figure 3.5 is the El Haddad correction which accounts for short crack growth by asymptotically joining the fatigue limit for crack initiation $\Delta\sigma_0$ and LEFM crack growth threshold ΔK_{th}. Furthermore, the LEFM threshold ΔK_{th} has been replaced by ΔK_{onset} because the onset of HCF crack growth can be influenced by the LCF loading part, leading to a potentially different threshold value (Byrne *et al.*, 2003). However, in this study such interactions between the LCF and HCF loading have been neglected. By accounting for the El Haddad correction the eq. 3.3 is rewritten as:

$$\Delta\sigma_{onset} = \frac{\Delta K_{onset}}{\sqrt{\pi(a + a_0(N))}\, Y(a + a_0(N))} \tag{3.4}$$

where $a_0(N)$ is the intersection between the LEFM limit and the initiation fatigue limit $\Delta\sigma_0(N)$ which decreases until the endurance limit is reached. The criterion for failure in this case is the probability of the HCF stress range $\Delta\sigma$ to be greater than the threshold $\Delta\sigma_{onset}$ and start contributing to crack growth. Such failure criteria are typically expressed as follows:

$$g(x) \leq 0 \tag{3.5}$$

Then, using the limit defined in eq. 3.4, it becomes:

$$g(x) \leq \Delta\sigma - \frac{\Delta K_{onset}}{\sqrt{\pi(a + a_0(N))}\, Y(a + a_0(N))} \tag{3.6}$$

with a failure probability of:

$$P_f = \int\limits_{g(x)\leq 0} f_X(x)\, dx \tag{3.7}$$

In this study, First-Order Reliability Method (FORM) will be used for its simplicity. Using FORM, the problem expressed in eq. 3.7 can be solved using approximations without having to resort to simulation based methods such as Monte Carlo (MC) simulations since this have a drawback common to all simulation methods: possibly requiring a prohibitive number of simulations in order to provide reliable results for low probability estimates.

The FORM approximation relies on the assumption that a transformation in the form $U = T(X)$ which maps the physical space to a standard space exists. Using this transformation, the problem in eq. 3.5 can be expressed as follows:

$$P_f = \int\limits_{g(x)\leq 0} f_X(x)\, dx = \int\limits_{g(T(X))\leq 0} \phi(u)\, du \tag{3.8}$$

where $\phi(u)$ is an n-dimensional standard normal density with independent components. We have chosen the Rosenblatt transform because it enables the analyst to impose dependency structures between random variables using copula theory. In this way, the Rosenblatt transform offers greater flexibility compared to other transformation methods like the Nataf transform (Lebrun et Dutfoy, 2009a,b). Please note that for independent random variables the Rosenblatt transform becomes:

$$U = \begin{bmatrix} \phi^{-1}\left(F_1\left(X_1\right)\right) \\ \phi^{-1}\left(F_2\left(X_2\right)\right) \\ \vdots \\ \phi^{-1}\left(F_n\left(X_n\right)\right) \end{bmatrix} \tag{3.9}$$

A schematic representation of the standard space is presented in Figure 3.6. In the standard space U, the probability of failure P_f can be obtained using either linear approximation (FORM) or quadratic approximation (SORM). Notice that the Most Probable Point (MMP), also named design point u^*, is located at the shortest distance between the origin and the limit state $g(U) = 0$. The distance to the MPP in the standard space U is called the Hasofer-Lind reliability index β_{HL} which is used as a metric to express the reliability level in our application.

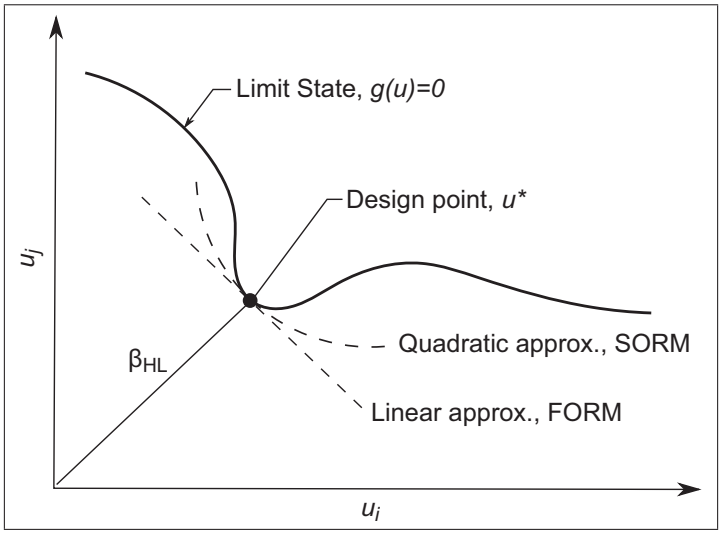

Figure 3.6 Schematic representation of FORM/SORM approximations in the standard space

Using the FORM approach, the probability of failure can be approximated directly from the Hasofer-Lind reliability index β_{HL} as follows:

$$P_f = 1 - \phi(\beta_{HL}) = \phi(-\beta_{HL}) \tag{3.10}$$

where $\beta_{HL} = \|u^*\|$, $\phi(\cdot)$ is the standard normal cumulative function and $u^* = min\|u^*\|$ for $g(U) \leq 0$. The Hasofer-Lind reliability index β_{HL} will be used to evaluate reliability in this study both for simplicity and to avoid working directly with approximated probability.

In the FORM methodology, two metrics are typically used to measure the influence of input variables on the reliability model. The first one is the importance factor which is calculated as follows:

$$\alpha_i^2 = \frac{(u_i^*)^2}{\beta_{HL}^2} \tag{3.11}$$

where α_i^2 is the importance factor of the parameter X_i with $\sum \alpha_i^2 = 1$. The importance factor is an indicator of the impact of modeling a given variable as random rather than deterministic. The second metric is the sensitivity factor ψ which is the derivative of the Hasofer-Lind reliability index β_{HL} with respect to the parameters Θ of the joint distribution X:

$$\psi = \frac{\partial \beta_{HL}}{\partial \Theta} \tag{3.12}$$

We refer the reader to the work of Rackwitz (Rackwitz, 2001) and the work of Ditlevsen and Madsen (Ditlevsen et Madsen, 2007) for a thorough overview of the use of FORM/SORM approximations in reliability analysis.

3.4 Case study

Our case study is based on the data observed on a low head Francis hydroelectric turbine runner from a power plant located in Quebec, Canada. This facility was chosen because strain measurements combined with an operation history over a five-year period were simultaneously available for one of the facility turbine runners. These *a posteriori* data are used to build realistic load patterns and spectra using different levels of simplifications. Such data can also be used for the validation of expected design values which are usually based on *a priori* assumptions.

In our case study, the following parameters are considered random:

a. Defect size, a.

b. HCF stress range, $\Delta\sigma_{HCF}$.

c. Startup transient amplitude, $\Delta\sigma_{startup}$.

d. Shutdown transient amplitude, $\Delta\sigma_{Shutdown}$.

e. Number of startups, $N_{Startup}$.

Each of these random parameters has to be characterized by distribution type, location and scale. Furthermore, if correlations are expected between parameters, the dependency structures must be characterized in the form of a copula. However, since no significant dependencies are expected between the chosen random parameters, they are considered independent in this study.

During the strain measurements, two blades were instrumented with strain gauges. The instrumented critical area is a cut-out located on the blade trailing edge near the runner crown on each blade as shown in Figure 3.7. Observed strains for this location are presented in Figure 3.2.

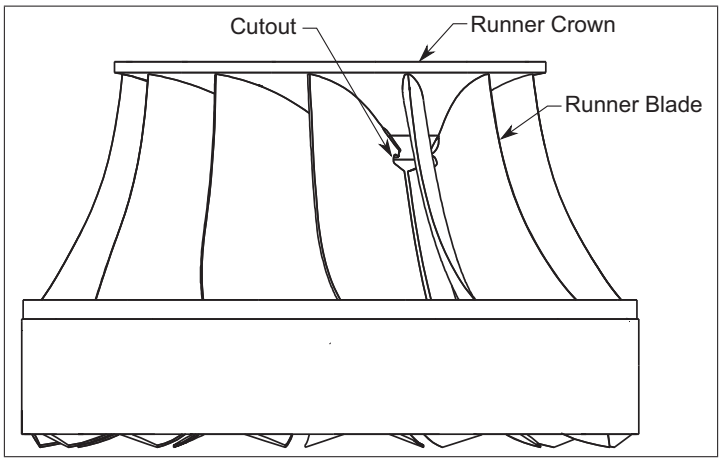

Figure 3.7 Francis runner diagram

Typically, critical flaws are expected to be either surfaces flaws or near surface embedded flaws. However, in this area, the critical location is near the corner of the cut-out region. Hence, the worst flaw type for reliability would be a corner flaw as shown in Figure 3.8 (Gagnon *et al.*, 2012b). This choice of flaw type is based on the assumption that any undetected embedded flaws near the surface in this region would be instantly re-characterized as a corner flaw right after the first load cycles. These first cycles can therefore be neglected. Notice that a semi-

circular corner flaw has only one parameter, i.e. the size a, eliminating the need to assess possible correlations between flaw parameters.

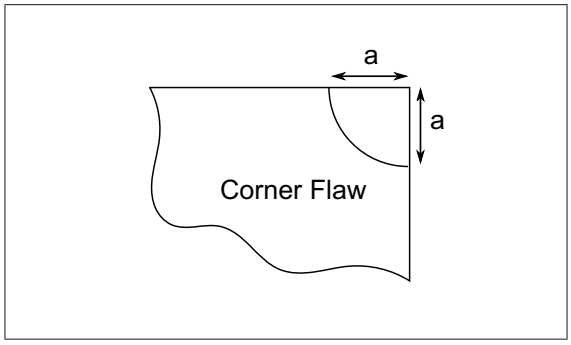

Figure 3.8 Flaw geometries

The strains measured at this location, shown in Figure 3.2, are used to identify the loading pattern characteristics needed to generate the simplified loading pattern presented in Figure 3.9. This loading pattern is more representative of the observed data than the typically assumed loading pattern shown in Figure 3.1 where the startup and shutdown transients are neglected. Furthermore, this loading pattern includes periodic excursions from normal operation (i.e. maximum opening in our simplified pattern) to spin no-load (SNL) which have been observed in the operation history of this runner. Those large load fluctuations generate stress fluctuations $\Delta\sigma_{SNL}$ which contribute significantly to crack propagation due to their amplitude. Notice that if the loading pattern in Figure 3.1 is to be used, both the startup and the SNL excursions would have the same LCF signature hence identical expected damage. Furthermore, if any other major strain fluctuations are observed they should also be considered.

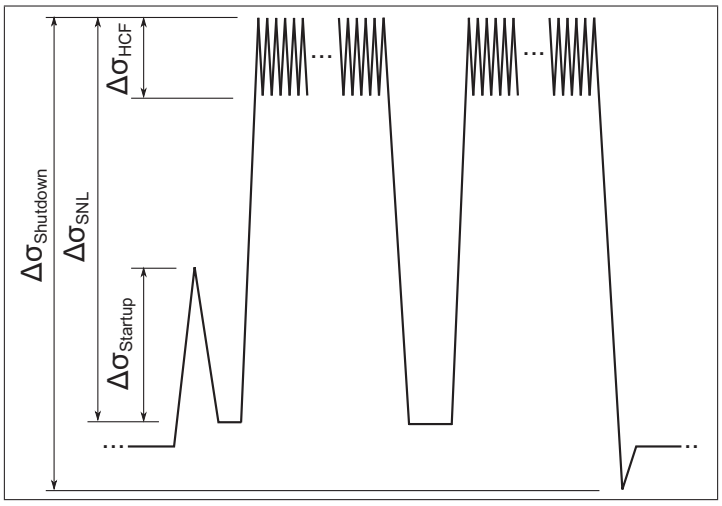

Figure 3.9 Proposed simplified loading pattern

The load spectrum is generated by combining the above loading pattern with the turbine operation history. In this case study, the operation history is based on a five-year period and a semi-Markov simulation method was used to extrapolate the history (Szczota *et al.*, 2011). The simulations giving the maximum and minimum number of startups from 400 simulations are presented in Figure 3.10. The probability distribution for the number of startups N estimated from these simulations is presented in Figure 3.11. Notice that the number of startups obtained is significantly lower than the typical design specifications of one startup per day and that the results are approximately linear over time.

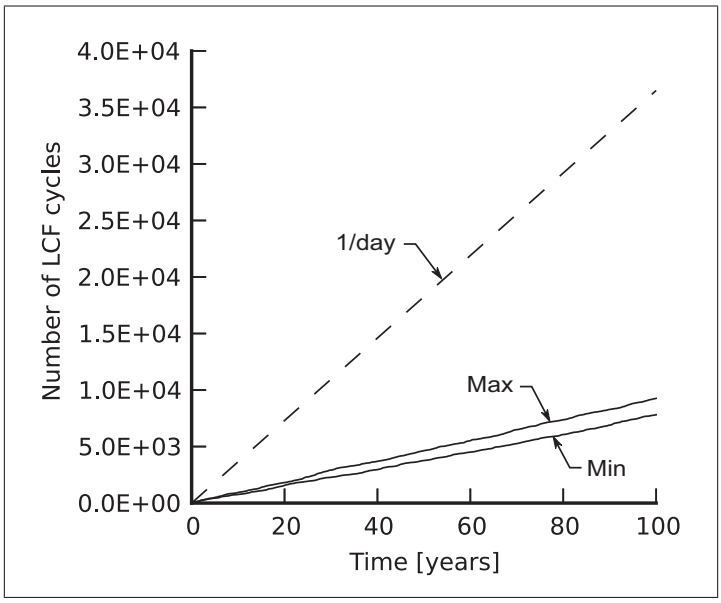

Figure 3.10 Extrapolated cumulative number of $\Delta\sigma_{Startup}$ cycles based on the studied runner's five-year history

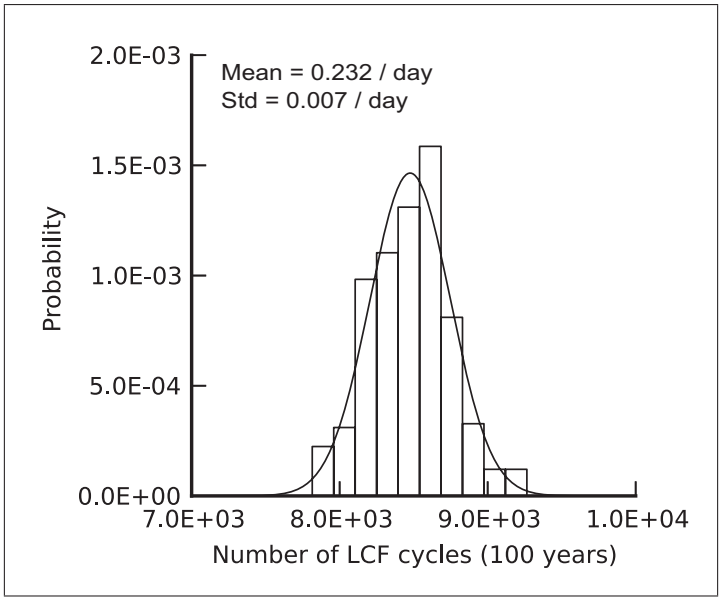

Figure 3.11 $N_{Startup}$ probability distribution over a 100 year period

From the runner history, we observe an almost constant ratio of 3 excursions to SNL for each startup. Because of this small variability, the number of excursions to SNL N_{SNL} is considered a deterministic constant. When both the number of startup $N_{Startup}$ and the number of excursion

to SNL N_{SNL} are combined, the design specification of 1/day becomes a probable value as shown in Figure 3.12. Both values are combined because they have the same amplitude when the load pattern in Figure 3.1 is used. This would reduce significantly the safety factor expected from the startup data only shown in Figure 3.10. Note that the excursions to SNL, as observed here, were likely not specified in the design requirements for this runner.

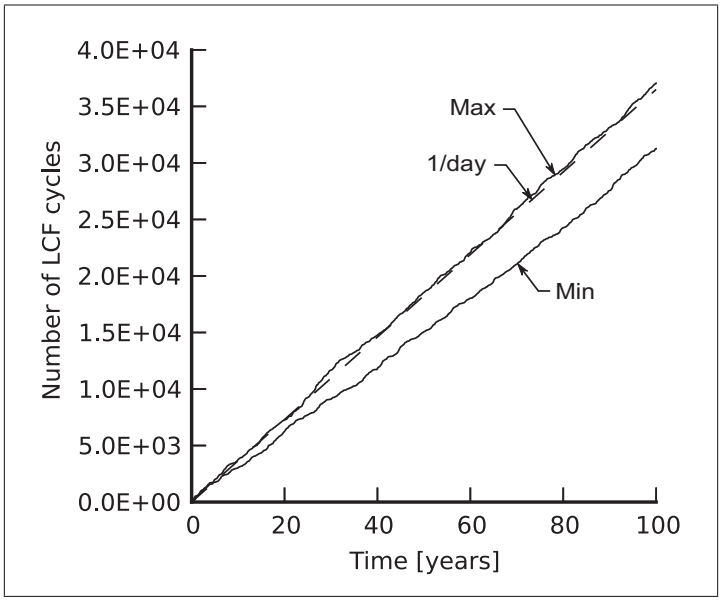

Figure 3.12 Extrapolated cumulative number of $N_{Startup}$ + N_{SNL} cycles

The load spectrum obtained from the combined load pattern and operation history is presented in Figure 3.13. In this study, the stress cycles are defined according to the Rychlik (Rychlik, 1987) rainflow definition. The damage from each stress cycle is accounted for when the cycle reaches its maximum value.

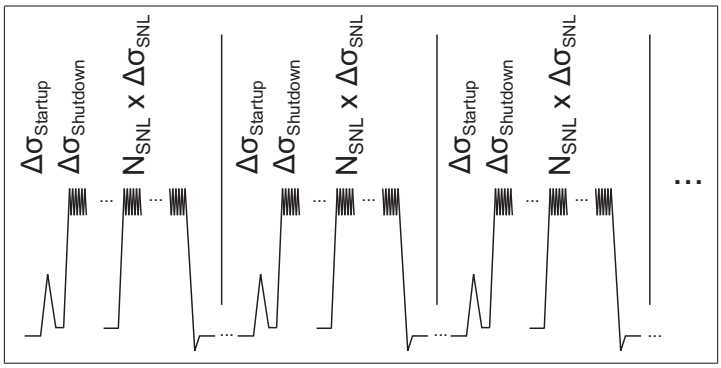

Figure 3.13 Proposed load spectrum

The estimated parameter values are presented in Table 3.1. All the random parameters except the number of startup $N_{Startup}$ have a Gumbel distribution with the following cumulative distribution:

$$F(x) = exp\left(-e^{\frac{-(x-\mu)}{\sigma}}\right) \tag{3.13}$$

The Gumbel distribution is a particular case of the Generalized Extreme Value (GEV) distribution which describes the uncertainty around the largest event of a sample (i.e. block maxima). This distribution was chosen because it has already been used in the literature to model both the extremes of load spectra (Johannesson, 2006) and the defect size (Murakami, 2002; Beretta *et al.*, 2006). Interestingly, such an assumption reasonably describes the largest events for a wide range of distributions such as the normal, log-normal and Weibull distributions. These distributions are approximately exponentially distributed above a high-enough threshold (Pickands III, 1975; Davison et Smith, 1990), hence they have an extreme value distribution of the Gumbel family (Coles, 2001). Please note that the parameter values for each random variable, except for the defect size, are based on the authors' opinions with regards to the available observed data. However, since no reliable data were available at the time of the study for the defect size parameter a, the location has been defined arbitrarily as half the typical allowable defect size of 3 mm combined with a scale value that allows the allowable size to be a probable value.

Tableau 3.1 Study case parameters

	Location	**Scale**	**Distribution**	**Units**
K_{th}	2.0	-	-	MPa $m^{1/2}$
a	1.5	0.5	Gumbel	mm
$\Delta\sigma_{HCF}$	26.0	1.0	Gumbel	MPa
$\Delta\sigma_{Startup}$	70.0	1.0	Gumbel	MPa
$\Delta\sigma_{Shutdown}$	120.0	2.0	Gumbel	MPa
$\Delta\sigma_{SNL}$	100.0	2.0	Gumbel	MPa
$N_{Startup}$	0.232	0.007	Normal	day^{-1}
N_{SNL}	3	-	-	$Startup^{-1}$

3.5 Results

Starting with the observed loading as a reference, three load spectra were modeled with different levels of simplification. The load spectra are the following:

a. The spectrum as presented in Figure 3.13 which uses the proposed simplified load pattern shown in Figure 3.9. This spectrum accounts for the transient events.

b. The spectrum without transients which uses the loading pattern in Figure 3.1 combined with a number of LCF cycles $N_{LCF} = N_{Startup}$ + N_{SNL} as shown in Figure 3.12.

c. The spectrum without transients which uses the loading pattern in Figure 3.1 combined with a number of LCF cycles $N_{LCF} = N_{Startup}$ as shown in Figure 3.10.

These three simplified loading spectra are compared both in terms of expected crack propagation and estimated reliability. The deterministic crack propagation results for the three simplified loading spectra and the observed loading spectrum generated using the measured loading (Figure 3.2) are compared in Figure 3.14. We notice that the results are closer to the observed loading for load spectrum which include transient events. The discrepancy becomes significantly larger as more features are neglected. Note that the loading pattern which accounts for

only the number of startups without transient (3) is the typically specified in design requirements for this type of runner. We observe, in our case study, that such assumptions could lead to significant bias between expected and actual reliability.

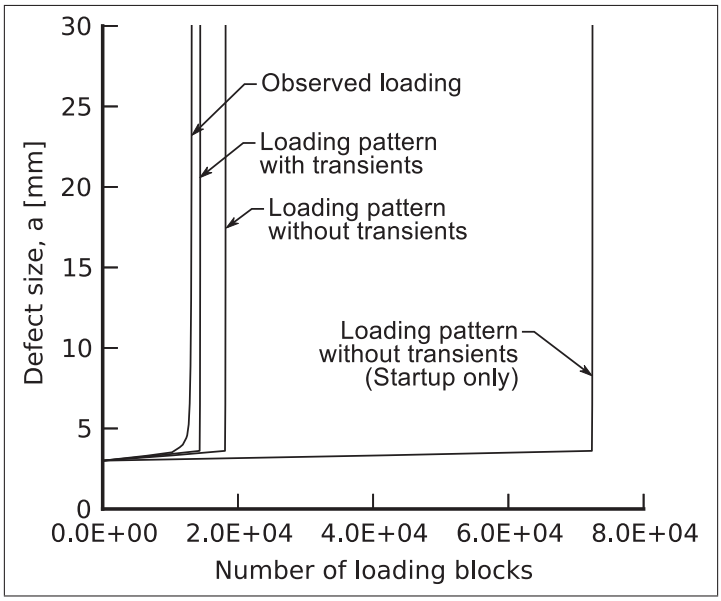

Figure 3.14 Deterministic crack propagation results

The reliability results for the three simplified loading spectra obtained using the parameter values in Table 3.1 are shown in Figure 3.15. These results are also compared to the results obtained when the defect size distribution scale value is divided by a factor of 2. By lowering the scale parameter, the defect size dispersion is reduced. This in turn, lowers the probability of large defects. We notice that lowering the probability of having large defects has significantly more influence on the reliability results than a change in loading pattern assumptions.

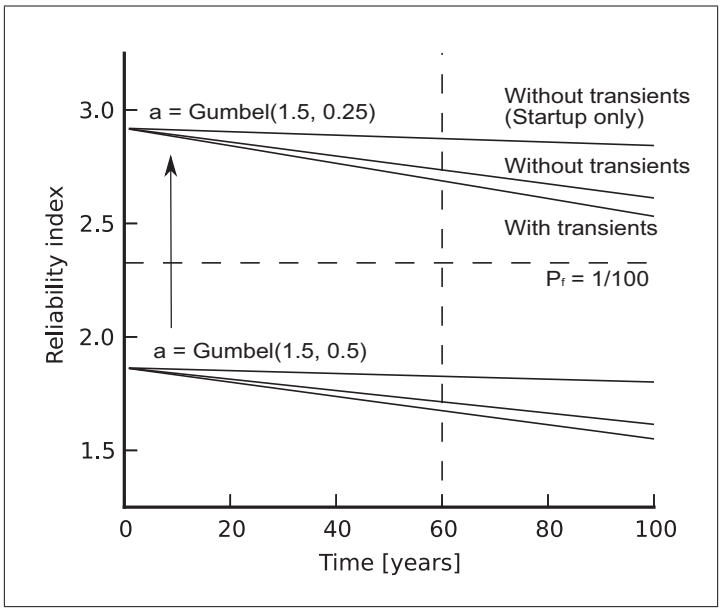

Figure 3.15 Reliability index as a function of time

The influence of the defect size a compared to the other parameters is even more obvious when looking at the importance factor at 60 years for the simplified load spectrum which includes transients on a pie chart as shown in Figure 3.16. In this figure, we observe that only the uncertainty around defect size a and the HCF stress range $\Delta\sigma_{HCF}$ contributes to the reliability index results. All the other parameters in this case could be considered deterministic. Note that these results completely conceal the influence of the the other parameters which are linked to the load spectra assumptions and LCF events.

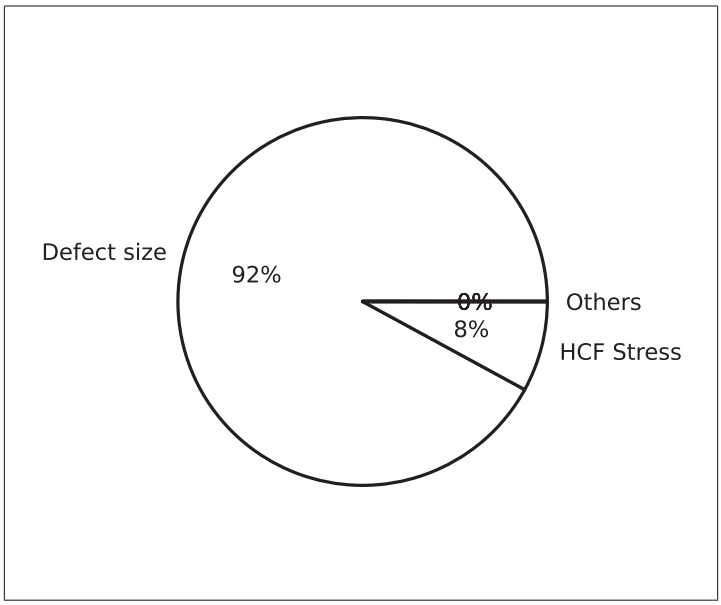

Figure 3.16 Importance factors for the load pattern with transients (1) at 60 years with a = Gumbel(1.5,0.25)

Furthermore, if we look at the sensitivity results for each of the parameters, shown in Figure 3.17, we still observe that the defect size a and HCF stress range $\Delta\sigma_{HCF}$ have a significant influence on the reliability index and again hide the influence of the other parameters which are mostly linked to load spectrum assumptions and LCF events.

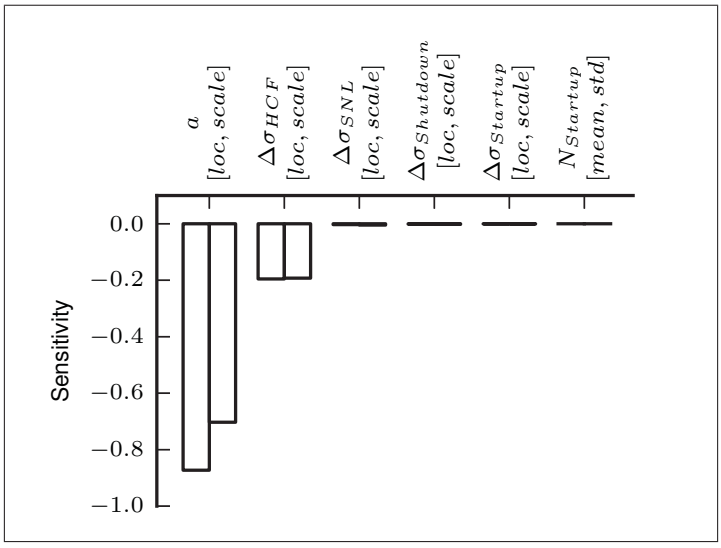

Figure 3.17 Reliability index sensitivity for load pattern with transients (1) at 60 years with a = Gumbel(1.5,0.25)

The observed lack of sensitivity to the parameters related to the LCF loading is mainly due to the slow rate at which the reliability decreases with time. To significantly influence the reliability, even after 60 years, the load pattern assumptions have to be changed ; not just their parameter values. The influence of these assumption changes cannot be highlighted by either sensitivity metrics.

3.6 Discussion

From the results presented in the previous section, if major transient events are neglected and only the number of startups are assumed, one could conclude that reliability is almost insensitive to the parameters related to the LCF part of the loading spectrum and that reliability does not change significantly with time. Our results show that not only some load spectrum assumptions can have significant influence on the expected reliability but that this influence is completely hidden by parameters like defect size a and HCF stress range $\Delta\sigma_{HCF}$. In this case study, typical metrics like importance factors and reliability index sensitivity factors were not able to highlight the influence of assumption changes. With both metrics, the influence of some significant parameters in our study is overlooked. Such results are in line with the work of Aven and Guikema (Aven et Guikema, 2011) which concludes that, for risk assessment, sensitivity analysis should also include the effect of assumptions choices as a rule.

However, our case study was conducted on only one specific runner design. Hence, care must be taken before generalizing the results from this study because the loads can vary significantly among different runner designs. We have observed that operation histories can differ significantly even for runners with identical designs emanating from the same hydroelectric facility. Furthermore, we note that the critical area investigated is a stress relief cut-out near the crown of the runner which is not a common feature found on hydroelectric turbine runners. Since the observed stress variations depend as much on operating conditions than on deform shape changes from one condition to another, such data might be difficult to standardize as they are design specific. For example, the maximum stress amplitude is observed in Figure 3.18 at the spin no-load condition, rather than the maximum opening condition found in our case study. Additionally, we observe for this runner design that the critical permanent regime is

not at the maximum wicket gate opening but at the spin-no-load condition. Unfortunately, in Figure 3.18, the transition between operating conditions and the shutdown transient were not available. Hence they cannot be shown.

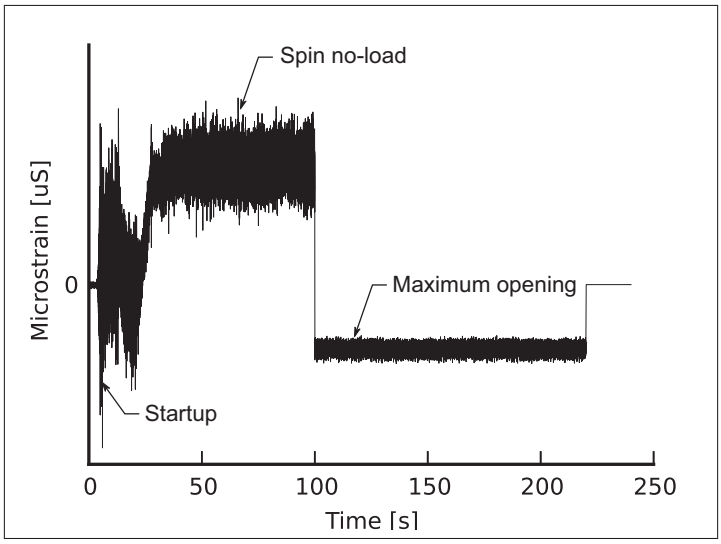

Figure 3.18 Example of a measured loading sequence from a different runner design

Such differences, if not correctly acknowledged during the runner design, may, lead to large discrepancies between predicted reliability and actual reliability.

3.7 Conclusions

The absence of observed data renders the reliability assessment of structures such as hydroelectric runners difficult. To alleviate this problem, some simplifications have to be made in order to minimize the number of parameters needed to generate the load spectrum used to assess the reliability of these large rotating structures. Our results show that the loading spectrum for such structures can be significantly simplified. In our case study, we observe that if the HCF onset is used as a failure criterion, the load spectrum can be limited to the following parameters without major reliability bias:

a. The maximum stress range of the startup transient.

b. The maximum stress range of the shutdown transient.

c. The frequency of startup/shutdown.

d. The maximum stress ranges generated by each major load change.

e. The frequency of each major load change.

f. The maximum stress range of the critical steady state regime.

Results obtained using deterministic crack growth show that such simplifications have limited impact on calculated life expectancy. Note that further simplifications have resulted in significant discrepancies in terms of deterministic crack growth and reliability estimates. Within these parameters, we observed that parameters 1 to 5 mainly influence the rate at which reliability decreases with time. On the other hand, the defect size and parameter 1 of the load spectrum influence initial reliability. Moreover, in our study, these two parameters tend to hide the influence of the other parameters when typical sensitivity analysis metrics are used. As a result, we believe that in the absence of observed data, fatigue reliability analysis should include an assessment of the influence of load spectrum assumptions. Currently, the lack of either standardized load spectrum or observed data from existing hydroelectric turbine runners in the literature make it difficult to construct such *a priori* assumptions. We hope that the data, results and methodology presented in this study will stimulate further research into the risk associated with such large rotating structures.

Acknowledgments

The authors would like to thank the *Institut de recherche d'Hydro-Québec* (IREQ), Andritz Hydro Ltd and the *École de technologie supérieure* (ÉTS) for their collaboration and financial contribution.

CONCLUSION

Dans cette thèse, nous avons entrepris d'approfondir la notion de fiabilité des aubes de turbines hydroélectriques. Les nouvelles exigences reliées à la déréglementation des marchés de l'électricité forcent les producteurs à opérer les turbines hydroélectriques dans des scénarios d'utilisation différents de ceux traditionnellement utilisés lors de la conception celles-ci. Ces nouveaux scénarios d'utilisation soulèvent deux questions fondamentales:

- Quelle est la limite à ne pas dépasser?
- Où sommes-nous situés par rapport à la limite?

Face à ces deux problématiques fondamentales, nous avons, dans cette thèse, contribué à répondre aux trois questions suivantes:

- Chapitre 1: Peut-on estimer l'incertitude sur le chargement d'un évènement transitoire?
- Chapitre 2: Comment définir l'état limite pour la fatigue d'une aube de turbine?
- Chapitre 3: Nos hypothèses sur le chargement ont-elles une influence sur la fiabilité?

Contributions et apports

Le chargement dynamique est principalement responsable du dommage en fatigue dans les structures. Nous avons mis en évidence dans les travaux préliminaires que nous avons effectués plusieurs problématiques reliées au chargement dynamique généré par les évènements transitoires lors du démarrage des turbines hydroélectriques (Gagnon *et al.*, 2010a,b). Une de ces problématiques est reliée à la nature stochastique de ces événements pour lesquels nous n'avons que peu de données observées. Le Chapitre 1 présente nos résultats sur la simulation de ce type d'événements transitoires (Gagnon *et al.*, 2012a). Les travaux que nous avons effectués sur ces phénomènes permettent d'entrevoir l'optimisation des automatismes qui régissent ces évènements comme une piste d'amélioration de la fiabilité en fatigue pour les turbines hydroélectriques.

Par la suite, dans le Chapitre 2, nous nous sommes attaqués aux deux questions fondamentales étudiées dans cette thèse. Nous avons proposé, dans ce chapitre, un état limite adapté au calcul de la fiabilité en fatigue des aubes de turbines hydroélectriques (Gagnon *et al.*, 2013a). Cet état limite permet d'estimer un indice de fiabilité proportionnel à la distance par rapport à celui-ci. L'état limite combine des informations qui étaient auparavant traitées de manière indépendante, et dont les interactions étaient négligées. Ces informations sont regroupées en trois catégories:

- Les paramètres du chargement de la structure ;
- Les propriétés en fatigue du matériau ;
- L'état de la structure et les caractéristiques des défauts contenus dans celle-ci.

L'état limite développé correspond au diagramme de Kitagawa (Kitagawa et Takahashi, 1976) combiné à la correction développée par El Haddad (El Haddad *et al.*, 1979). Cette limite habituellement utilisée pour définir la zone de vie infinie d'un matériau n'est pas nouvelle, mais elle n'avait jamais été appliquée dans le contexte de l'évaluation de fiabilité en fatigue.

Par la suite, la méthodologie a été utilisée au Chapitre 3 pour étudier l'influence des hypothèses sur le chargement en l'absence de données observées. Nos résultats confirment l'importance des événements transitoires identifiés au Chapitre 1. Nous constatons que pour évaluer les risques, il ne faut pas seulement évaluer la sensibilité des résultats par rapport aux valeurs utilisées, mais aussi par rapport aux choix du modèle et des paramètres.

Originalité de la thèse

L'originalité des travaux effectués a permis d'initier plusieurs projets de recherche à l'intérieur desquels nous avons joué un rôle de coordination et d'intégration. L'ensemble des publications que nous avons effectuées en lien avec les travaux de recherche de cette thèse est, par ordre chronologique:

- Gagnon, M., S. A. Tahan, P. Bocher, et D. Thibault. 2010a. « Impact of startup scheme on Francis runner life expectancy ». *IOP Conference Series: Earth and Environmental Science*, vol. 12, n° 1, p. 012107
- Gagnon, M., S.-A. Tahan, P. Bocher, et D. Thibault. 2010b. « Impact of startup scheme on Francis runner life expectancy and reliability ». In *28th CMVA seminar, 27-29 of October 2010, Quebec*
- Szczota, M., M. Gagnon, A. Tahan, L. Marcouiller, et D. Thibault. 2011. « Modeling Operation History of Hydroelectric Turbines ». In *HydroVision International, July 19-22, Sacramento, California, USA*
- Gagnon, M., A. Tahan, P. Bocher, et D. Thibault. 2012a. « On the stochastic simulation of hydroelectric turbine blades transient response ». *Mechanical Systems and Signal Processing*, vol. 32, n° 0, p. 178-187
- Gagnon, M., S.-A. Tahan, P. Bocher, et D. Thibault. 2012b. « The role of high cycle fatigue (HCF) onset in Francis runner reliability ». *IOP Conference Series: Earth and Environmental Science*, vol. 15, n° 2, p. 022005
- Arpin-Pont, J., M. Gagnon, S.-A. Tahan, A. Coutu, et D. Thibault. 2012. « Strain gauge measurement uncertainties on hydraulic turbine runner blade ». *IOP Conference Series: Earth and Environmental Science*, vol. 15, n° 6, p. 062042
- Poirier, M., A. Tahan, M. Gagnon, et A. Coutu. 2012. « Extrapolation des signaux de chargement mesurés sur des aubes de turbine hydroélectrique de type Francis ». In *CMVA Machinery Vibration, Reliability and Maintenance Seminar, 24-26 Octobre 2012, Niagara Falls, ON*
- Gagnon, M., A. Tahan, P. Bocher, et D. Thibault. 2013a. « A probabilistic model for the onset of High Cycle Fatigue (HCF) crack propagation: Application to hydroelectric turbine runner ». *International Journal of Fatigue*, vol. 47, n° 0, p. 300-307
- Gagnon, M., A. Tahan, P. Bocher, et D. Thibault. 2013b. « Influence of load spectrum assumptions on the expected reliability of hydroelectric turbines: A case study ». *submitted to Structural Safety*

Perspectives

Nous n'avons toutefois pas réussi à répondre à toutes les questions générées au cours de cette recherche. La première problématique est la forte influence que les defauts contenus dans la structure ont sur la fiabilité (Gagnon *et al.*, 2013a, 2012b). Nous avons démontré dans les Chapitres 2 et 3 que les paramètres liés aux caractéristiques des défauts ont une importance significative sur la fiabilité des aubes de turbines hydroélectriques. Par contre, aucune étude dans notre revue de la littérature n'est reliée à l'estimation des défauts pour les matériaux, géométries et procédés de fabrication spécifiques aux turbines hydroélectriques. Compte tenu de la sensibilité de notre modèle à ces caractéristiques, nous jugeons qu'il y a là un potentiel important de développement.

Un autre groupe de paramètres, mis en évidence par nos travaux, sont les propriétés du matériau. Dans nos travaux de recherche, les propriétés utilisées proviennent de standards internationaux (British Standards Institute, 2005). Ces valeurs sont adéquates dans l'optique du développement d'une méthodologie, de la conception ou du calcul de la probabilité de rencontrer les exigences de ces standards. Par contre, ces valeurs ne permettent pas d'évaluer la fiabilité réelle de la structure. Pour ce faire, une meilleure compréhension de paramètres tels que le seuil de propagation K_{th} en présence de chargement combiné HCF/LCF pour les matériaux employés dans la fabrication des turbines hydroélectriques s'avère souhaitable. Nous détenons que très peu de données expérimentales pour ces matériaux. Ceci limite significativement notre compréhension de la transition entre la propagation causée par le chargement LCF et celle générée par le chargement HCF.

Un troisième aspect à ne pas négliger est la nature du chargement. Ce dernier est au centre de la majorité des travaux présentés dans cette thèse. L'incertitude sur le chargement dépend de plusieurs facteurs tels que: la séquence des opérations des groupes turbine-alternateurs, les paramètres hydrauliques des centrales hydroélectriques et les paramètres de conception mécanique des turbines. De plus, on doit y ajouter, l'incertitude générée par les méthodes de mesure utilisées pour quantifier ces paramètres et la quantité restreinte de données disponibles. Dans cette thèse, uniquement l'aspect stochastique des démarrages de la turbine a été étudié.

Toutefois, tel que présenté dans le Chapitre 3, le démarrage n'est qu'un des paramètres du chargement. Plusieurs autres paramètres du chargement relié aux transitoires lors de l'arrêt et aux changements de puissances n'ont pas été étudiés malgré que ceux-ci possèdent une influence non négligeable sur la fiabilité estimée (Gagnon *et al.*, 2013b).

Nous avons développé dans cette thèse la capacité d'agréger les données nécessaires pour obtenir la fiabilité. Par contre, les méthodes necessaires à l'obtention de ces données de manière adéquate n'a pas été traitée. Nous espérons que les travaux présentés dans cette thèse permettront de stimuler la recherche dans ce domaine d'application en ingénierie.

Épilogue

Les perspectives de recherche générées par les travaux présentés dans cette thèse ont permis d'initier plusieurs activités de recherche tant en parallèle et qu'à la suite de ceux-ci. Certaines de ces activités ont été complétées avant la fin des travaux présentés dans cette thèse. À ce titre, mentionnons les travaux de maîtrise de Szczota *et al.* (2011); Szczota (2012) et Arpin-Pont *et al.* (2012); Arpin-Pont (2012). De plus, certains travaux sont toujours en cours: les travaux de Poirier *et al.* (2012) qui sont effectués dans le cadre d'une maîtrise sur l'extrapolation du chargement en régime permanent des turbines hydroélectriques et qui se terminera à l'été 2013, les travaux de doctorat d'Hamid Habibzadeh Boukani initiés en 2012 sur les méthodes non destructives d'inspection des aubes de turbines hydroélectriques et les travaux de Firas Ben Salah dans une maîtrise sur l'interpolation spatiale des mesures de déformations qui ont débuté en 2013. On remarque aussi certaines activités entreprises en parallèle aux nôtres par des chercheurs du centre de recherche d'Hydro-Québec (IREQ). Notons, à ce titre, les travaux sur la modélisation des phénomènes transitoires à l'aide de la mécanique des fluides de Nicolle *et al.* (2012). Finalement, mentionnons l'implantation du modèle de fiabilité présenté dans cette thèse dans les outils de prédiction et diagnostic de la dégradation des turbines hydroélectriques actuellement en développement à l'IREQ.

BIBLIOGRAPHIE

Altamura, A. et S. Beretta. 2012. « Reliability assessment of hydraulic cylinders considering service loads and flaw distribution ». *International Journal of Pressure Vessels and Piping*, vol. 98, n° 0, p. 7-88.

Annis, C. 2004. « Probabilistic Life Prediction Isn't as Easy as It Looks ». *Journal of ASTM International*, vol. 1, p. 1-12.

Anthes, R. J. 1997. « Modified rainflow counting keeping the load sequence ». *International Journal of Fatigue*, vol. 19, n° 7, p. 529-535.

Arpin-Pont, J. 2012. « Méthode de détermination des incertitudes de mesures par jauges de déformation ». Master's thesis, École de technologie superieure.

Arpin-Pont, J., M. Gagnon, S.-A. Tahan, A. Coutu, et D. Thibault. 2012. « Strain gauge measurement uncertainties on hydraulic turbine runner blade ». *IOP Conference Series: Earth and Environmental Science*, vol. 15, n° 6, p. 062042.

ASTM Standard E1049. 2011. « Standard Practices for Cycle Counting in Fatigue Analysis ».

Atzori, B. et P. Lazzarin. 2002. « A three-dimensional graphical aid to analyze fatigue crack nucleation and propagation phases under fatigue limit conditions ». *International Journal of Fracture*, vol. 118, p. 271-284.

Atzori, B., P. Lazzarin, et G. Meneghetti. 2003. « Fracture mechanics and notch sensitivity ». *Fatigue & Fracture of Engineering Materials & Structures*, vol. 26, n° 3, p. 257-267.

Aven, T. 2012. « The risk concept - historical and recent development trends ». *Reliability Engineering & System Safety*, vol. 99, p. 33-44.

Aven, T. et S. Guikema. 2011. « Whose uncertainty assessments (probability distributions) does a risk assessment report: the analysts' or the experts'? ». *Reliability Engineering &amp ; System Safety*, vol. 96, n° 10, p. 1257-1262.

Ayala-Uraga, E. et T. Moan. 2007. « Fatigue reliability-based assessment of welded joints applying consistent fracture mechanics formulations ». *International Journal of Fatigue*, vol. 29, p. 444-456.

Bedrosian, E. 1963. « A product theorem for Hilbert transforms ». *Proceedings of the IEEE*, vol. 51, n° 5, p. 868-869.

Beretta, S., C. Anderson, et Y. Murakami. 2006. « Extreme value models for the assessment of steels containing multiple types of inclusion ». *Acta Materialia*, vol. 54, n° 8, p. 2277-2289.

Bloom, J. M. et J. C. Ekvall, 1983. *Probabilistic Fracture Mechanics and Fatigue Methods: Applications for Structural Design and Maintenance, ASTM STP 798*. American Society for Testing and Materials.

Breitung, K. 1989. « Asymptotic approximations for probability integrals ». *Probabilistic Engineering Mechanics*, vol. 4, n° 4, p. 187-190.

British Standards Institute. 2005. « Guidance on some methods for the assessment of flaws in welded construction, BS7910 ».

Bryan, D. F. et J. M. Potter, 1980. *Effect of Load Spectrum Variables on Fatigue Crack Initiation and Propagation, ASTM STP 714*. American Society for Testing and Materials.

Byrne, J., R. F. Hall, et B. E. Powell. 2003. « Influence of LCF overloads on combined HCF/LCF crack growth ». *International Journal of Fatigue*, vol. 25, n° 9-11, p. 827-834.

Carboni, M., A. Cerrini, P. Johannesson, M. Guidetti, et S. Bereta. 2008. « Load spectra analysis and reconstruction for hydraulic pump components ». *Fatigue & Fracture of Engineering Materials & Structures*, vol. 31, p. 251-261.

Castillo, E., A. Fernandez-Canteli, H. Pinto, et M. L. Ruiz-Ripoll. 2008. « A statistical model for crack growth based on tension and compression Wöhler fields ». *Engineering Fracture Mechanics*, vol. 75, p. 4439-4449.

Cerrini, A., P. Johannesson, et S. Beretta. 2006. « Superposition of manoeuvres and load spectra extrapolation ». *Applied Mechanics and Materials*, vol. 5-6, p. 255-262.

Chryssanthopoulos, M. K. et T. D. Righiniotis. 2006. « Fatigue reliability of welded steel structures ». *Journal of Constructional Steel Research*, vol. 62, p. 1199-1209.

Ciavarella, M. et F. Monno. 2006. « On the possible generalizations of the Kitagawa-Takahashi diagram and of the El Haddad equation to finite life ». *International Journal of Fatigue*, vol. 28, n° 12, p. 1826-1837.

Coles, S., 2001. *An introduction to statistical modeling of extreme values*. Springer series in statistics. Springer.

Coutu, A., M. Gagnon, et C. Monette. 2007. « Life Assessment of Francis Runners Using Strain Gage Site Measurements ». In *WaterPower XV, Chattanooga, USA*.

Cross, R. J., A. Makeev, et E. Armanios. 2006. « A Comparison of Predictions From Probabilistic Crack Growth Models Inferred From Virkler's Data ». *Journal of ASTM International*, vol. 3, p. 1-11.

Davison, A. C. et R. L. Smith. 1990. « Models for Exceedances over High Thresholds ». *Journal of the Royal Statistical Society. Series B (Methodological)*, vol. 52, n° 3, p. 393-442.

Ditlevsen, O. et H. O. Madsen, 2007. *Structural reliability methods*. Internet edition 2.2.7.

Divenah, L. L. et J.-Y. Beaufils. 2004. « Large Commercial Aircraft Loading Spectra: Overview and State of the Art ». *Journal of ASTM International*, vol. 1, n° 10, p. 1-13.

Doerfler, P., M. Sick, et A. Coutu, 2013. *Flow-Induced Pulsation and Vibration in Hydroelectric Machinery: Engineer's Guidebook for Planning, Design and Troubleshooting*. Springer London.

Doker, H. 1997. « Fatigue crack growth threshold: implications, determination and data evaluation ». *International Journal of Fatigue*, vol. 19, n° 93, p. 145-149.

Dressler, K., B. Grunder, M. Hack, et V. B.: Kottgen. 1996. « Extrapolation of Rainflow Matrices ». *SAE, technical paper 960569*.

El Haddad, M. H., T. H. Topper, et K. N. Smith. 1979. « Prediction of non propagating cracks ». *Engineering Fracture Mechanics*, vol. 11, n° 3, p. 573-584.

Ellens, M., J. Provan, G. McLean, et M. Sanders. 1997. Fatigue and reliability assessment incorporating computer strain gage network data. Braun, A. A. et L. N. Gilbertson, editors, *Applications of Automation Technology to Fatigue and Fracture Testing and Analysis: Third Volume, ASTM STP 1303*, p. 19-32. American Society for Testing and Materials.

Flandrin, P., G. Rilling, et P. Goncalves. Février 2004. « Empirical Mode Decomposition as a Filter Bank ». *IEEE Signal Processing Letters*, vol. 11, p. 112-114.

Gagnon, M., S. A. Tahan, P. Bocher, et D. Thibault. 2010a. « Impact of startup scheme on Francis runner life expectancy ». *IOP Conference Series: Earth and Environmental Science*, vol. 12, n° 1, p. 012107.

Gagnon, M., S.-A. Tahan, P. Bocher, et D. Thibault. 2010b. « Impact of startup scheme on Francis runner life expectancy and reliability ». In *28th CMVA seminar, 27-29 of October 2010, Quebec*.

Gagnon, M., A. Tahan, P. Bocher, et D. Thibault. 2012a. « On the stochastic simulation of hydroelectric turbine blades transient response ». *Mechanical Systems and Signal Processing*, vol. 32, n° 0, p. 178-187.

Gagnon, M., S.-A. Tahan, P. Bocher, et D. Thibault. 2012b. « The role of high cycle fatigue (HCF) onset in Francis runner reliability ». *IOP Conference Series: Earth and Environmental Science*, vol. 15, n° 2, p. 022005.

Gagnon, M., A. Tahan, P. Bocher, et D. Thibault. 2013a. « A probabilistic model for the onset of High Cycle Fatigue (HCF) crack propagation: Application to hydroelectric turbine runner ». *International Journal of Fatigue*, vol. 47, n° 0, p. 300-307.

Gagnon, M., A. Tahan, P. Bocher, et D. Thibault. 2013b. « Influence of load spectrum assumptions on the expected reliability of hydroelectric turbines: A case study ». *submitted to Structural Safety*.

Genet, G. 2006. « A statistical approach to multi-input equivalent fatigue loads for the durability of automotive structures ». PhD thesis, Chalmers University of Technology and Göteborg University.

Grigoriu, M., 1995. *Applied non-Gaussian processes: examples, theory, simulation, linear random vibration, and MATLAB solutions*. PTR Prentice Hall.

Gurley, K. R., M. A. Tognarelli, et A. Kareem. 1997. « Analysis and simulation tools for wind engineering ». *Probabilistic Engineering Mechanics*, vol. 12, n° 1, p. 9-31.

Heng, A., S. Zhang, A. C. C. Tan, et J. Mathew. 2009. « Rotating machinery prognostics: State of the art, challenges and opportunities ». *Mechanical Systems and Signal Processing*, vol. 23, p. 724-739.

Heuler, P. et H. Klatschke. 2005. « Generation and use of standardised load spectra and load-time histories ». *International Journal of Fatigue*, vol. 27, n° 8, p. 974-990.

Hohenbichler, M. et R. Rackwitz. 1988. « Improvement Of Second Order Reliability Estimates by Importance Sampling », vol. 114, n° 12. p. 2195-2199.

Hu, W., Y. C. Tong, K. F. Walker, D. Mongru, R. Amaratunga, et P. Jackson. 2006. *A review and assessment of current airframe lifing methodologies and tools in air vehicles division*. Technical report. Air Vehicles Division Defense Science and Technology Organization.

Huang, N. E. et Z. Wu. Juin 2008. « A review on Hilbert-Huang transform: Method and its applications to geophysical studies ». *Rev. Geophys.*, vol. 46, n° 2, p. RG2006.

Huang, N. E., Z. Shen, S. R. Long, M. C. Wu, H. H. Shih, Q. Zheng, N. C. Yen, C. C. Tung, et H. H. Liu. March 1998. « The empirical mode decomposition and the Hilbert spectrum for nonlinear and non-stationary time series analysis ». *Proceedings of the Royal Society of London. Series A: Mathematical, Physical and Engineering Sciences*, vol. 454, n° 1971, p. 903-995.

Huang, N. E., Z. Wu, S. R. Long, K. C. Arnold, X. Chen, et K. Blank. 2009. « On Instantaneous Frequency ». *Advances in Adaptive Data Analysis*, vol. 1, n° 2, p. 177-229.

Hydro-Québec. 2011. « Rapport annuel 2011 ». <http://www.hydroquebec.com/publications/fr/rapport_annuel/>.

IEA. 2012. *Technology roadmap: Hydropower*. Technical report. OECD/IEA.

IEEE. 1990. « IEEE Standard Glossary of Software Engineering Terminology ». *IEEE Std 610.12-1990*.

Jha, S. K., J. M. Larsen, et A. H. Rosenberger. 2008. « Towards a Physics-Based Description of Fatigue Variability Behavior in Probabilistic Life Prediction ». *Engineering Fracture Mechanics*.

Johannesson, P. 1999. « Rainflow analysis of switching markov loads ». PhD thesis, Lund Institute of Technology.

Johannesson, P. 2006. « Extrapolation of load histories and spectra ». *Fatigue and Fracture of Engineering Materials and Structures*, vol. 29, n° 3, p. 209-217.

Johannesson, P. et J.-J. Thomas. 2001. « Extrapolation of Rainflow Matrices ». *Extremes*, vol. 4, p. 241-262.

Kappas, J. 2002. *Review of risk and reliability methods for aircraft gas turbine engines*. Technical report. Airframes and Engines Division, Aeronautical and Maritime Research Laboratory.

Kareem, A. 2008. « Numerical simulation of wind effects: A probabilistic perspective ». *Journal of Wind Engineering and Industrial Aerodynamics*, vol. 96, n° 10-11, p. 1472-1497.

Kitagawa, H. et S. Takahashi. 1976. « Applicability of fracture mechanics to very small cracks ». In *ASM Proceedings of 2nd International Conference on Mechanical Behaviour of Materials, Metalspark, Ohio.* p. 627-631.

Klemenc, J. et M. Fajdiga. 2000. « Description of statistical dependencies of parameters of random load states (dependency of random load parameters) ». *International Journal of Fatigue*, vol. 22, n° 5, p. 357-367.

Klemenc, J. et M. Fajdiga. 2002. « A neural network approach to the simulation of load histories by considering the influence of a sequence of rainflow load cycles ». *International Journal of Fatigue*, vol. 24, n° 11, p. 1109-1125.

Klemenc, J. et M. Fajdiga. 2004. « An improvement to the methods for estimating the statistical dependencies of the parameters of random load states ». *International Journal of Fatigue*, vol. 26, n° 2, p. 141-154.

Klemenc, J. et M. Fajdiga. 2005. « Prediction of loading spectra under diverse operating conditions by a localised basis function neural network ». *International Journal of Fatigue*, vol. 27, n° 5, p. 555-568.

Klemenc, J. et M. Fajdiga. 2006. « Predicting smoothed loading spectra using a combined multilayer perceptron neural network ». *International Journal of Fatigue*, vol. 28, n° 7, p. 777-791.

Klemenc, J. et M. Fajdiga. 2008. « Improved modelling of the loading spectra using a mixture model approach ». *International Journal of Fatigue*, vol. 30, n° 7, p. 1298-1313.

Lange, C. H. 1996. *Probabilistic fatigue methodology and wind turbine reliability*. Technical report. SAND 96-1246, Sandia National Laboratories, Albuquerque, NM.

Lanteigne, J., M. Sabourin, T. Bui-Quoc, et D. Julien. 2007. « A comprehensive research program on crack propagation characteristics of the base material used in hydraulic turbine runners ». In *WaterPower XV, Chattanooga, USA*.

Lanteigne, J., M. Sabourin, T. Bui-Quoc, et D. Julien. 2008. « The Characteristics of the Steels used in Hydraulic Turbine runners ». In *IAHR 24th Symposium on Hydraulic Machinery and Systems, October 27-31, Foz do Iguassu*.

Lebrun, R. et A. Dutfoy. 2009a. « An innovating analysis of the Nataf transformation from the copula viewpoint ». *Probabilistic Engineering Mechanics*, vol. 24, n° 3, p. 312-320.

Lebrun, R. et A. Dutfoy. 2009b. « Do Rosenblatt and Nataf isoprobabilistic transformations really differ? ». *Probabilistic Engineering Mechanics*, vol. 24, n° 4, p. 577-584.

Liao, M. 2009. « Probabilistic modeling of fatigue related microstructural parameters in aluminum alloys ». *Engineering Fracture Mechanics*, vol. 76, n° 5, p. 668-680.

Liu, Y. et S. Mahadevan. 2009. « Probabilistic fatigue life prediction using an equivalent initial flaw size distribution ». *International Journal of Fatigue*, vol. 31, p. 476-487.

Murakami, Y., 2002. *Metal fatigue: effects of small defects and nonmetallic inclusions*. Elsevier, Oxford, UK.

Nagode, M. et M. Fajdiga. 1999. « The influence of variable operating conditions upon the general multi-modal Weibull distribution [service life prediction] ». *Reliability Engineering & System Safety*, vol. 64, n° 3, p. 383-389.

Nagode, M., J. Klemenc, et M. Fajdiga. 2001. « Parametric modelling and scatter prediction of rainflow matrices ». *International Journal of Fatigue*, vol. 23, n° 6, p. 525-532.

Naudascher, E. et D. Rockwell, 1994. *Flow-Induced Vibrations: An Engineering Guide*. Dover Civil and Mechanical Engineering Series. Dover Publications.

Nicholas, T., 2006. *High Cycle Fatigue: A Mechanics of Materials Perspective*. Elsevier.

Nicolle, J., J.-F. Morissette, et A.-M. Giroux. 2012. « Transient CFD simulation of a Francis turbine startup ». *IOP Conference Series: Earth and Environmental Science*, vol. 15, n° 6, p. 062014.

Nuttall, A. H. 1966. « On the quadrature approximation to the Hilbert transform of modulated signals ». *Proceedings of the IEEE*, vol. 54, n° 10, p. 1458-1459.

Olhede, S. et A. T. Walden. 2004. « The Hilbert spectrum via wavelet projections ». *Proceedings of the Royal Society of London. Series A: Mathematical, Physical and Engineering Sciences*, vol. 460, n° 2044, p. 955-975.

Olhede, S. et A. T. Walden. 2005. « A generalized demodulation approach to time-frequency projections for multicomponent signals ». *Proceedings of the Royal Society A: Mathematical, Physical and Engineering Science*, vol. 461, n° 2059, p. 2159-2179.

Percival, D. B. et A. T. Walden, 2000. *Wavelet Methods for Time Series Analysis*. Cambridge University Press.

Pickands III, J. 1975. « Statistical Inference Using Extreme Order Statistics ». *The Annals of Statistics*, vol. Vol. 3, No. 1, p. 119-131.

Poirier, M., A. Tahan, M. Gagnon, et A. Coutu. 2012. « Extrapolation des signaux de chargement mesurés sur des aubes de turbine hydroélectrique de type Francis ». In *CMVA Machinery Vibration, Reliability and Maintenance Seminar, 24-26 Octobre 2012, Niagara Falls, ON*.

Potter, J. M. et R. T. Watanabe, 1989. *Development of Fatigue Loading Spectra, ASTM STP 1006*. American Society for Testing and Materials.

Priestley, M. B. 1965. « Evolutionary Spectra and Non-Stationary Processes ». *Journal of the Royal Statistical Society. Series B (Methodological)*, vol. 27, n° 2, p. pp. 204-237.

Rackwitz, R. 2001. « Reliability analysis - a review and some perspectives ». *Structural Safety*, vol. 23, n° 4, p. 365-395.

Rychlik, I. 1987. « A new definition of the rainflow cycle counting method ». *International Journal of Fatigue*, vol. 9, n° 2, p. 119-121.

Rychlik, I. 1993. « Note on cycle counts in irregular loads ». *Fatigue & Fracture of Engineering Materials & Structures*, vol. 16, n° 4, p. 377-390.

Rychlik, I. 1996. « Simulation of load sequences from rainflow matrices: Markov method ». *International Journal of Fatigue*, vol. 18, p. 429-438.

Sabourin, M., D. Thibault, D.-A. Bouffard, et M. Lévesque. 2010. « Hydraulic Runner Design Method for Lifetime ». *International Journal of Fluid Machinery and Systems*, vol. 3, n° 4, p. 301-308.

Sankararaman, S., Y. Ling, et S. Mahadevan. 2011. « Uncertainty quantification and model validation of fatigue crack growth prediction ». *Engineering Fracture Mechanics*, vol. 78, n° 7, p. 1487-1504.

Schijve, J. Mai 2003. « Fatigue of Structures and Materials in the 20th Century and the State of the Art ». *Materials Science*, vol. 39, n° 3, p. 307-333.

Sharpe, P. S., B. M. Hillberry, et B. A. Craig. 2004. « Fatigue Life Variability Prediction Based on Crack Forming Inclusions in a High Strength Alloy Steel ». *Journal of ASTM International*, vol. 1, n° 8, p. 1-14.

Skorupa, M. 1998. « Load interaction effects during fatigue crack growth under variable amplitude loading - A litterature review. Part I: Empirical trends ». *Fatigue & Fracture of Engineering Materials & Structures*, vol. 21, n° 8, p. 987-1006.

Socie, D. 2001. « Modelling expected service usage from short-term loading measurements ». *International Journal of Materials & Product Technology*, vol. 16, p. 295-303.

Socie, D. F. et M. A. Pompetzki. 2004. « Modeling variability in service loading spectra ». *ASTM Special Technical Publication*, , p. 46-57.

Sykora, M. 2006. « Advanced Load Effect Model for Probabilistic Structural Design ». *Acta Polytechnica*, vol. 46, p. 28-34.

Szczota, M. 2012. « Modélisation de l'historique d'opération de groupes turbine-alternateur ». Master's thesis, École de technologie superieure.

Szczota, M., M. Gagnon, A. Tahan, L. Marcouiller, et D. Thibault. 2011. « Modeling Operation History of Hydroelectric Turbines ». In *HydroVision International, July 19-22, Sacramento, California, USA*.

Thieulot-Laure, E., S. Pommier, et S. Fréchinet. 2007. « A multiaxial fatigue failure criterion considering the effects of the defects ». *International Journal of Fatigue*, vol. 29, n° 9-11, p. 1996-2004.

Tong, Y. C. 2001. *Literature review on aircraft structural risk and reliability analysis*. Technical report. DSTO Aeronautical and Maritime Research Laboratory.

Tovo, R. 2001. « On the fatigue reliability evaluation of structural components under service loading ». *International Journal of Fatigue*, vol. 23, n° 7, p. 587-598.

Tvedt, L. 1988. « Second order reliability by an exact integral ». In *Proc. of the IFIP Working Conf. Reliability and Optimization of Structural Systems*. p. 377-384.

Wang, L. 2007. « Stochastic modeling and simulation of transient events ». PhD thesis, Department of Civil Engineering and Geological Sciences, University of Notre Dame, Notre Dame, IN.

Wang, X., M. Rabiei, J. Hurtado, M. Modarres, et P. Hoffman. 2009. « A probabilistic-based airframe integrity management model ». *Reliability Engineering &amp ; System Safety*, vol. 94, n° 5, p. 932-941.

Wen, Y. K. et P. Gu. 2004. « Description and Simulation of Nonstationary Processes Based on Hilbert Spectra ». *Journal of Engineering Mechanics*, vol. 130, n° 8, p. 942-951.

Wen, Y. K. et P. Gu, 2005. *The Hilbert-Huang Transform in Engineering*, chapter Simulation of Nonstationary Random Processes Using Instantaneous Frequency and Amplitude from Hilbert-Huang Transform, p. 191-212. CRC Press.

Wu, W. F. et C. C. Ni. 2007. « Statistical aspects of some fatigue crack growth data ». *Engineering Fracture Mechanics*, vol. 27, p. 2952-2963.

Wu, W. et C.C. Ni. 2003. « A study of stochastic fatigue crack growth modeling through experimental data ». *Probabilistic Engineering Mechanics*, vol. 18, p. 107-118.

Wu, W. et C.C. Ni. 2004. « Probabilistic models of fatigue crack propagation and their experimental verification ». *Probabilistic Engineering Mechanics*, vol. 19, p. 247-257.

Wu, Z. et N. E. Huang. Juin 2004. « A study of the characteristics of white noise using the empirical mode decomposition method ». *Royal Society of London Proceedings Series A*, vol. 460, p. 1597-1611.

Wu, Z. et N. E. Huang. 2009. « Ensemble Empirical Mode Decomposition: a Noise-Assisted Data Analysis Method ». *Advances in Adaptive Data Analysis*, vol. 1, n° 1, p. 1-41.

Xiong, J. J. et R. A. Shenoi. 2008. « A load history generation approach for full-scale accelerated fatigue tests ». *Engineering Fracture Mechanics*, vol. 75, p. 3226-3243.

Yuanfang, H., L. Guangning, et F. Shiying, 2012. *Resarch on prototype hydro-turbine operation*. ForeignLanguages Press Co. Ltd.